# THE DIRECT CONNECTION OF GENERATORS TO HVDC CONVERTERS WITH AN EMPHASIS ON SERIES EXCITATION

STUART JAMES MACDONALD

A thesis presented for the degree of Doctor of Philosophy
in Electrical and Electronic Engineering at the
University of Canterbury, Christchurch, New Zealand.

November 1994

# Abstract

The underlying theme of this thesis has been the investigation of the direct connection of generators to HVdc converters. The first ever direct connection harmonic test measurements are presented. The accuracy of present steady state and dynamic simulation models is assessed.

A novel variation of the direct connection, called the series excitation is proposed. In this system the dc line current is fed back in series with the dc output to provide the excitation requirements of the generators. A steady state formulation is developed to investigate its operational advantages and limitations. State variable and EMTDC models are used to predict the dynamic behaviour.

The time consuming nature of dynamic simulation algorithms has encouraged the search for effective differential equation initialisation procedures. A Newton–Raphson technique is applied to a state variable transient converter simulation programme in a bid to reduce steady state computation times.

# Publications

Arrillaga, J., Macdonald, S.J., Watson, N.R. and Watson, S. "Direct Connection of Series Self-Excited Generators and HVDC Converters," IEEE Winter Power Meeting, Columbus, Ohio, February 1993.

Arrillaga, J., Macdonald, S.J., Watson, N.R. and Watson, S. "Series Self-Excited HVDC Generation,"*Proceedings of the IEE, Pt C*, Vol. 140, No.2, March 1993, pp.141–146.

Arrillaga, J., Camacho, J.R., Macdonald, S.J. and Arnold, C.P. "Operating characteristics of unit and group connected generator–HVDC converter schemes,"*Proceedings of the IEE, Pt C*, Vol. 140, No.6, November 1993, pp.503–508.

Macdonald, S.J., Enright, W., Arrillaga, J., O'Brien, M.T."Test Results from Benmore HVdc station with the generators operating in Group Connected Mode,"*CIGRE Joint Working Group 11/14–09*,August 1994.

# Acknowledgements

There are a number of people that deserve mention for their direct and indirect contributions to this thesis. Some of them have helped me to see the wood through the trees while others have been good friends ever willing to lend an ear.

I would like to thank my supervisor J Arrillaga for his guidance throughout the course of this work but especially for his patience. The financial and technical assistance of Trans Power New Zealand is gratefully recognised.

My thanks to Drs C P Arnold, N R Watson for their assistance and support and in particular Drs Jose Camacho, Aurelio Medina, Allan Miller, Alan Wood and J Zavahir for their friendship. Thanks again to Alan Wood for his many helpful suggestions.

My best wishes go to fellow postgraduates Glenn Anderson, Roger Brough, Shiun Chen, Quang Dinh, Wade Enright, Du Ping, Bruce Smith, Simon Todd, David Waterworth, Tim Wilkinson. May all their papers be duly accepted.

Finally, and most importantly, I wish to acknowledge the ever strong support and encouragement of my parents and family during the years of study, and to the dearest thing to me, Maria.

QUANTUM IN ME FUIT

# CONTENTS

# LIST OF FIGURES

# LIST OF TABLES

# Glossary

| | |
|---|---|
| $\alpha$ | converter firing angle |
| $\alpha_{min}$ | minimum converter firing angle |
| $\alpha_{nom}$ | nominal converter firing angle |
| $\chi$ | generator vector phase angle |
| $\delta$ | partial derivative operator |
| $\Delta$ | average state vector difference |
| $\epsilon$ | error tolerance |
| $\gamma$ | inverter gamma |
| $\hbar$ | harmonic order |
| $\mu$ | commutation angle |
| $\eta_l$ | line efficiency |
| $\eta_l^g$ | group connection line efficiency |
| $\eta_l^u$ | unit connection line efficiency |
| $\eta_t$ | turbine efficiency |
| $\phi_{gap}$ | machine air gap flux |
| $\phi_n$ | state transition matrix for the "nth" sub–interval |
| $\Phi$ | state transition matrix |
| $\Psi$ | flux linkage |
| $\Psi_a, \Psi_b, \Psi_c$ | three phase stator flux linkages |
| $\Psi_d$ | direct axis flux linkage |
| $[\Psi_{dqo}]$ | vector of dqo flux linkages |
| $\Psi_l(t)$ | inductor flux vector |
| $\Psi_n$ | flux linking inductor "n" |
| $\Psi_o$ | zero sequence flux linkage |
| $\Psi_q$ | quadrature axis flux linkage |
| $[\Psi_s]$ | vector of three phase stator flux linkage |
| $\rho$ | derivative with respect to time |
| $\Re$ | magnetic circuit reluctance |
| $\tau$ | three phase to two phase transformation matrix |
| $\theta$ | rotor position angle (degrees) |
| $\omega$ | synchronous speed |
| $\xi$ | dummy integration variable |
| $\zeta$ | generator vector phase angle |
| $a_n$ | sinusoidal inductance coefficient |
| $A_{yz}$ | coefficient matrix (i.e. $A_{l\alpha}$) |
| $b_n$ | sinusoidal inductance coefficient |
| $B_{yz}$ | coefficient matrix (i.e. $B_{l\alpha}$) |
| $c_n$ | sinusoidal inductance coefficient |
| $C_\hbar$ | $\hbar$th current harmonic |
| $d_n$ | sinusoidal inductance coefficient |
| $e_n$ | sinusoidal inductance coefficient |
| $E$ | machine internal EMF |
| $E''$ | generator subtransient EMF (rms phase-neutral) |

| | |
|---|---|
| $E_{nom}$ | nominal machine internal EMF |
| $f$ | denotes "function of" |
| $f_v$ | forcing function for the "vth" time step |
| $F$ | summation of forcing function terms |
| $g$ | algebraic control equation |
| $G_n$ | generator "n" |
| $h$ | time step |
| $i$ | current |
| $i_c(t)$ | capacitor current vector |
| $i_{km}$ | current flowing between nodes $k$ and $m$ |
| $i_l(t)$ | inductor current vector |
| $i_n$ | current flowing in inductor "n" |
| $I$ | identity matrix |
| $I_a$ | phase a stator current |
| $I_{ac}$ | ac current |
| $I_b$ | phase b stator current |
| $I_b^r, I_b^s$ | base rotor, stator current |
| $I_c$ | phase c stator current |
| $I_d$ | direct axis current |
| $I_{dc}$ | dc current |
| $[I_{dqo}]$ | vector of dqo currents |
| $I_f$ | field current |
| $I_{kd}$ | direct damper winding current |
| $I_{km}$ | history term current source |
| $I_{kq}$ | quadrature damper winding current |
| $I_n$ | vector of history term current sources |
| $I_{nom}$ | nominal dc current |
| $I_o$ | zero sequence current |
| $I_q$ | quadrature axis current |
| $[I_s]$ | vector of three phase stator currents |
| $I_{sat}$ | knee point of excitation saturation curve |
| $I_y$ | current in branch type "y" |
| $j$ | imaginary operator |
| $J$ | jacobian or sensitivity matrix |
| $k$ | constant |
| $k_f$ | generator excitation constant |
| $k_f^s$ | saturated generator excitation constant |
| $K_{yz}$ | connection matrices (i.e. $K_{\gamma\alpha}$) |
| $L$,$[L]$ | inductance, inductance matrix |
| $L_a$ | leakage inductance |
| $L_b^r, L_b^s$ | base rotor, stator inductance |
| $L_f$ | field leakage inductance |
| $L_{kd}$ | direct axis damper leakage inductance |
| $L_{kf}$ | field to damper winding mutual inductance |
| $L_{kq}$ | quadrature axis damper leakage inductance |
| $L_{md}$ | direct axis mutual inductance |
| $L_{mq}$ | quadrature axis mutual inductance |

| | |
|---|---|
| $L_{yz}$ | self and mutual terms of the $[L]$ |
| $M$ | contraction mapping operatpr |
| $MVAR_i$ | inverter reactive power consumption |
| $n$ | whole number |
| $N$ | number of state variables |
| $p$ | per unit generator power |
| $P$ | transmitted dc power |
| $P_n$ | nominal dc power |
| $P_b^r, P_b^s$ | base rotor, stator power |
| $Q_c(t)$ | capacitor charge vector |
| $[R]$ | diagonal resistance matrix |
| $R_a$ | armature resistance |
| $R_{eq}$ | equivalent resistance |
| $R_f$ | field resistance |
| $R_{kd}$ | direct axis damper resistance |
| $R_{kq}$ | quadrature axis damper resistance |
| $R_l$ | line resistance |
| $t$ | time in seconds |
| $T$ | the period |
| $T'_{do}$ | direct axis transient open circuit time constant |
| $T''_{do}$ | direct axis subtransient open circuit time constant |
| $T''_{qo}$ | quadrature axis subtransient open circuit time constant |
| $u$ | applied voltage vector |
| $v$ | integer |
| $v_{km}$ | voltage between nodes $k$ and $m$ |
| $V$ | voltage |
| $V_a$ | phase a stator voltage |
| $V_{ac}$ | ac voltage |
| $V_b$ | phase b stator voltage |
| $V_b^r, V_b^s$ | base rotor, stator voltage |
| $V_c$ | phase c stator voltage |
| $V_d$ | direct axis voltage |
| $V_{dc}$ | dc voltage |
| $[V_{dqo}]$ | vector of dqo voltages |
| $V_f$ | field voltage |
| $V_{\hbar}$ | $\hbar$th voltage harmonic |
| $V_i$ | inverter dc voltage |
| $V_l(t)$ | inductor voltage vector |
| $V_n$ | nominal voltage of a generator–converter group |
| $V_{nom}$ | nominal dc voltage |
| $V_o$ | zero sequence axis voltage |
| $V_q$ | quadrature axis voltage |
| $V_r$ | rectifier voltage |
| $[V_s]$ | vector of three phase stator voltages |
| $x$ | state variable vector |
| $x''$ | generator subtransient reactance |
| $x_c$ | commutation reactance |

| | |
|---|---|
| $x_o^v$ | present state variable vector |
| $x_o^{v+1}$ | new state variable estimate |
| $x_t$ | transformer leakage reactance |
| $X_d$ | generator direct axis reactance |
| $X_d'$ | direct axis transient reactance |
| $X_d''$ | generator direct axis subtransient reactance |
| $X_q''$ | generator quadrature axis subtransient reactance |
| $X_l$ | armature leakage reactance |
| $X_o$ | zero sequence reactance |
| $X_q$ | quadrature axis reactance |
| $Z_b^r, Z_b^s$ | base rotor, stator impedance |
| $Z_n$ | nodal impedance matrix |

Abbreviations

| | |
|---|---|
| ac | alternating current |
| dc | direct current |
| pu | per unit |
| AVR | automatic voltage regulator |
| CCC | constant current control |
| CEA | constant extinction angle |
| CHART | continuous harmonic analysis in real time |
| D | direct (axis) |
| DAQ | data acquisition unit |
| EMF | electro magnetic force |
| EMTDC | electro magnetic transient direct current |
| EMTP | electro magnetic transient programme |
| FASST | fast steady state |
| HVdc | high voltage direct current |
| MMF | magneto motive force |
| OLTC | on load tap changer |
| PSCAD | power systems computer aided design |
| Q | quadrature (axis) |
| STM | state transition matrix |
| TCS | transient converter simulation |
| THD | total harmonic distortion |

# Chapter 1
# INTRODUCTION

The human races burning ambition seems to be to harness and control nature. There is a never ending pursuit to explain *how* and *why* physical processes occur, we are left with a sense of frustration as the deep mysteries of our existence continue to elude us.

Progress in science and the creation of knowledge is facilitated by two complementary methodologies, experiment and theory. The conditions of the experiment are rigidly controlled so that single parameter variations produce a resultant effect that can be observed. By logical deduction and reasoning a theoretical model of the process can be formed. This model describes the given process in the common language of mathematics and can be tested and validated (or otherwise) against the real system. It provides a basis for further theoretical improvements and can perhaps direct areas of the experimental research. The two paths go hand in hand and must more or less advance together.

Many natural processes are governed by mathematical differential equations, for example the propagation of light or the simple harmonic motion of a pendulum, the solid foundations of which were laid by the ubiquitous calculus of Newton. Faraday became the father of Electromagnetism when he discovered that the current induced in a coil was proportional to the rate of change of flux linking that coil. Faraday's experimental efforts were recognised when the unit of capacitance, the Farad, was named after him. The phenomena of electromagnetism has also become inextricably bound up with the differential equation.

Until the advent of the digital computer the complexity and number of equations used to explain physical processes were limited because the calculations were performed entirely by hand. While computers cannot think, they are readily programmed to rapidly deal with and solve large and complex sets of equations in a systematic fashion. Computer speed and storage abilities look set to increase further and this ensures that larger more complex and sophisticated problems will be attempted.

This capability has been well exploited in the field of electrical circuit analysis, to name just one application. The construction of electrical machines has changed very little for the last fifty years, yet the computer has greatly advanced the performance analysis of these devices. The extent and sophistication to which computer simulation algorithms have developed now blurs the distinction between that which is experimental and that which is theoretical.

The age of electrical ac and dc Power

At the turn of the century the first electrical machines generated dc power for commercial and residential lighting. However the use of this energy was problematic because the distribution voltage was low. Consequently the current bearing copper conductors had to be thick (and therefore costly) to reduce resistive losses and prevent voltage regulation. Alternatively the generator units had to be positioned close to their loads which was also inefficient.

The realisation of the ac transformer overcame the immediate problem of electricity distribution but the goal of an alternating current electrical system had to wait until suitable alternators and motors were available. Once the polyphase concept was decided upon as the optimum configuration the generation of power was centralised leading to greater efficiency of generation and supply.

The technical and economic advantages of dc power transmission lines are well known. The development of the first truly high voltage mercury–arc valve by the ASEA company of Sweden in the 1940's opened the doors for HVdc technology to stake its claim to long distance transmission. In 1954 a 10MW Sweden–Gotland inter island link was built and since then 49 other links have been commissioned to give a total installed capacity of 36,000 MW.

As world energy sources are depleted and remote hydro, gas or low grade coal reserves are exploited, it is expected the number of HVdc schemes will increase. Conventional HVdc systems interconnect and strengthen ac systems. Large amounts of filtering is provided at the converter terminals to absorb converter station characteristic harmonics. At remote generating stations, where the generated power is supplied almost exclusively to the link, there is little or no local load or interconnected ac system and hence no strict need for a filtered ac bus bar.

A new proposal, called the Direct Connection, proposes to directly connect the generators to HVdc converters aiming to reduce the cost and greatly simplify the sending end system by dispensing with the ac switchyards and filters. This idea is receiving serious consideration in academic journals and by electrical engineering bodies. A further simplification, called the Series Excitation, removes entirely the need for machine excitation systems by feeding back the dc line current in series to excite the generators.

Before a new scheme such as the one above can be built many system design parameters must be known. Computer dynamic simulation packages are modern design tools that can be used to predict the influence of the given parameters on the system operation. A drawback of these methods is that they consume large amounts of computer time to arrive at a solution. Improving the efficiency of these theoretical tools is thus also of prime importance.

Thesis Outline

This thesis has been by and large computer based and thereby theoretical. Existing *tried and true* computer algorithms have been used, and in some cases modified, to predict the steady state and transient performances of the direct and series connections.

Chapter 2 briefly introduces the direct connection concept and comments on its strengths and weaknesses. The salient design aspects are reviewed and the suitable methods of system analysis discussed.

A clear deficiency of the technical discussions so far is that no practical data, which is of vital importance to system designers, has been available. Chapter 3 reports on the first large scale harmonic measurements of a direct connection variant, called the group connection. The experimental circumstances are described and the implications of the harmonic measurements are discussed. The accuracy of present steady state and dynamic simulations is assessed. Further to the harmonic tests the operating and efficiency characteristics of two direct connection alternatives, the unit and group connections, are explored.

Chapter 4 deals with the innovative proposal of the series excitation. In this system the dc line current is fed back to excite the generating station synchronous machines to further simplify the rectifying station. A steady state model is developed to illustrate the operating advantages and deficiencies of this arrangement. The series–group connection of generators to HVdc converters, such that the transmission voltage is boosted at low powers, is also discussed.

A modified state variable machine model is proposed in Chapter 5 to investigate the behaviour of the series excitation scheme under the transient conditions of power fluctuations and system faults. The EMTDC based simulations are complemented by the time honoured Transient Converter Simulation algorithm.

Even after huge advances in computer processor speed, detailed modeling of generator converter units or large nonlinear problems in general can become intractable. Chapter 6 discusses the use of a Newton–Raphson numerical technique to initialise dynamic simulation algorithms.

The conclusions are drawn in Chapter 7 and ideas for future work discussed.

# Chapter 2
# DIRECT CONNECTION SCHEMES

## 2.1 Conventional HVdc Transmission

In many HVdc schemes around the world, large blocks of power are transferred over long distances between ac systems. However the transmission distance is not the sole criterion that will determine the choice of dc technology. HVdc transmission has some distinctive advantages over ac transmission systems. While the rectifier and inverter station costs are quite high and ac filters need to be installed to absorb converter harmonics, the transmission line towers are more compact. Moreover the ac systems at each end of the transmission line need not be synchronised. Long ac transmission lines can be prone to phase voltage unbalance requiring transposition of the phases and even expensive reactive compensating equipment to regain symmetrical three phase waveforms. This is not a problem for dc power transmission which also has a very fast speed of response.

The injection of large amounts of power into the primary transmission system can appreciably increase the fault level which increases ac system circuit breaker duty. In such cases the practice has been to construct a new primary transmission level at a higher voltage which will pose increasingly intolerable environmental constraints in the future. A back to back infeed can circumvent this problem as was the case for the Kingsnorth (1974) scheme where it was necessary to connect into an area of high load density. Back to Back converters can also be implemented to couple unsynchronised ac systems or two ac systems of different frequency as with the Eel River project (1972) and the Sakuma interconnection of 1965 (50–60 Hertz) respectively. Operating experience with the Pacific Intertie (1970) where an HVdc transmission line operates in parallel with ac transmission lines has shown to improve the transient stability of the whole system.

In other cases such as the Sweden–Gotland (1954) and New Zealand (1965) schemes, the transmission distance was not the primary factor. The voltage rating of the undersea cables made the dc alternative the most attractive.

A simplified diagram of a single pole of a conventional HVdc rectifier station is depicted in Figure(2.1). The schematic could equally well represent an inverter system because the power flow can be bidirectional. The converter bus has harmonic filters which aim to prevent characteristic converter harmonics from penetrating into the generator plant or further into the ac system. If nearby sources of generation exist then these may be connected through a transformer level to the converter bus. Converter transformer on load tap changing (OLTC) will be implemented to assist with reactive power control.

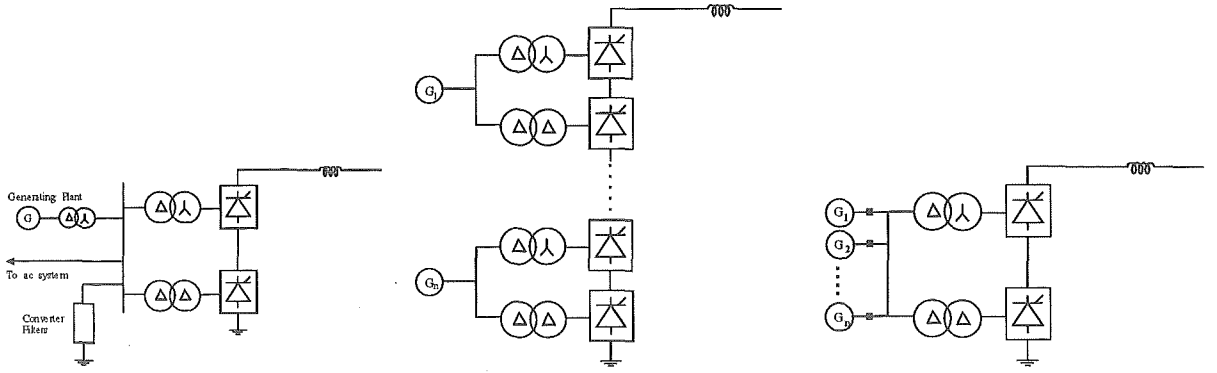


(a) Conventional (b) Unit Connection (c) Group Connection

**Figure 2.1** HVdc Transmission

## 2.2 Direct Connection Configurations

The direct connection of generators to HVdc converters was first proposed a little over 20 years ago [Calverley *et al.*, 1973], and two possible realisations are the unit and group connections shown in Figure(2.1)b and c respectively.

There are a number of applications that could be well suited to such a scheme. When isolated sources of energy are exploited, the transmission of large blocks of power to load centres by dc transmission is an attractive option. In remote locations with little or no local load or interconnecting ac system, the generating plant will almost exclusively supply the converters. Without the need for an ac system at the generating source, the direct connection could provide a very compact design. The construction of new generators situated near their load centres and the injection of a large amount of electricity into the primary transmission system (as already mentioned) may pose tremendous technical and environmental problems. In this case the use of a direct connected back to back link may be a viable means of providing reinforcement.

The main advantage is a great simplification of the sending end system by dispensing with the intermediary filtered ac bus bar. Feasibility studies have shown that doing away with generator transformers, on load tap changers, ac filters and associated switchyards would reduce the station cost by about one third [Ingram, 1988]. As well as the initial capital saving further saving accrue as the low number of components should reduce maintenance costs and improve reliability. The generator frequency is not fixed to a common ac system base and hence variable turbine speed operation is possible to maximise overall generation efficiency [Arrillaga *et al.*, 1992],[Naidu and Mathur, 1989]. Furthermore generator self excitation, sub harmonic oscillations and transient overvoltage phenomena, effects usually attributed to filter banks, are eliminated.

It has been suggested [Arrillaga *et al.*, 1991] that, while the direct connection can be designed to provide any specified nominal power, the absence of filters may limit the operational capability at larger currents levels and thus reduce the ability of the link to provide temporary power increases. In the absence of filters the generator must supply all the reactive power of the converter. Another disadvantage is that characteristic harmonic currents flow in the generator stator windings causing additional losses and parasitic torques. The harmonic voltages impressed upon the stator windings

cause extra insulation stresses and aging. Furthermore an external source must be found for the station auxiliaries if variable speed is to be considered.

In the unit connection each generator is connected to its own twelve pulse converter. Each of these "units" is completely independent of the rest. On the other hand, the generators of the group connection are connected to a common bus which supplies a single 12–pulse converter group. The number of transformers and bridges has been significantly reduced however each machine requires a circuit breaker and synchronising mechanisms.

## 2.3 Steady State Characteristics

The conventional (i) and the direct connection (ii) characteristics are shown in Figure(2.2). Both systems have a nominal operating point A for a given nominal $\alpha$ ($\alpha_{nom}$).

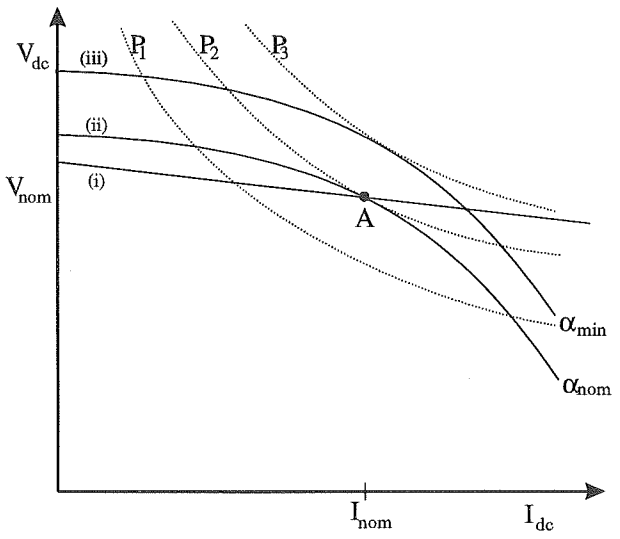


**Figure 2.2** The Conventional and Direct Connection Characteristics

### 2.3.1 Temporary Overload Capability

The HVdc link may be required to deliver extra synchronising power to the receiving ac system following an inverter fault, which for the conventional system does not present a problem. The dc current can be increased without suffering a poor voltage regulation, allowing temporary overload capability subject to maximum overload current limits.

At the nominal point A the direct connected system commutation angle will be close to 30 degrees. The machine excitation controllers are relatively slow acting and hence the level of machine excitation is considered fixed. Further dc current increases cause simultaneous commutations on both bridges which effectively increases the commutation reactance and results in a larger voltage regulation slope. The extra power conversion capability can be deduced from where the power locus curves meet the voltage characteristic and it can be seen that increasing the line current actually results in less transmitted power. Hence the overload capability of the direct connection is poor compared to the conventional system.

Power increases to stabilise the inverter system must be implemented quickly by a fast acting strategy. The most efficient way of achieving this is by operating at a slightly higher nominal firing angle. The firing angle reserve, i.e. the difference between $\alpha_{nom}$ and $\alpha_{min}$, can be used to provide temporary power increases as shown by curve (iii) of Figure(2.2).

The use of fast machine static excitation is also possible however it will be operating at a high firing angle, and inefficiently, most of the time.

## 2.4 Design considerations

The final design will be dictated by the performance requirements of the system and there will be compromises to arrive at the best overall system performance. Unit or group connection of the generators can be implemented or some hybrid combination to achieve the desired flexibility.

### 2.4.1 Commutation Reactance

There are two contributors to the commutation reactance, i.e. the transformer leakage and machine subtransient reactances [Arrillaga, 1983]. It is desirable to keep the commutation interval as short as practically possible to minimise the dc voltage commutation reduction. By choosing a low nominal firing angle, some restriction may be placed on transformer leakage and machine sub transient reactances in order to keep the commutation angle below 30 degrees. This may also limit the temporary extra power capability however the harmonic current generation will be a minimum.

The selection of a slightly higher nominal converter firing angle will increase the cost of the converter valves [Salgado *et al.*, 1986]. The reactive power consumption of the converter will also be higher and reflected in the MVA rating of the generators. The commutation angle will be reduced which will increase the harmonic current content flowing in the machine windings. On the positive side however fast temporary power reserve is available to stabilise the inverter system and there is less need to lower machine and transformer reactances to bring the commutation angle to some acceptable limit.

### 2.4.2 Diode Rectifiers

The common control strategy in HVdc schemes is for the inverter to be operating as close as practically possible to its extinction angle limit to minimise the reactive power consumption at the inverter i.e. constant extinction angle (CEA) control. The rectifier then acts in constant current control (CCC) mode by adjusting firing angle typically in the range of 10–20 degrees. Some authors have suggested replacing the rectifier thyristors with diodes to further simplify the sending end system [Bowles, 1981][Hungsasutra and Mathur, 1989]. Complex controls and firing circuitry would be eliminated and maintenance costs would be further reduced. Machine excitation would thus become the sole means of rectifier voltage control and the inverter would regulate the dc current.

A significant rectifier cost saving is provided and the generator harmonic currents will be a minimum. Again some restrictions may have to be imposed on the allowable transformer leakage and machine subtransient reactance values. The inverter will operate at higher extinction

angles thereby consuming more reactive power. Under these conditions, however, the chance of commutation failure would be significantly reduced.

The greatest restriction appears to be the loss of one degree of controllability. On detection of a dc line fault the normal practice is to advance the converter firing angle so that the stored smoothing reactor energy is removed. In a diode scheme, fast ac circuit breaker action can isolate the generators from the circulating fault current, and the machine excitation control can reduce terminal over voltages, yet the energy in the smoothing inductance will take a long time to naturally decay. DC circuit breaker technology now exists [Long *et al.*, 1990] to speedily remove residual energy from the fault circuit however the link re–energisation without converter firing angle control could be slow [Hungsasutra and Mathur, 1989].

### 2.4.3 Variable speed operation for hydro units

In the normal case of hydro generation the fixed blade turbine is designed to have maximum efficiency at the nominal head and the rated power of the generator. Hence during seasonal head fluctuations or at reduced power settings the turbine conversion of energy is inefficient. The ability to optimise the speed for particular head and load condition allows an extra degree of freedom permitting gains to be made. These gains must be weighed against some limitations as will be explained next. The speed range boundaries will be mainly limited by what levels of cavitation (if any) are acceptable. Therefore variable speed can be used to avoid areas of cavitation and rough operation at the expense of not fully optimising the turbine efficiency.

From an electrical point of view high rotational speeds will correspond to higher power levels and it is expected that additional heating of the machine will be compensated by greater air cooling keeping the machine within thermal limits. At lower speeds the induction will be reduced however so will the machine and transformer impedances. Moreover lower rotational speeds will be associated with lower power settings assuming the efficiency is to be maximised. To this end a recent paper has suggested that economical transmission voltages will be maintained at low speeds [Arrillaga *et al.*, 1992]. It is difficult to estimate the effects of variable speed on the machine losses because they occur due to the skin effect and are thus frequency dependent.

Under variable speed operation the dc line voltage harmonic frequencies will vary and hence a tuned dc filter cannot be used. The lack of a dc filter may also mean unacceptably high levels of electromagnetic interference. Intermodulation between the inverter and rectifier terminals may cause small amounts of intermodulated currents to flow. It is even possible that the natural resonance of the dc line could be excited by such intermodulation.

### 2.4.4 Generator Harmonic Rating

The rating of converter transformers is well understood from practical experience with conventional HVdc schemes. From the generator point of view it is desirable to operate with a commutation angle close to 30 degrees so that harmonic current generation and harmonic losses are at a minimum, although the commutation losses will be higher. Because there are no asymmetries it is expected that the negative sequence thermal capacity shall, in the main, compensate for the extra harmonic loading.

## 2.5 Methods of Analysis

Before a scheme will be built the operational capability, steady state periodic waveforms and transient responses will be thoroughly investigated. The accuracy of the results will depend on the simulation methods employed.

### 2.5.1 Steady State Simulation

In the conventional HVdc the presence of filters at the converter bus makes the commutating voltage sinusoidal and measurable. The commutation reactance is then simply the leakage reactance of the transformer. The operational capability can therefore be derived from steady state formulae on the basis of specified and perfectly sinusoidal commutating voltages and fixed commutation reactances.

For a synchronous machine directly connected to a converter without filters the terminal voltages are distorted and no longer sinusoidal. The commutating point has been referred inside the machine where it is not accessible. The commutations, which are brief phase to phase short circuits are controlled by the generator subtransient behaviour. The system commutation reactance now comprises the transformer leakage reactance plus the generator subtransient reactance. The analysis is more complicated because the machine contribution to the commutation reactance and the commutating voltage are not exactly known.

Non salient machines have a fairly uniform air gap between rotor and stator leading to practically invariant reactances for different load conditions. Hence in this case the formulation of a constant commutating voltage behind the subtransient reactance is often an acceptable approximation.

### 2.5.2 Dynamic Simulation

If the machine is salient then the rotor permeance around the air gap is not constant, the characteristic machine inductances are functions of rotor position and the harmonic coupling in the machine can no longer be considered in terms of linear generator equivalents. More sophisticated models are required to predict the interactions between generator and converter.

Dynamic simulation is the solution of differential equations to determine circuit voltages and currents. Because the system is sufficiently non linear and an accurate knowledge of waveforms is required then dynamic simulation is appropriate. Electrical circuit simulation programmes can be divided into two types; State Variable and Electromagnetic Transient and these have evolved primarily to investigate the reaction of systems for transient fault disturbances. In many cases (i.e. where only the periodic steady state waveforms are to be determined) dynamic simulation is excessively powerful and reduced formulations, of which [Sudhoff and Wasynczuk, 1993] [Yikang He and Yaoming Wang, 1990] are two examples, can be used to represent bi–lateral generator–converter interactions.

### 2.5.3 Finite Elements

In circuits containing electromagnetic devices (i.e transformers or electric machines) the most complete representation can be accomplished with finite element analysis. In these techniques the

magnetic field potential is calculated considering the detailed physical geometry of the component. Finite element models will be needed to accurately estimate damper bar, saturation and eddy current losses of the generator especially if variable speed operation is to be assessed. The calculation sequence is exceedingly time consuming and at present there are problems interfacing the magnetic solution to external twelve pulse electrical networks.

## 2.6 Conclusions

The direct connection of generators to HVdc converters is being given serious consideration for a number of important applications. These include the transmission of bulk electrical power from isolated energy sources and the interconnection of new generation plant into existing ac networks where an ac tie would pose technical difficulties. In such cases there is no strict need for a filtered ac bus bar at the rectifier terminal.

The removal of filters and any attendant transformer levels, switchyards etc, leads to a gross simplification of the rectifier terminal which significantly reduces the construction and maintenance costs. There are a host of technical benefits that arise from the absence of filters such as a reduction of over voltages and the elimination of low frequency oscillations. Furthermore variable speed can be utilised to optimise hydro to electrical energy conversion.

The flow of characteristic converter harmonic currents in the generator windings causes additional losses and pulsating torques. The generators also must supply the reactive power demands of the converters and consequently the temporary overload capability is reduced. The system design will very much depend on the desired performance requirements. At present the accurate analysis of salient generator converter interactions requires computer intensive dynamic simulation. While this may be the best compromise between speed and accuracy, detailed finite element models may be necessary to properly assess the machine losses.

# Chapter 3

# DIRECT CONNECTION HARMONIC TESTS AND EFFICIENCIES

The foregoing chapter briefly described the potential benefits and pertinent design issues of directly connected generators and HVdc converters. This chapter constitutes *new* information related to such schemes and is divided into two sections. The first contains harmonic test measurements from the New Zealand HVdc system. To show important operational differences between unit and group connections, respective transmission efficiencies combining turbine and line characteristics are calculated in the second section. The implications for the inverter reactive power demand at reduced power settings are also discussed.

## 3.1 Harmonic Tests

Issues relating to the design and rating of generators are now becoming increasingly the focus of direct connection studies. While the steady state capability, operational aspects and transient behaviour are well documented from a theoretical point of v iew [CIGRE Joint Working Group 11/14-09, 1993], there is no practical information on the operation of such schemes and particularly the harmonic content and required ratings of the generator units involved. This section describes harmonic tests that were carried out at the Benmor e station of the New Zealand HVdc link. The test results are also used to assess the accuracy of currently used simulation techniques.

### 3.1.1 The Benmore HVdc Terminal

The New Zealand HVdc link transmits surplus hydro power from the South Island to major load centres in the North Island. The recently upgraded link consists of a parallel arrangement of two 12–pulse mercury–arc valve converters on Pole 1 and a new thyristor–valve 12–pulse converter on Pole 2. The older Pole 1 mercury–arc valve and new thyristor equipment is rated for 270kV and 350kV respectively. The nominal line current is 2kA and hence the overall maximum continuous power transfer is 1240MW from South to North.

For the sake of simplicity only the circuit and components involved in pole 1 are shown in Figure(3.1). The station harmonic filters, F1 and F2, are connected on the tertiaries of T2 and T5. Hence when either of the interconnecting transformers (T2 or T5) are removed from service, poles 1A or 1B can operate in group connection. Electrically there is no difference between unit and group connections in the sense that the generators, for a given load and firing angle condition should see the same harmonic voltages and currents. Therefore the group connected harmonic test results should also be of general applicability to unit connection schemes.

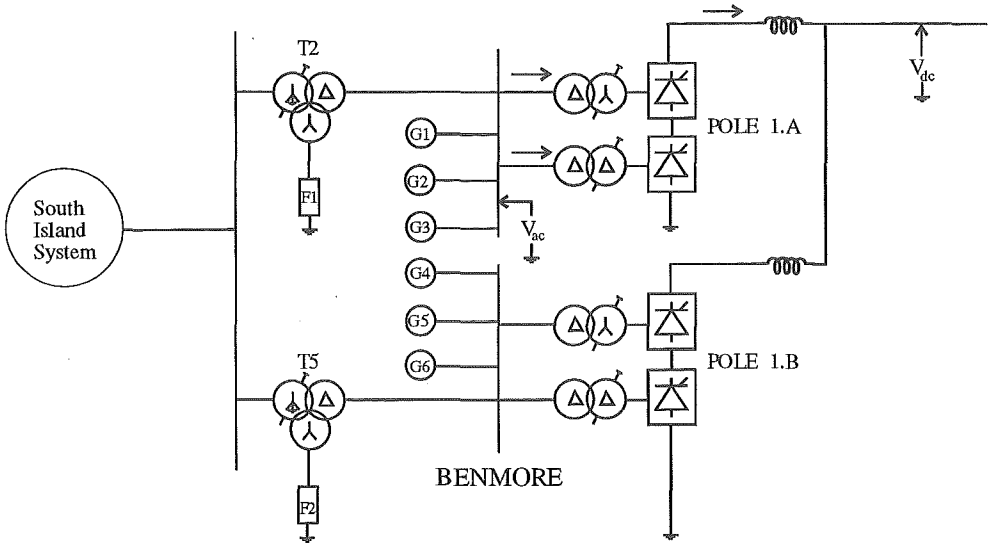


**Figure 3.1** Pole 1 of the New Zealand HVdc Link

By arrangement with TRANS POWER, the National Grid Company, the system was available for harmonic tests in the group connected mode (i.e. with no filters and the ac system disconnected) during a recent period of maintenance for transformer T2. The maximum power transmitted under this condition was 212 MW (80 % of full power) with three generator units (G1–G3) connected on pole 1A.

### 3.1.2 Measurement Equipment

The harmonic measurements were made with a Hewlet Packard Data Acquisition Unit (DAQ) which forms part of the Benmore instrumentation to capture system transients. The usual DAQ traces are derived from filtered control system waveforms and are consequently of no use for harmonic studies.

Three extra channels were installed to record the generator's terminal voltage in one phase and the corresponding currents in each of the two transformers of the 12–pulse converter; these two currents were subsequently added to derive the total generator stator current. Hence it was assumed that the three phase waveforms were balanced. A thorough harmonic analysis would entail measuring the three phase generator voltage and current quantities, however this option was expensive in terms of technician cost. In general, high rate sampling of many waveforms is not problematic because the DAQ is equipped with an optical disk drive which can save approximately 600 megabytes of information to each optical disk.

Other existing channels of interest were the dc voltage, the Pole 1A current and the converter firing angle. The measuring points are labelled on Figure(3.1) as arrows for the current transformers and voltmeter symbols as voltage transformers. The current and voltage transducers were of magnetic type and assumed to be linear.

### 3.1.3 Experimental Procedure

The pole 1A mercury–arc valve converter was deblocked and a steady operating point of 350 Amps, 260kV at 15 degrees firing angle was achieved. In all of the measurements the firing angle was maintained at 15 degrees. The waveforms were sampled at 8192 bits per second for a 5 second interval. Further half–pole dc current increments were performed, and after allowing sometime for the system to stabilise, the waveforms were again sampled. In practice it was difficult to fix the frequency at 50 hertz especially if the machines were lightly loaded and hence small frequency deviations were experienced over the sampling period. This frequency variation led to care being exercised when the spectra of the waveforms were computed.

Owing to the difficulty in maintaining a constant generating frequency it is recommended that future tests should use more accurate FFT processing synchronised with the actual fundamental frequency, such as provided by the CHART instrumentation [Miller, 1992]. Moreover a higher sampling frequency should be used in future so that valve conduction periods can be more accurately measured and the effects of spectral leakage reduced. Based on 50Hz, 8192 bits per second corresponds to one sample approximately every 2.2 electrical degrees and hence the determination of $\mu$ is subject to great error. The best estimate of $\mu$ was obtained by measuring the whole valve conduction interval because the zero crossings are simplest to detect, and then by subtracting 120 degrees.

The dc current range varied from 350 to 785 amps; a typical set of time data recorded is shown in Figure(3.2) for the case of a half pole dc current of 650 Amps. In all cases the uncharacteristic harmonic levels were insignificant. Moreover the presence of dc side filters also made the dc voltage harmonics negligible and hence only the generator characteristic harmonic content is discussed.

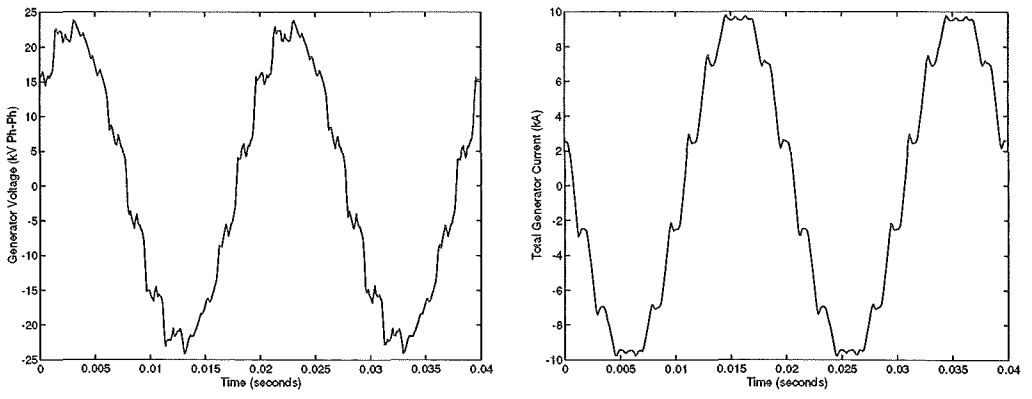


**Figure 3.2** Typical Generator Voltage and Current Waveforms

### 3.1.4 Generator Rating

The possibility of a direct connection was envisaged in the design of the Benmore generators although restrictions were imposed on the nominal power rating (lowered to 102.3 MVA) and the current harmonic content under such operating conditions. The ratings are listed in table(3.1) together with the actual maximum current harmonics monitored during the tests. Clearly none of

the specified maximum limits were exceeded at the power levels involved.

| Harmonic | rating (pu) | recorded (at 212 MW) |
|---|---|---|
| 11th | 0.0744 | 0.0422 |
| 13th | 0.0595 | 0.0267 |
| 23rd | 0.0193 | 0.0067 |
| 25th | 0.0154 | 0.0037 |

**Table 3.1** Machine Stator Current Harmonics

If the dynamic simulation results are extrapolated in the high current region to the rated half–pole power of 270 MW, the rated harmonic currents are still not exceeded.

Conventional generators normally have extra thermal capacity to sustain 10% of negative sequence loading [Uhlman, 1975]; however negative sequence is practically absent in the unit connected mode and the extra capacity compensates for the harmonic loading. Thus the total harmonic distortion of the current was well within 10% of fully rated generator positive sequence current for all operating points including the rated power case investigated with the PSCAD dynamic simulation.

The maximum total harmonic distortion (THD) of the generator current was determined to be 5.4%.

### 3.1.5 Steady State Simulation

To represent generator AVR action, a fixed terminal voltage $V_{ac}$ is specified. The following machine relations based on the phasor diagram of Figure(3.3) then apply.

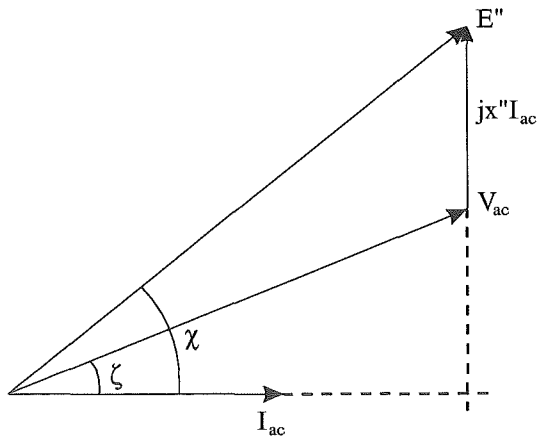


**Figure 3.3** Machine Sub–Transient Phasor Diagram

$$V_{ac}cos\zeta = E''cos\chi \tag{3.1}$$

$$V_{ac}sin\zeta = E''sin\chi - I_{ac}x'' \tag{3.2}$$

where $E''$ and $x''$ are the subtransient voltage (rms phase–neutral) and reactances respectively and $I_{ac}$ is the rms stator current. In preliminary studies such as these it is often assumed that the machine subtransient reactance around the air gap is constant. In this case an average value

$$x'' = \frac{X_d'' + X_q''}{2} \tag{3.3}$$

is often acceptable. Squaring and adding gives

$$V_{ac}^2 = [E''cos\chi]^2 + [E''sin\chi - I_{ac}x'']^2 \tag{3.4}$$

The equations that represent the 12–pulse HVdc converter [Arrillaga, 1983] are

$$I_{ac} = \frac{2\sqrt{6}}{\pi} I_{dc} \tag{3.5}$$

$$cos\chi = \frac{1}{2}[cos\alpha + cos(\alpha + \mu)] \tag{3.6}$$

$$I_{dc} = \frac{\sqrt{3}E''}{\sqrt{2}x_c}[cos\alpha - cos(\alpha + \mu)] \tag{3.7}$$

$$V_{dc} = \frac{6\sqrt{2}}{\pi}\sqrt{3}E''cos\alpha - \frac{6x_c}{\pi}I_{dc} \tag{3.8}$$

where $\alpha$ is the converter firing angle, $\mu$ the commutation angle and $x_c$ the commutation reactance. The quantity $x_c$ is made up of the machine subtransient component and the leakage reactance of the converter transformer. $V_{dc}$ and $I_{dc}$ are the dc voltage and current respectively. For arbitrarily specified $I_{dc}$, $\alpha$ and $x_c$, equations(3.4),(3.6) and (3.7) can be solved iteratively for $\mu$, $\chi$ and $E''$.

>From the value of $\mu$ determined above for some given system operating point, characteristic ac current and voltage harmonics can be estimated in the following manner.

### 3.1.5.1 AC current harmonics

Assuming that the current change over the commutation interval is linear, the current waveform for a 6–pulse bridge is shown in Figure(3.4)a.

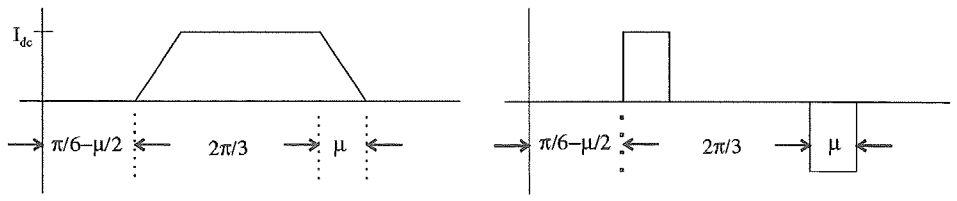


(a) Current waveform (b) Voltage Waveform

**Figure 3.4** Waveforms for harmonic analysis

The frequency spectrum coefficients of this waveform is then given by

$$C_{\hbar} = \frac{2\sqrt{3}}{\pi}\frac{1}{\hbar}\frac{sin\frac{\hbar\mu}{2}}{\frac{\hbar\mu}{2}} \tag{3.9}$$

where $\hbar = 6n \pm 1$ (n is a whole number) and $\mu$ is in radians.

#### 3.1.5.2 AC voltage harmonics

The characteristic 6–pulse harmonic voltage spectrum is approximated by 2 rectangular voltage pulses of width $\mu$ (Figure(3.4)b). The height of each pulse is a function of $\alpha$, $\mu$ and the ratio of the machine subtransient reactance to the total commutation reactance, leading to the following expression for the voltage harmonics

$$V_{\hbar} = \frac{4\sqrt{3}}{\pi}\frac{x''}{x''+x_t}\left[sin\left(\frac{\pi}{6}+\alpha+\frac{\mu}{2}\right) - \frac{1}{2}cos\left(\alpha+\frac{\mu}{2}\right)\right]\frac{sin\frac{\hbar\mu}{2}}{\hbar} \tag{3.10}$$

Because the converter transformers are displaced by 60 electrical degrees, the 12–pulse current and voltage harmonics can also be deduced from equations(3.9) and (3.10). Alternatively the harmonic voltages can be evaluated by multiplying the harmonic currents by harmonic impedances.

### 3.1.6 Comparison between Test and Simulation Results

Figures (3.5) and (3.6) compare the recorded machine current and voltage harmonic levels with those predicted by steady state and dynamic simulations.

#### 3.1.6.1 The Steady State Solution

The steady state formulation estimates of $\mu$ correspond quite well with the measured values as shown in Table(3.2), although lower levels of characteristic harmonics were predicted. The agreement for the harmonic voltages in this case is considered fortuitous.

| $I_{dc}$ (kA) | measured $\mu$ | predicted $\mu$ |
|---|---|---|
| 0.35 | 10 | 10.9 |
| 0.40 | 12 | 12.0 |
| 0.50 | 14 | 14.1 |
| 0.55 | 15 | 15.1 |
| 0.60 | 15 | 16.0 |
| 0.65 | 16 | 16.9 |
| 0.75 | 17 | 18.6 |
| 0.78 | 18 | 19.0 |

**Table 3.2** Steady State and measured $\mu$

It has been suggested that at rated powers $\mu$ will be close to 30 degrees and the ac current will be almost sinusoidal. It does not, however, follow that the machine terminal voltage is sinusoidal

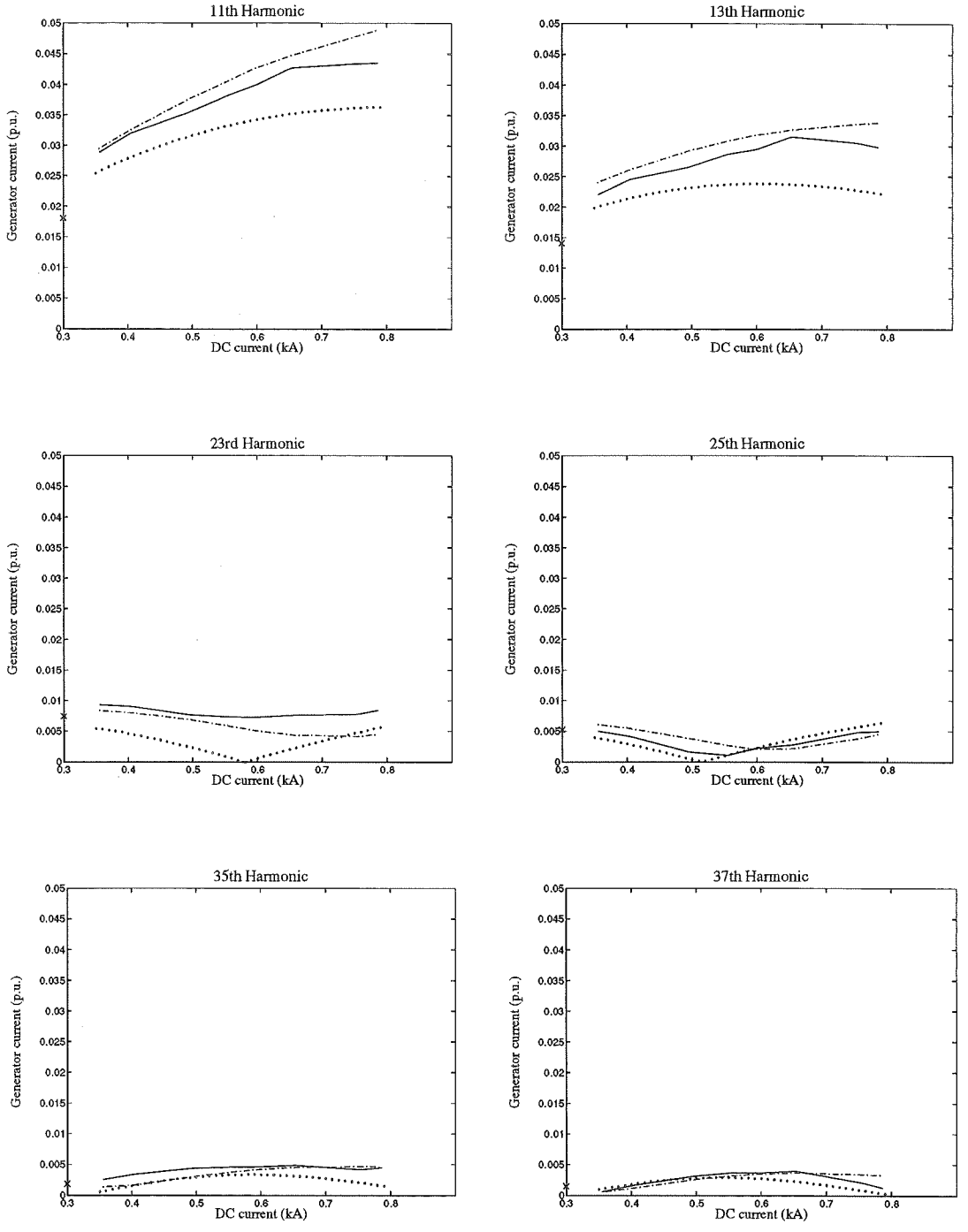


**Figure 3.5** Harmonic comparison of recorded generator current with dynamic simulation; *Recorded data=Solid, PSCAD=Dash–Dash, Steady state equations=Dot*

as well because this very much depends on the parameters of the machine. It has been proposed that the steady state analysis could be further simplified by considering the converter terminal voltage as the commutating voltage. Even if the machine voltage and current are sinusoidal the machine component of the commutation reactance must be included to avoid under estimating $\mu$.

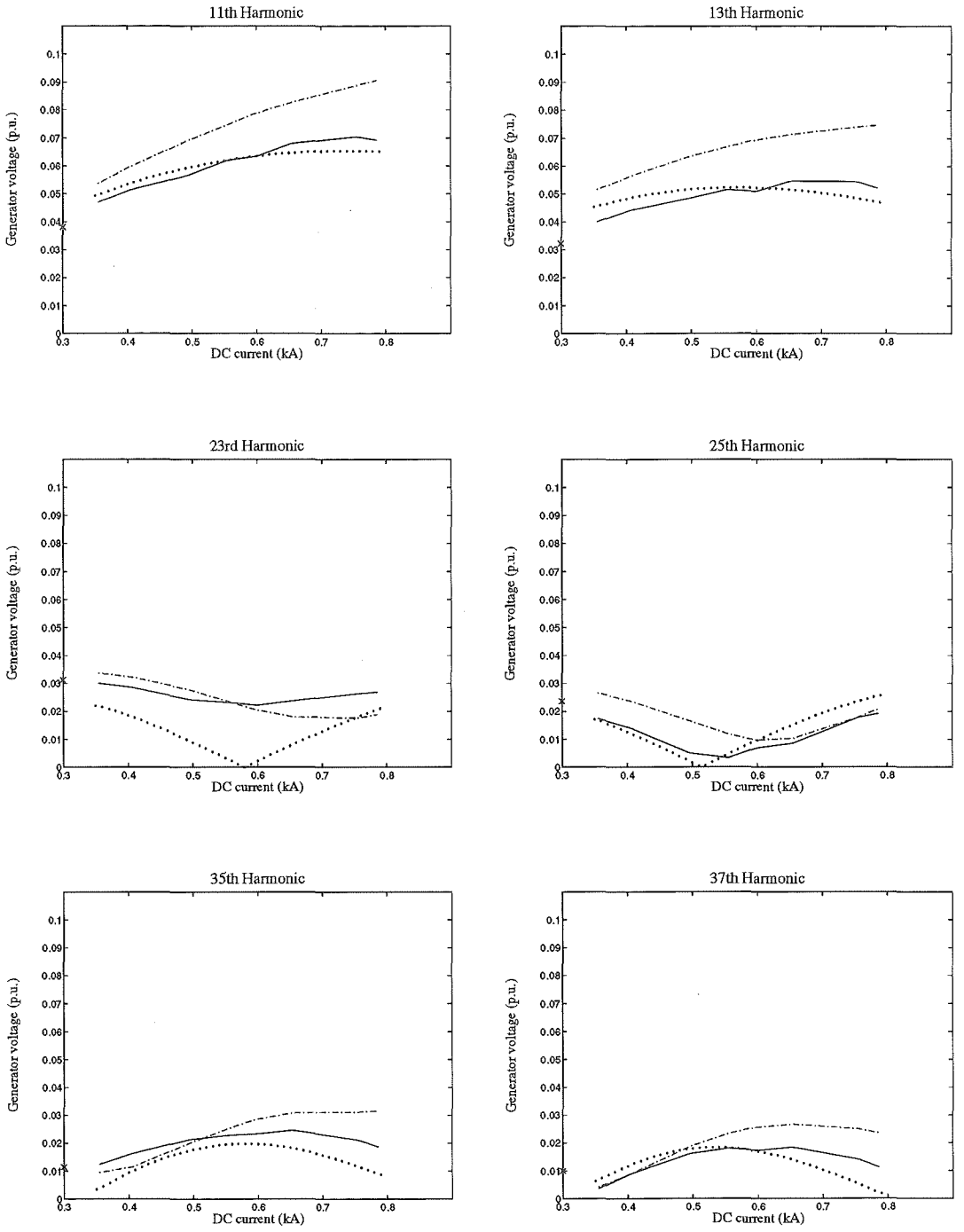


**Figure 3.6** Harmonic comparison of recorded generator voltage with dynamic simulation; *Recorded data=Solid, PSCAD=Dash–Dash, Steady state equations=Dot*

### 3.1.6.2 The Dynamic Solution

The PSCAD [Manitoba HVdDC Research Centre, 1994] dynamic simulation package has been used in the harmonic prediction, the data for which is contained in Appendix A. Overall the harmonic current levels are quite close to the test results as they are less influenced by the

generating operating conditions and more by the dc link firing and current control, which were fixed during the tests.

To give some perspective to the difference between the harmonic current estimations, Figure(3.7) compares one quarter cycle of the measured time domain, PSCAD and steady state current waveforms for the case having a dc current of 785 amps. There appears to be significant differences in the plotted per unit values of Figure(3.5), yet the time domain data seems to be in very good agreement.

However, the harmonic voltages are particularly sensitive to the specified machine subtransient reactances [Kettleborough *et al.*, 1983]. This explains the quite large discrepancy between the simulation and measured voltage harmonics. The parameter values of machine armature leakage, $X_l$, and $X_q''$ are *estimated* quantities only. By reducing $X_q''$ (and consequently reducing $X_l$ which depends on $X_q''$) the voltage harmonics resemble more the measured data without affecting much the harmonic current levels.

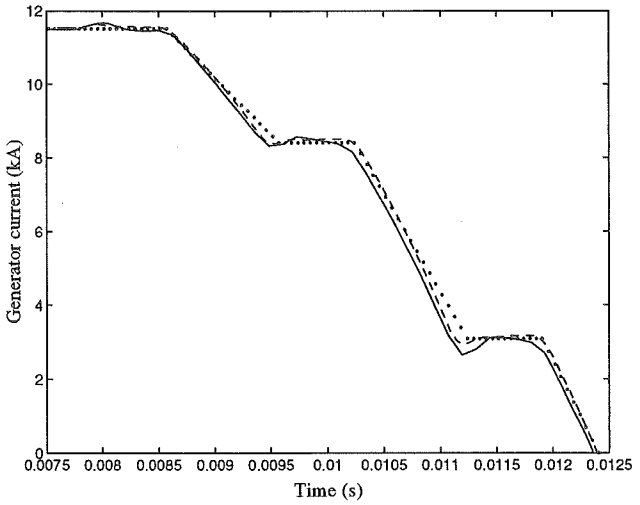


**Figure 3.7** Comparison of Current Waveforms; *Recorded data=Solid, PSCAD=Dash–Dash, Steady state equations=Dot*

The total harmonic current distortion remains constant from 0.65 to 0.785kA at 5.4%, the rate of increase of the 11th harmonic slows and the levels of 13th harmonic actually reduce. This trend is not mirrored by the PSCAD simulation as illustrated by Figure(3.8). Why not is unclear and a more thorough investigation is needed in this matter.

The Transient Converter Simulation programme [Arrillaga *et al.*, 1977] was also used to estimate the harmonics and a comparison with the measured data is shown in Figure(3.9) only for the harmonic currents. The PSCAD predicted trends appear to be more consistent with the measured data than those of the TCS programme.

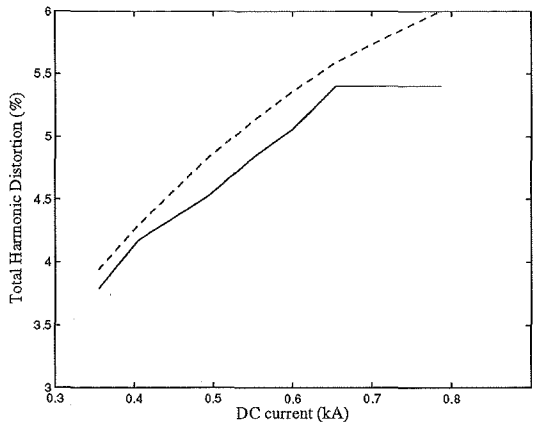


**Figure 3.8** Total Harmonic Distortion; *Recorded data=Solid, PSCAD=Dash–Dash*

### 3.1.7 Future Harmonic Tests

The application of CHART would greatly improve the efficiency of the harmonic data collection. It should also be possible to take a more comprehensive set of readings of the individual machine operating conditions such as field excitation, real and reac tive power, and temperature. It is hoped that readings at nearer full machine power of 90MW will be possible to extend the results already reported upon.

In the course of the experiments an extra operating point was gathered, i.e. 4 machines, 300 amps at 54Hz. This result is indicated by a cross on figures (3.5) and (3.6) and doesn't comply with the trends already described. It is therefore believed that frequency deviations of $\pm$ 5Hz operating frequency will have a measurable effect on the characteristic ac voltage and current characteristic harmonics. Hence, if allowable, it would be interesting to have the freedom to vary the frequency during the next trials. Furthermore achieving operating points at various firing angles should also be possible if the generator AVR controller can be manipulated.

The experimental procedures proposed above contain an element of risk however it is known from commissioning tests in the mid 1960s that the maximum power limit of each generator is 90MW under 12–pulse operation [O'Brien, 1993]. Moreover with the CHART system in place making continuous measurements, it will be immediately detectable if unacceptable levels of harmonic currents are flowing in the system.

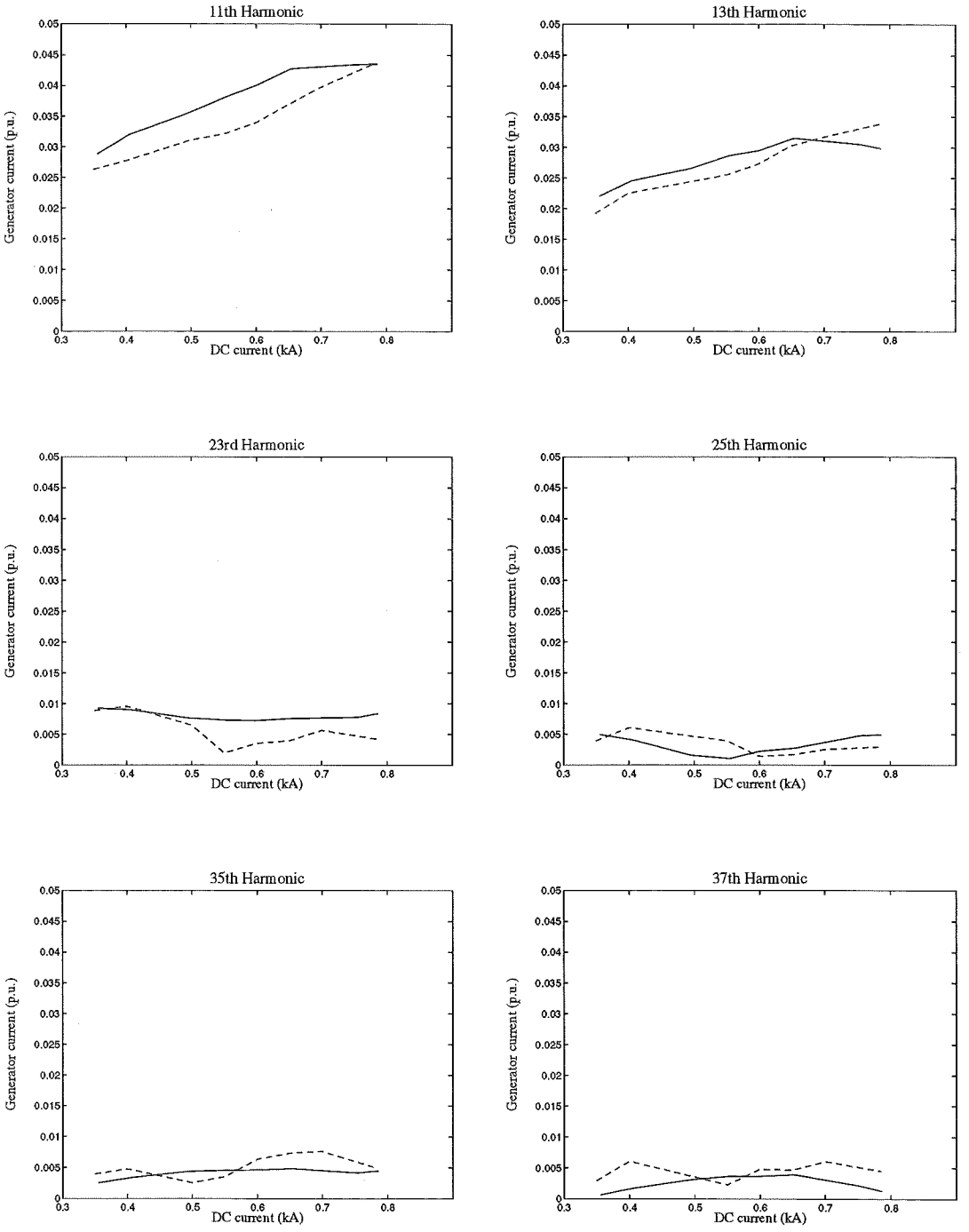


**Figure 3.9** Harmonic comparison of recorded generator current with dynamic simulation; *Recorded data=Solid, TCS=Dash–Dash*

## 3.2 Efficiency Considerations

As stated in section(2.2) the unit and group connections are two possible direct connection arrangements. As seen from the inverter there are no differences between the two schemes when all the generators are in service. However significant differences become apparent at reduced

power settings.

In order to avoid low generator turbine efficiency and severe cavitation problems for hydro machines, the number of generators in service must be reduced at low power levels. For the unit connection the dc line voltage is proportional to the number of units in service and hence at reduced dc powers the transmission voltage is lowered. The implications of this are twofold: firstly the transmission line losses are proportionally higher and secondly, current control reverts to the inverter increasing its reactive power demand. Conversely the group connection maintains a constant dc voltage irrespective of the number of machines in service.

It has been shown that for reducing active power levels, operation with fewer machines demands increasing reactive power provision at the inverter end [Arrillaga *et al.*, 1993c], a condition unlikely to be acceptable. The derivation of respective transmission efficiency formulae, comprising turbine and line efficiencies, are however given here.

### 3.2.1 Turbine Efficiency

Assuming fixed frequency operation (i.e. 50Hz) and constant water head level, the turbine efficiency, $\eta_t$, will be dependent on the power loading. The performance characteristics of a 90 MW turbine in [Jaquet, 1986] were used at a selected water head of 86 metres. Thus the turbine efficiency $\eta_t$ for a power range 45 to 90 MW (Figure(3.10)) could be approximated by a 3rd order polynomial

$$\eta_t = -0.6735p^3 + 1.1620p^2 - 0.4151p + 0.9220 \tag{3.11}$$

with $\eta_t$ being the turbine efficiency and $p$ is the turbine power in per unit on a 90MW base.

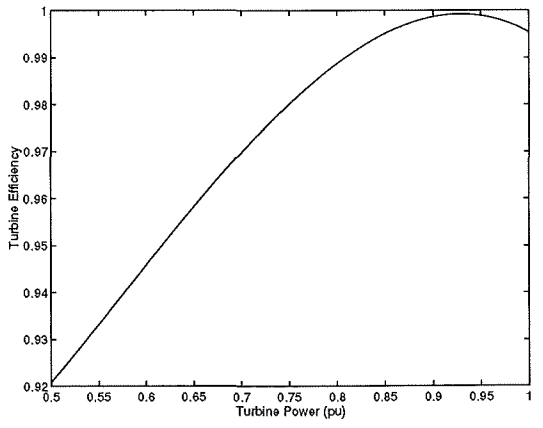


**Figure 3.10** Turbine characteristic

### 3.2.2 Line Efficiency

For a given nominal dc power, the line voltage is the critical factor affecting line efficiency. By comparison the generator, transformer and converter plant efficiencies are high and practically constant. Thus for the purpose of this comparison the efficiency of an HVdc transmission line can be expressed as

$$\eta_l = \frac{V_i}{V_r} = 1 - \frac{\Delta V_l}{V_r} \tag{3.12}$$

where $V_i$ and $V_r$ are the inverter and rectifier voltages respectively and $\Delta V_l$ is the voltage drop along the line.

$\Delta V_l$ is approximately

$$\Delta V_l = R_l.I_{dc} \tag{3.13}$$

where $R_l$ is the resistance of the line and $I_{dc}$ is the dc current in kA.

For the conventional unit connection the rectifier end voltage is proportional to the number of generating units.

$$V_r = nV_n \tag{3.14}$$

where $n$ is the number of units and $V_n$ is the nominal voltage of each unit. Combining equations (3.12),(3.13) and (3.14) yields the unit connection line efficiency

$$\eta_l^u = 1 - \frac{R_l \times I_{dc}}{nV_n} \tag{3.15}$$

In the group arrangement the rectifier voltage $V_r$ is maintained at the nominal line voltage, and hence the group line efficiency can be expressed as

$$\eta_l^g = 1 - \frac{R_l \times \frac{P}{V_r}}{V_r} \tag{3.16}$$

where P is the power setting.

For conventional unit and group configurations the appropriate line efficiency formula was combined with the turbine efficiency to give the respective Transmission efficiency characteristics.

### 3.2.3 Unit and group connection efficiencies

A 6 machine test system based on the Benmore terminal data in Appendix A is compared to an equivalent 6 machine unit connection for which the nominal voltage of each unit, $V_n$, was 45kV.

The transmission efficiencies versus power with one to six machines in service are shown in Figure(3.11). With fewer units in service, the line efficiency reduction in the case of the unit connection predominates. The opposite effect occurs with the group connection, where the nominal dc voltage can be maintained with lower powers and machine numbers. Hence the group connection provides higher overall operating efficiencies with reducing active powers.

Regarding unit connection performance, the crossings between the efficiency curves in Figure(3.11) (i.e. points A and B) indicate the power boundaries for the number of units to be used at maximum efficiency. Even then the efficiencies are considerably lower than for the group connection.

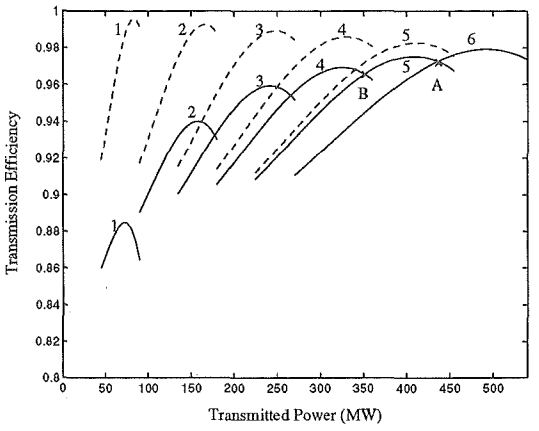


**Figure 3.11** Transmission efficiencies for unit (solid line) and group (dotted line) connections

## 3.3 Conclusions

Before a direct connection scheme will be constructed, manufacturers and utilities will have to be convinced that the scheme is viable. One major concern has been that the characteristic converter harmonics would cause severe detriment to the generators. Many contributions have pursued methods of calculating the operating conditions of directly connected systems yet a psychological barrier has remained for lack of hard physical evidence.

The Benmore terminal of the New Zealand HVdc system regularly operates as a group connected scheme, and has done on and off since commissioning over 25 years ago. To address the lack of concrete information, the first direct connection harmonic measurements have been presented. The experience gained will be used for future measurement opportunities as they arise. In all cases the generator harmonic current levels were well below specified maximum ratings. Moreover extension of the conservative dynamic simulations to rated powers yielded harmonic current levels below these specified maximums as well.

PSCAD dynamic simulation studies show good agreement as far as determining current harmonics is concerned, although future tests may reveal that conservative estimates are provided at rated powers due to simplified nature of the models used. Conservative estimates of the voltage harmonics were provided and this reflects the uncertainty of the subtransient machine parameters. A steady state formulation gave optimistic estimates of the harmonic current levels.

Operating characteristics for two direct connection schemes (the unit and group) were investigated. The group connection can maintain a constant dc voltage at reduced dc power levels which keeps the transmission efficiency high and the inverter reactive power consumption low. The unit connection on the other hand, assuming the need for efficient generation, has a reduced dc voltage when units are removed from service which, while maintaining a high turbine efficiency, significantly reduces the line efficiency and progressively increases the inverter reactive power consumption.

# Chapter 4
# THE SERIES EXCITATION

The direct connection is like a dc machine except turned inside out. The motivation for this new proposal comes from the traditional series field dc machine. By performing the commutations statically, incorporating a transformer between the rotating machine and the commutating switches, and feeding the exciter in series with the rectifier output, it is possible to create what could be referred to as a high voltage series field dc generator.

## 4.1 The Series Excitation Concept

The conventional direct connection affords a considerable reduction in the number of components at an HVdc rectifier station. The series excitation proposes to simplify and reduce the cost of the station even further by finding an alternative machine excitation source. The proposed configuration for the series excited unit connected generator converter group is illustrated in Figure(4.1). The generator rotor windings, connected in series on the ground side of the converter, take the place of the smoothing reactor. In the absence of the conventional excitation the operation of the series excitation is controlled by the converter.

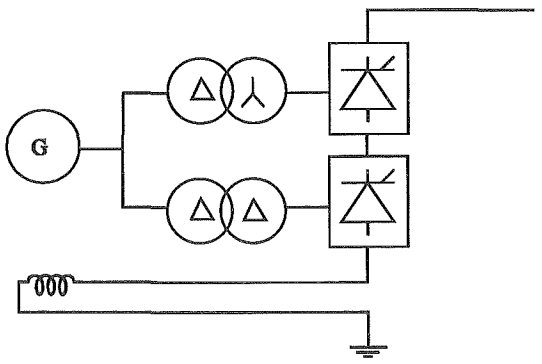


**Figure 4.1** The series excitation principle

### 4.1.1 Energisation and Blocking

For the rectifiers to start delivering power to the link, the generators require exciting current. If the dc link is already supplying power via other connected generator–converter units the incoming set will immediately receive excitation current. In the absence of any other operating units the dc link will be energised by the receiving end converters, which will temporarily operate in the rectification mode via normal constant current control action.

Converter blocking, in the series connected alternative, presents no special problem with respect to the separate excitation alternative, both cases requiring a bypass path if a group is to be disconnected. In the series excitation case a three set of quick isolators per unit will be required to permit the connection and disconnection of individual excitation units without interrupting the main dc line current. The first isolator, to connect a resistor in parallel with the exciter winding, the second to by pass the winding and the third to remove it from service altogether. The isolators and resistor constitute the only additional requirement of the generator. The field winding current will be considerably smoother than in the conventional static exciter and this should reduce the harmonic rating of the rotor.

### 4.1.2 Steady State Formulation

To investigate the steady state behaviour of the series excitation a modified version of the steady state simulation of Chapter(3) is used. For the series excited machine driven at a constant speed, the generator EMF is proportional to the dc current, i.e.

$$E = k_f.I_{dc} \tag{4.1}$$

With reference to the phasor diagram of Figure(4.2) the commutating voltage (i.e. $E''$), assuming a symmetrical rotor, is implicitly specified by the equation

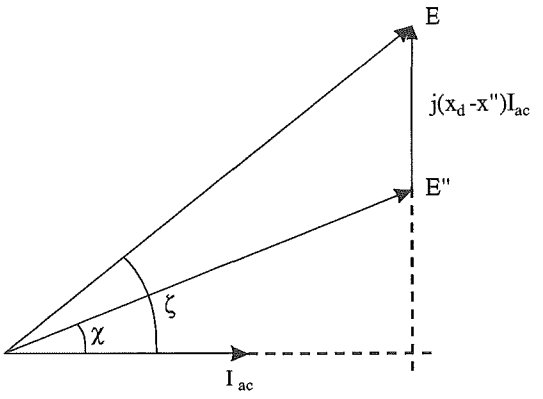


**Figure 4.2** Nonsalient machine representation

$$E^2 = [E''.cos(\chi)]^2 + [E''.sin(\chi) + I_{ac}(X_d - x'')]^2 \tag{4.2}$$

where $X_d$ is the direct axis reactance of the machine. The equations that represent a line commutated 6–pulse HVdc converter are

$$I_{ac} = \frac{2\sqrt{6}}{\pi} I_{dc} \tag{4.3}$$

$$cos\chi = \frac{1}{2}[cos\alpha + cos(\alpha + \mu)] \tag{4.4}$$

$$I_{dc} = \frac{\sqrt{3}E''}{\sqrt{2}x_c}[cos\alpha - cos(\alpha + \mu)] \tag{4.5}$$

and all other variables have been previously defined.

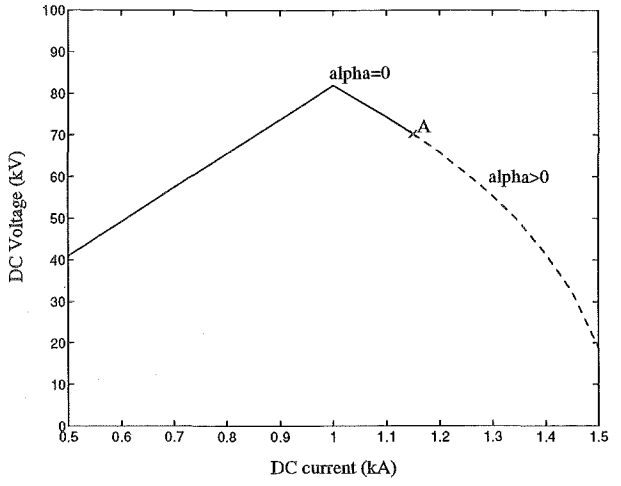


**Figure 4.3** Limitation of applicability of Steady State formulation

Equations (4.1) to (4.5) together with control specifications can be used in an iterative solution to derive the seven variables identified in the formulation, i.e. $I_{dc}, E, E'', I_{ac}, \alpha, \mu, \chi$. In the following studies $I_{dc}$, $\alpha$ and $x_c$ are the known quantities and the iteration solution determines $E''$, $\mu$ and $\chi$. Finally the dc voltage can be determined from equation(4.6) below.

$$V_{dc} = \frac{6\sqrt{2}}{\pi}\sqrt{3}E''cos\alpha - \frac{6x_c}{\pi}I_{dc} \tag{4.6}$$

The limitations stipulated in Chapter(3) equally apply to this formulation, i.e. the machine is nonsalient, the dc current is perfectly smooth and for the 12–pulse converter $\mu$ is restricted to less than 30 degrees.

In practice the machine field windings will saturate at higher current levels and thus it is appropriate to specify E as a piecewise linear function. Hence equation(4.1) is clarified as

$$\begin{aligned} E &= k_f I_{dc} && I_{dc} < I_{sat} \\ E &= k_f I_{sat} + k_f^s(I_{dc} - I_{sat}) && I_{dc} \geq I_{sat} \end{aligned}$$

where $I_{sat}$ is the knee point of the saturation curve and $k_f^s$ is excitation slope in the saturation region.

To illustrate the formulation's limitation of applicability, Figure(4.3) shows (with the dotted line) how past point A requires increasingly larger $\alpha$ for increased dc current such that the solution of equations(4.1) to (4.6) does not violate the condition on $\mu$. At extended power settings and currents with regions of commutation overlap, dynamic simulation is used.

### 4.1.3 Basic Characteristics

Figure(4.4) shows the derivation of the nominal operating point A for three rectifier alternatives, i.e. the conventional configuration (i), a separately excited unit connection (ii), and the proposed series excited unit connection (iii). All of them share the same constant current control characteristic

(iv) and inverter characteristics depicted with a broken line. Curve (i) can be seen as a special case of equation (4.6) where $E''$ is replaced by the converter terminal voltage. Curve (ii) directly represents equation (4.6) and curve (iii) results from the iterative solution.

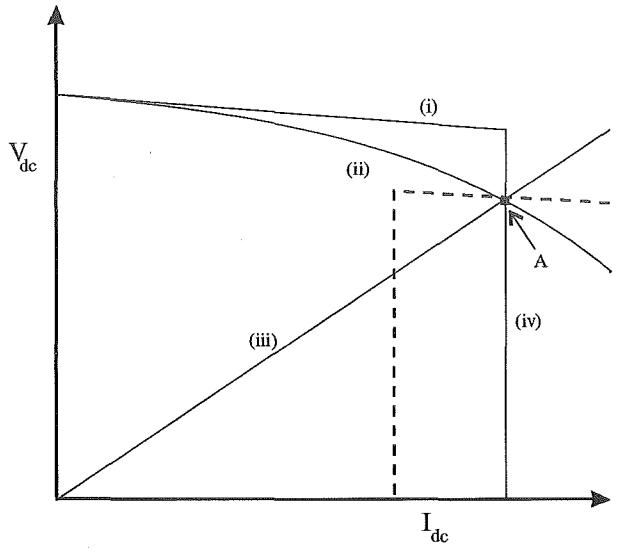


**Figure 4.4** Operating point derived from conventional and unit connected schemes

In Figure(4.5) the conventional characteristics have been left out to simplify the description of the series connection. If the inverter voltage increases the rectifier reduces its firing angle until it reaches the $\alpha_{min}$ limit (point B in Figure(4.5)). If the inverter voltage increases beyond $V_{i2}$ the direct current reduces and at point C the current control is transferred to the inverter (i.e. current setting $I_i^s$).

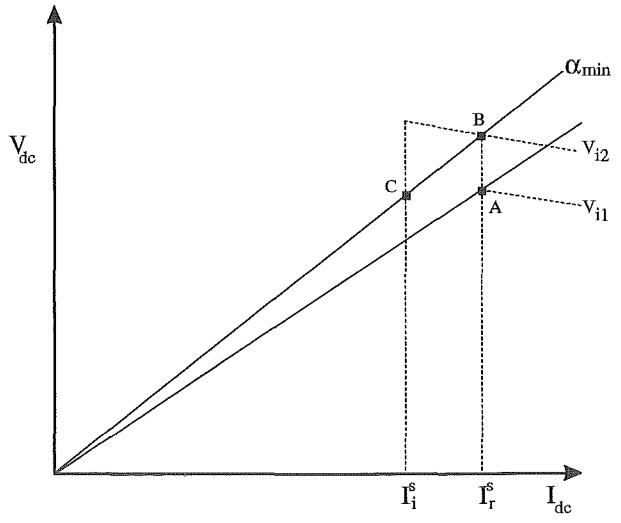


**Figure 4.5** Steady state characteristics of series unit connection

The series unit connection is seen to have a very large positive voltage regulation as compared with the relatively small negative slope of the conventional scheme. This effect should simplify the changeover of current control from the inverter to the rectifier as there is no alternative crossing in

the transition region (a problem earlier encountered in conventional schemes with weak systems at the receiving ends). Inverter voltage reductions will reverse the sequence, i.e. going from operating point C to B to A. Similar reasoning for the case of constant power control leads to the characteristics of Figure(4.6). For a specified power $P_r^s$ the operating point A is under rectifier constant power control. Inverter voltage increases will take the operating point to B, beyond which point the rectifier loses controllability. The current then drops along the $\alpha_{min}$ characteristic until the power margin setting is reached (at point C) and will remain there under inverter constant power control $P_i^s$.

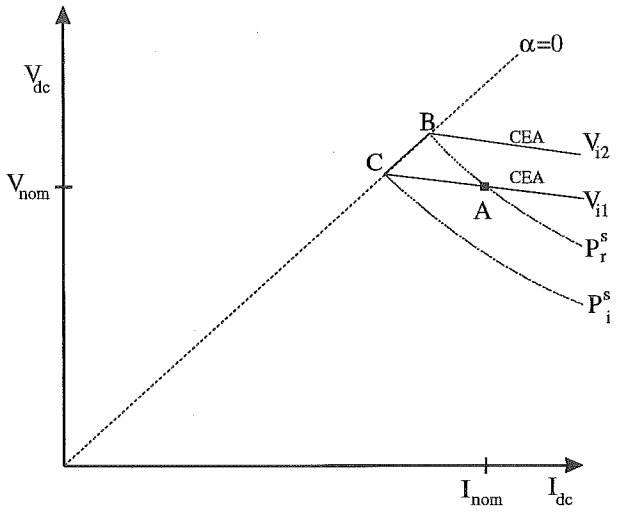


**Figure 4.6** Operating point derived from constant power and constant extinction angle characteristics

## 4.2 Comparisons between Unit and Series Connections

A typical 90 MW generator is used for the comparison between the conventional and series excited unit connection schemes. Details of the generator, transformers and converter are given in Appendix B. In the comparisons that follow, the characteristics in the regions where the commutation overlap exceeds 30 degrees have been derived using time domain simulation.

### 4.2.1 Operating Range

Optimum transmission efficiency is achieved when the direct voltage can be kept constant for the complete range of specified power levels. Series excitation can not maintain the nominal voltage at low powers because the machine EMF reduces with the line current. This effect is illustrated in Figure(4.7) where a nominal operating point (A) is selected which for the separate excitation case provides 55kV and 1kA at a firing angle of 20 degrees. Using series excitation, point D (at $\alpha = 0$) marks the lower current limit (670A) of operation at full efficiency.

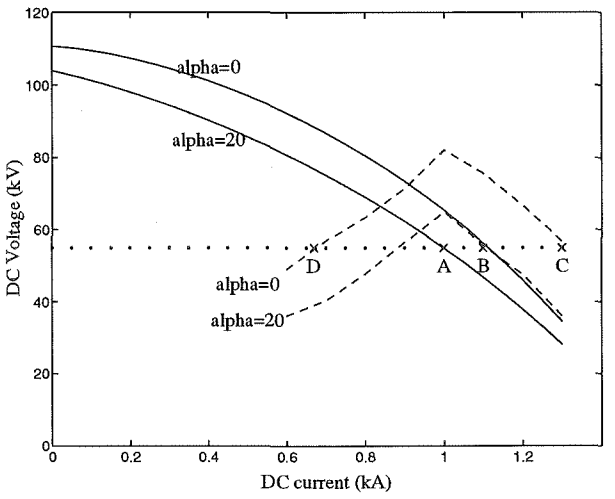


**Figure 4.7** Operating ranges of conventional (solid lines) and series (dotted lines) excitations

In theory the separately excited scheme can maintain full voltage down to zero current but in practice power transmission at such power levels is unlikely to use all the generators and therefore the separately excited unit scheme will also operate at lower than optimal transmission efficiencies.

Extending the power range beyond the nominal operation point presents no problem to the series connection because the excitation increases proportionally with the load subject to the machine field winding saturation characteristic. There is, however a limit (point C) beyond which the commutation voltage drop increases faster than the current and the output power decreases. This limit occurs at 1.3kA (or 75MW) in the test system. Under constant excitation the separately excited scheme meets the minimum alpha characteristic at point B, which corresponds with 61MW. The separately excited scheme could also be made to operate at point C by providing extra excitation however, apart from the extra rating of the static exciter, such extended range would require the excitation rectifiers to operate at very large firing angles most of the time.

### 4.2.2 Temporary Overload Capability

Compared with conventional generation/HVdc transmission schemes the unit connection alternative has very limited power overload capability owing to a larger commutation reactance which reduces the rectified voltage at higher currents. To improve the transient stability margins at the inverter end it is important to provide some temporary conversion capability at the rectifier following fault clearance. However, to be effective, the implementation of the current setting must be fast acting (i.e. rather by firing angle than excitation control). Assume to illustrate the effect, that no excitation change takes place immediately after fault clearance, the $\alpha = 0$ characteristics in Figure(4.8) give an indication of the relative maximum temporary capabilities of the conventional and series alternatives.

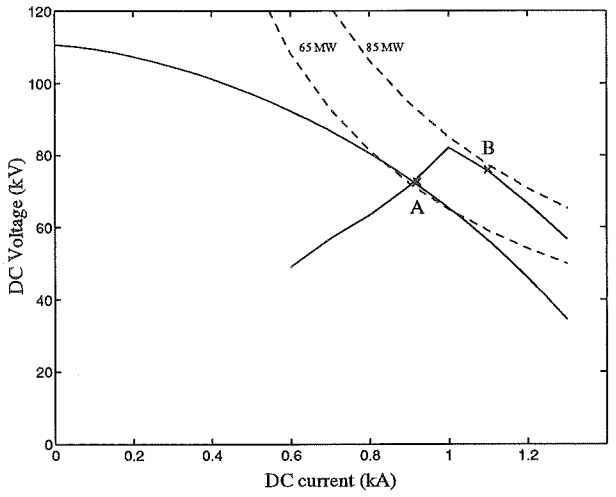


**Figure 4.8** Overload Capability of Conventional and Series excitations

In each case the power curve tangent to the maximum voltage characteristic determines the unrestricted power conversion capability. These are 66MW (point A) and 83MW (point B) for the conventional and series configurations respectively, or an increase of 25 percent in favour of the last mentioned. This increase will be lower in practice if fast acting field forcing is used with the separate excitation.

## 4.3 Series–Group Connection

A large power station will have a number of generating machines; for a multiple machine system two possible arrangements of the generators are shown in Figure(4.9). Because the characteristics previously derived are equally applicable, it is not possible to maintain the nominal voltage at low power levels.

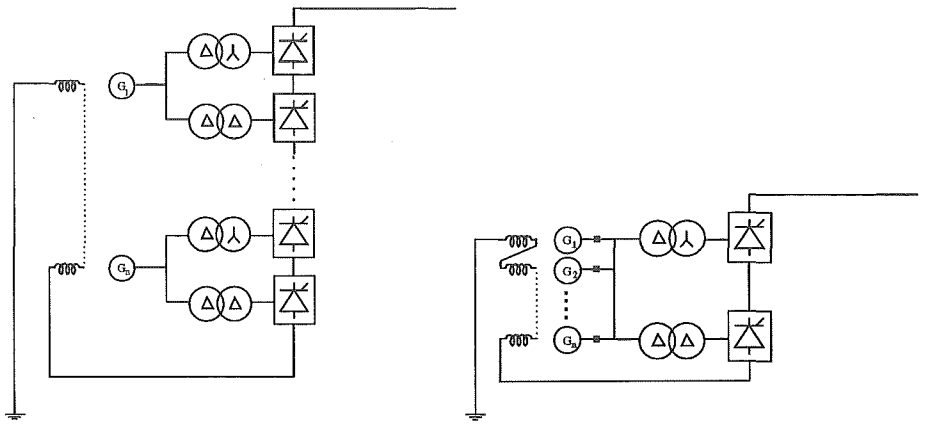

(a) series–unit (b) series–group

**Figure 4.9** Multi machine series excitation systems

This is illustrated in Figure(4.10), where the nominal operating point (A) is obtained with the rectifier on constant power ($P_{ds}$) and the inverter on constant extinction angle (CEA) control. However, when the range of rectifier firing angle control has been used, the output voltage will reduce linearly following the minimum $\alpha$ characteristic.

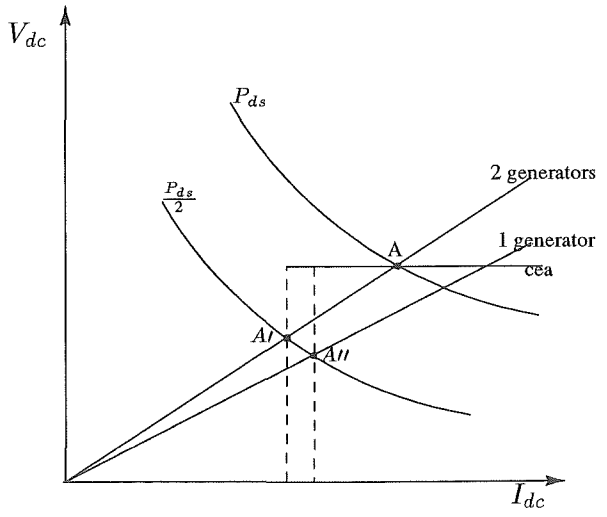


**Figure 4.10** Operating Points derived from constant power and constant extinction angle characteristics

If a lower power setting (say $\frac{P_{ds}}{2}$) is used, the new operating point is $A'$, with the inverter in control of the power. In order to maintain high turbine efficiency at lower powers the number of generators in service should be reduced. However this alternative is impractical with the unit

connected alternative, because the voltage reduces in proportion to the number of generators. When applied to the group connection, the use of fewer generators increases slightly the commutation reactance. As a result, the dc voltage is further lowered by a slightly increased commutation voltage reduction, Hence the operating point moves from $A'$ to $A''$ to deliver the desired power level. At point $A''$ the dc current is higher and the resistive line losses are also proportionally higher. This effect partly offsets the benefit of a higher turbine efficiency. Apart from lower transmission efficiencies, operating at points $A'$ or $A''$ transfers the power control to the inverter and thus increases its reactive power requirements.

### 4.3.1 Dual Excitation Arrangement

Normally the nominal dc currents used in HVdc schemes will exceed the generator excitation requirement. This suggests the alternative connection illustrated in Figure(4.11) for a four machine group connected scheme. It is a two stage arrangement which permits halving the number of machines without reducing the common bus voltage.

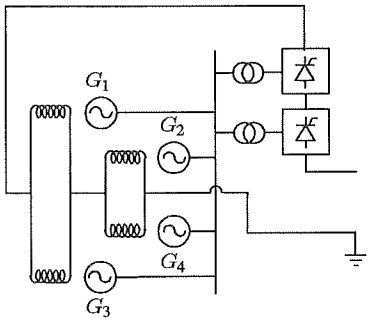


**Figure 4.11** Alternative field winding connection

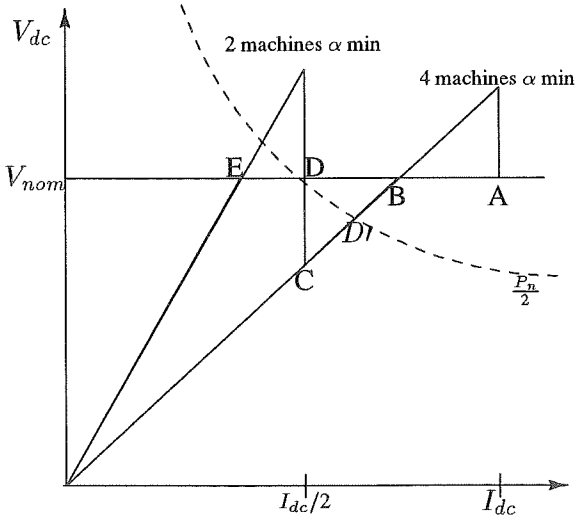


**Figure 4.12** Maximum Voltage Characteristics derived from the steady state formulation

The resulting steady state characteristic, illustrated in Figure(4.12), shows an obvious im-

provement over the previous configuration. Below point B, which determines the limit of rectifier constant current control, the dc voltage begins to fall down the path of the minimum $\alpha$ characteristic. At point C, when the dc current reduces to half the nominal rating, two generators are disconnected (e.g. $G_3$ and $G_4$, or $G_1$ and $G_2$) such that each remaining rotor receives the full dc current.

However there is no need to continue down the linear characteristic below $D'$ because the same power setting (shown in the dotted line) can be obtained more efficiently by halving the number of machines at that point, i.e. transfering the operation to point D. The new configuration (at point D) returns the power control to the rectifier end, which will initially operate at a large firing angle; further power reductions will use the available firing angle and at point E power control will again transfer to the inverter end. From this point the voltage output will again reduce linearly with the dc current.

### 4.3.2 Case study

To understand the operational implications of the new excitation arrangement a six machine system with 2 sets of three paralleled field windings in series is investigated and compared with a conventional separately excited unit connection system. The test system is rated at $2kA$ and $270kV$ dc comprising six of the same $90MW$ machines already used. The line resistance $R_l$ is 5.93 Ohms. It is assumed that the field windings are configured such that 660 amps (i.e. $\frac{1}{3}$ of the dc line current) provides the nominal excitation of each machine and that they are linear in the 0 to 660 amp region as shown by curve (i) in Figure(4.13). The system transmission efficiency and the inverter reactive power consumption are to be specifically considered.

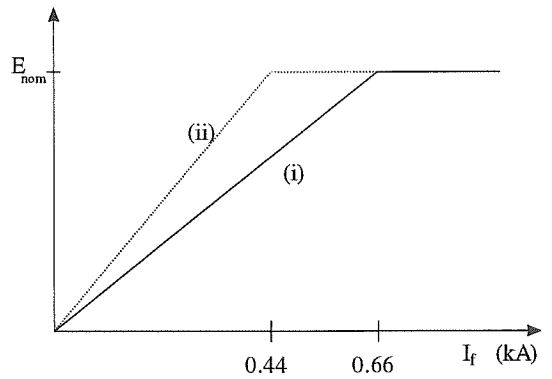


**Figure 4.13** Machine field excitation characteristics

Figure(4.14) shows the voltage profile for the six machine system derived with the steady state formulation of section(4.1.2). A similar mode of operation, as described in the section(4.3.1), is employed so that the voltage for a given power is maximum. From now on the nominal voltage will be considered to be the rated voltage and the characteristics are for the minimum alpha characteristic $\alpha = 0$.

#### 4.3.2.1 Efficiency Curves

The efficiency curves for new system based on the formulae in section(3.2) are compared in Figure(4.15) with a conventional 6 machine unit connection system. The dotted lines correspond

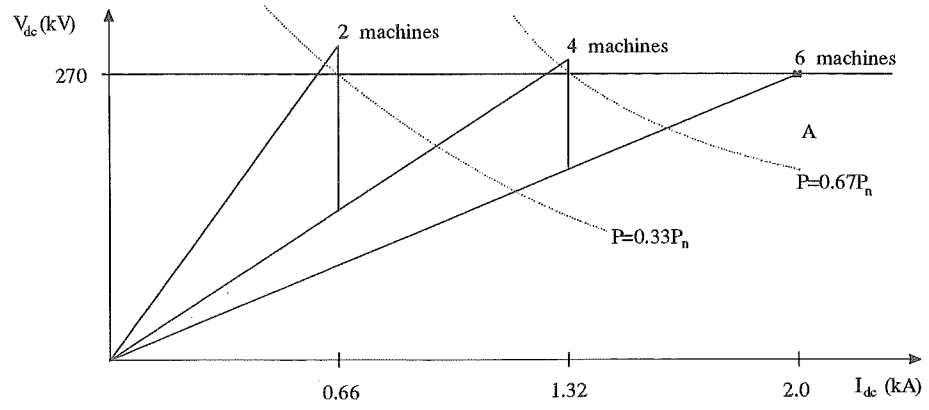


**Figure 4.14** series–group with excitation characteristic (i)

to 2,4 and 6 machines of the series–group excitation whilst the solid lines refer to 2 to 6 machines in the conventional unit connection.

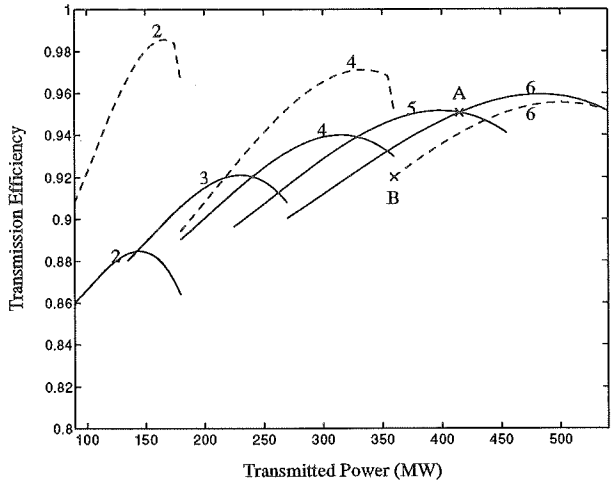


**Figure 4.15** Efficiency comparison between conventional and series–group excitations

In the case of the conventional unit connection the appropriate number of generators in service can be selected for a given power such that the efficiency can be maximised, i.e. at point A, for reducing dc power, it becomes more efficient to deliver power with 5 machines instead of 6.

The series–group can operate with an odd number of machines provided the non generating field winding is keep in the circuit to ensure the machine excitations remain balanced. It turns out however, that while from a turbine efficiency point of view it would be desirable to have the 3 and 5 machine option, the removal of the 4th and 6th machines respectively significantly increases the commutation reactance which reduces the dc voltage such that the transmission efficiency is lowered. Therefore from an efficiency point of view it seems unfeasible to operate with 3 or 5 machines.

Overall the series–group system is not as flexible for two reasons. A multiple number of two

machines must be in service and is to a large extent governed by the delivered power. Hence, for reducing dc power, only at point B can two machines be disconnected. This restriction could pose a severe limitation should one machine suffer an outage condition as, in all likelihood, its corresponding paired machine needs also to be removed and the link capability is considerably reduced.

#### 4.3.2.2 Inverter Reactive Power Consumption

While the transmission efficiency is an important consideration, the implications for the receiving inverter system must also be taken into account. Assuming $\gamma = 20$ degrees at the nominal rated operating point then an approximate expression for the inverter reactive power consumption $(MVAR_i)$

$$MVAR_i = 275.I_{dc}.sin(cos^{-1}(\frac{V_i}{275})) \tag{4.7}$$

can be derived as a function of the inverter voltage and the dc current for this particular system.

Assuming that the overall efficiency is to be maximised, the required reactive power compensation at the inverter is computed for a power range of 90 to 540MW.

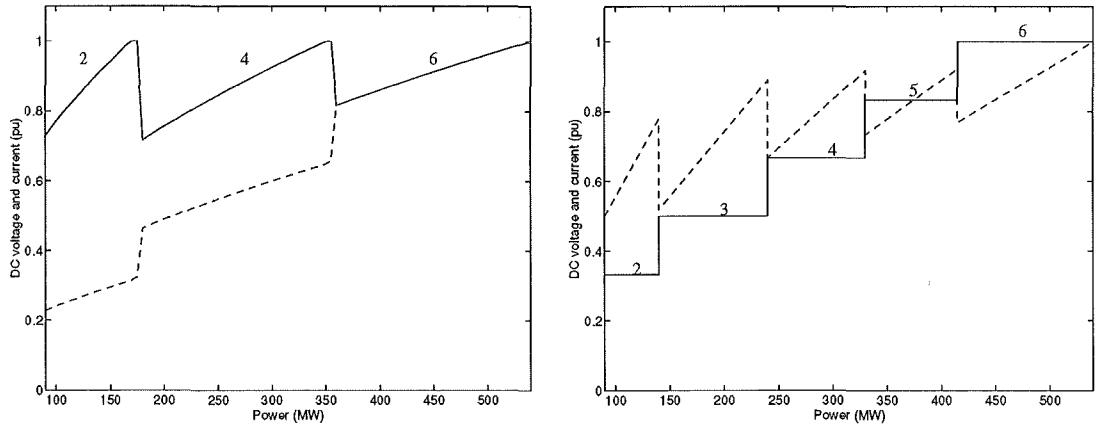


(a) series–group (b) conventional unit

**Figure 4.16** DC voltage and current profiles in pu for maximum efficiency; *dc voltage=solid line, dc current=dotted line*

Figure(4.16)a shows how the series–group arrangement has declining dc voltage and current trends with reduced power settings and this by and large reduces reactive power consumption at the inverter. The unit connection maintains a high dc voltage at high power which makes the reactive power consumption lower in the high power region (Figure(4.16)b). At reduced powers the line voltage falls yet the dc current levels remain high which increases the peak reactive consumption.

Figure(4.17) shows how the unit connection has a larger peak reactive power requirement $(436MVAR)$ than the series–group arrangement $(288MVAR)$. This is partially offset with higher transmission efficiency in the higher power range. From this study it is clear that the efficiency is dominated by the turbine characteristic while the reactive power consumption is strongly dependent on the dc voltage. Therefore for the series–group configuration it seems

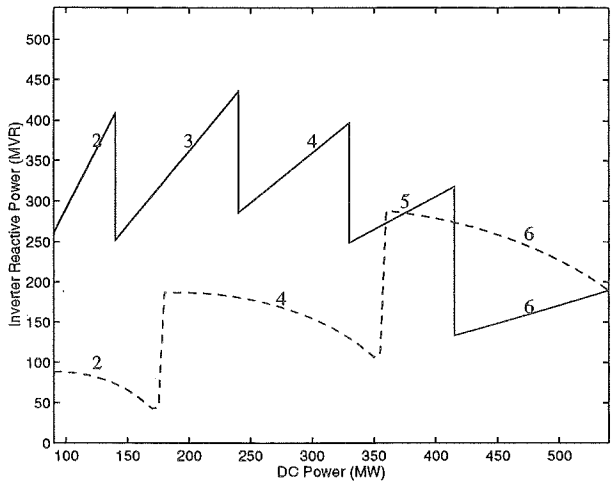


**Figure 4.17** Comparison between conventional (solid line) and series–group (dotted line)

unlikely that the efficiency will be improved unless it is possible to generate with any desired number of machines, i.e. anything from 2 to 6.

#### 4.3.2.3 Systems with larger numbers of machines

In theory it should be possible to extend the idea to systems with even larger numbers of machines. For a given nominal machine MVA rating however, as the number of paralleled field windings is increased a corresponding increase in the number of field turns on each rotor will be necessary to provide the same nominal excitation. This will increase the size and cost of the machine rotors. The efficiency, while improved, will be sub–optimal because two machines must still be removed from service at one time.

### 4.3.3 Redesigning the rotor circuit to sustain the dc voltage

Curve (i) of Figure(4.18) represents the voltage profile at the minimum alpha characteristic at a nominal operating point A. By increasing the number of field turns, an operation point C is achieved and rectifier firing control can pare back the dc voltage to the nominal level. Hence while the nominal voltage can now be maintained from point A to B, a higher nominal firing angle, the limitations of greater rectifier valve costs and reactive power consumption at the rectifier must be accepted.

#### 4.3.3.1 Modified Saturation Characteristic

Alternatively the field windings are designed so that the nominal excitation is provided before the nominal power of the machine is reached, after which saturation occurs so that the machines do not become over excited. As an example consider the field circuit characteristic of curve(ii) in Figure(4.13) where the nominal excitation is reached at a dc current of 0.44kA (but the windings are still rated to carry 0.66kA).

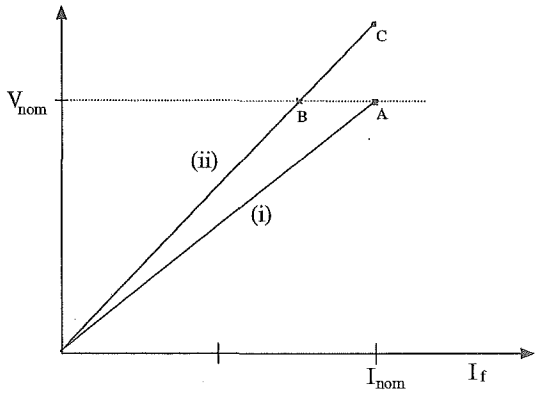


**Figure 4.18** Effect of increased rotor turns

#### 4.3.3.2 Improved Voltage characteristic

The new dc voltage current characteristic (solid line) is laid over the previous characteristic, of Figure(4.14), (dotted line) for comparison in Figure(4.19). Firstly it can be seen that an almost completely constant dc voltage can be maintained at all power levels and secondly that anything from 2 to 6 machines can operate normally. The ability to operate with an odd number of machines, as opposed to section(4.3.2.1) where 3 and 5 machine operation was not possible, is a direct benefit of maintaining a higher level of machine excitation so illustrated in Figure(4.13).

Rectifier firing angle control, or constant current control, is necessary however to keep the dc voltage at the desired value. The maximum value required for this particular system was 26 degrees and this will increase the costs of the valves. Operating at a large rectifier firing angle could in some cases increase the overall MVA rating of the generators. This is not the case here because large firing angle operation occurs at reduced link power settings ensuring the total generator MVA remains below the nominal rating.

#### 4.3.3.3 Efficiency and Reactive Power Characteristics

By being able to maintain the dc voltage and operate with the optimal number of machines, the series–group with the modified field characteristic has a far superior efficiency and inverter reactive power consumption characteristics as illustrated in Figures(4.20) and (4.21). Operation at high values of $\alpha$ will keep the levels of current harmonics (and therefore the system losses) at a high level however. In fact the characteristics are almost identical to a separately excited group connection scheme with the same number of machines.

#### 4.3.3.4 Rotor design Implications

As the nominal field current is reduced, the number of field turns has to be increased to provide the same excitation. In all probability the amount of steel at the same time in the rotor also has to reduce to ensure that the rotor saturates and these requirements may pose difficulties i.e. larger field windings coupled with less mechanical strength. The field windings while saturating at a lower nominal value still need to carry large currents.

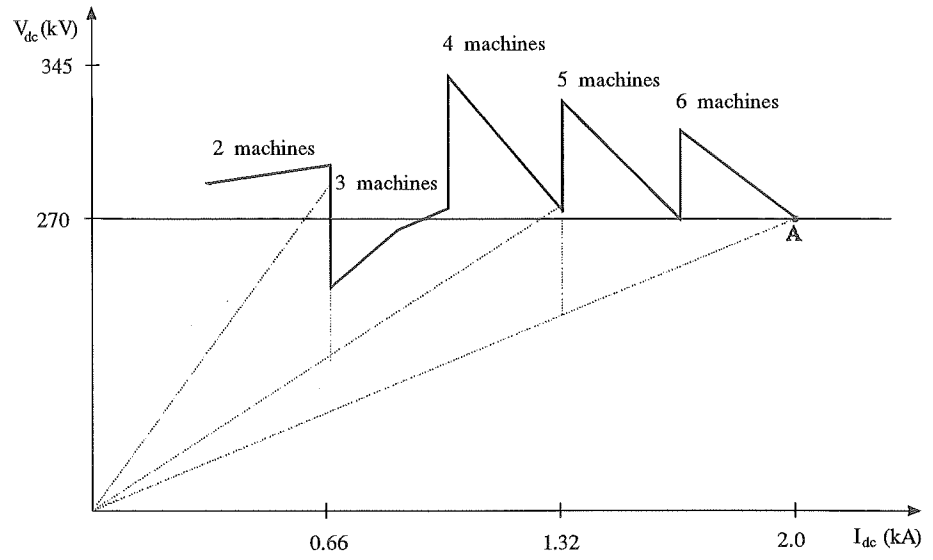


**Figure 4.19** Voltage profile with redesigned field characteristic

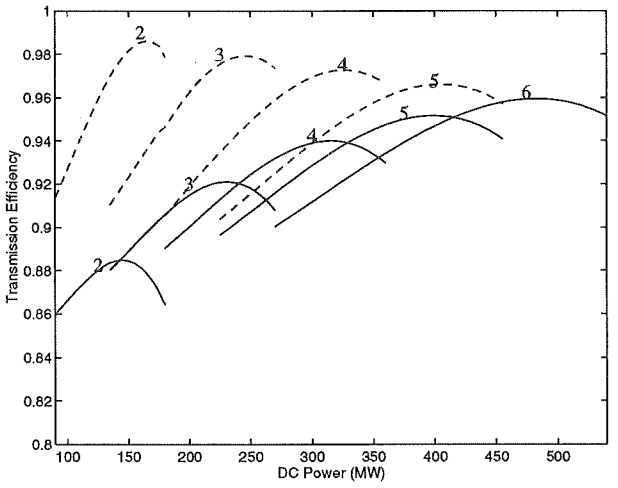


**Figure 4.20** Efficiency comparison between conventional (solid line) and series–group (dotted line)

## 4.4 Conclusions

In line with the main direct connection purpose, the new series excitation scheme permits further simplification of the converter, generator plant and considerable cost savings. It eliminates entirely the need for machine excitation and control systems.

A steady state formulation has been developed which combines generator phasor diagrams with converter equations in an iterative model, which has been validated and complemented by dynamic simulation. Using a conventional 90MW generator as a reference the theoretical models have predicted that series excitation extends the region of fast temporary power conversion capability, which should help to maintain transient stability at the inverter end.

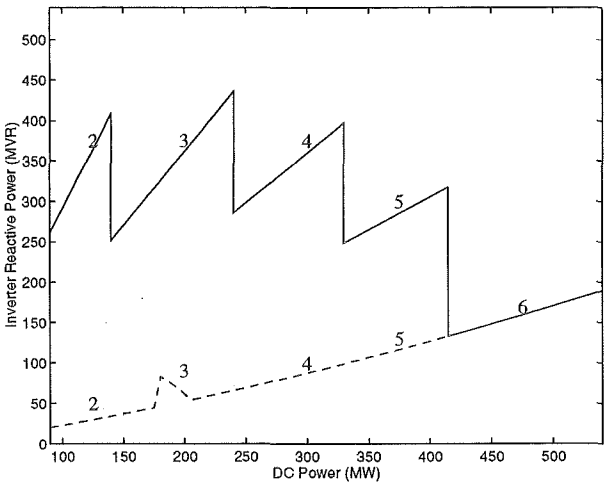


**Figure 4.21** Comparison between conventional (solid line) and series–group (dotted line)

The simulation predicts that the series excitation is less efficient at low power. By using a modified field connection arrangement it has been shown that the voltage may be boosted at low powers. The transmission efficiency and operational aspects of the series–group connection have been investigated and compared to the conventional unit connection. The series–group has superior transmission efficiency in the low to mid power range and a significantly lower peak inverter reactive power requirement. Operation is however restricted to an even number of generators to prevent dc voltage reduction and reduced transmission efficiency. Because of the need for equal machine field current sharing, a generator outage will necessitate the removal from service of a second generator. This reduces the link capability and constitutes a major disadvantage of the series–group arrangement.

In conjunction with the new field winding arrangement, the field saturation characteristic was modified such that the windings saturated before the nominal power of the machine was reached. This meant that the dc voltage could be maintained at an almost constant level with rectifier current control. Moreover operation with any desired number of machines is possible. The necessary redesign of the field circuits would increase the cost of the rotor and converter valves, however this may well be justified in light of the tremendously improved transmission efficiency and significantly reduced inverter reactive power demand. In theory there should be no limit to the number of machines in the series–group system, the only requirement is that the shared dc current provide the nominal excitation of each machine.

# Chapter 5

# THE DYNAMIC PERFORMANCE OF THE SERIES EXCITATION

When referring to the dynamic or transient response of direct connection schemes there is potential for confusion. During the steady state operation, the generator is driven from one subtransient state to the next by the periodic switching of the converter. Therefore in this chapter the dynamic response or performance refers to the behaviour of the system under abnormal operating conditions (i.e. faults), rather than the succession of commutating transients.

## 5.1 Synchronous Machine Theory

The previous chapter detailed the steady state operational capabilities of series excited systems. The goal of this chapter is to outline a cornerstone of synchronous machine theory which is then applied to evaluate the dynamic responses of the series excitation. Perhaps the best all round text is that of [Adkins and Harley, 1975] although a number of other excellent books can also be consulted [Kimbark, 1968].

### 5.1.1 Salient and Nonsalient Machines

There are two broad classes of synchronous machine; salient and non salient. The phenomena of saliency is caused by the physical construction of the machine and refers to the different magnetic properties of the rotor (or stator) on two different axes of symmetry. These two axes are usually referred to as the direct (D) and quadrature (Q) axes. For purposes of the rest of the discussions it is assumed the rotor is the salient member of the system, typical rotor constructions are shown in Figure(5.1) [1].

In any synchronous machine whether salient or non–salient the distribution of flux will be complicated. For practical purposes the most critical region for determining the flux is in the machine air gap. Consider a synchronous motor being driven by sinusoidal terminal waveforms and drawing sinusoidal currents. Balanced three phase currents in balanced three phase windings set up a constant magneto motive force (MMF) wave that rotates around the air gap at synchronous speed. The magnetic flux in the air gap will depend on the reluctance of the magnetic circuit($\Re$), or the radial permeability of the air gap, and the counter MMF of the field circuit i.e.

$$\phi_{gap} = \frac{MMF_{stator} - MMF_{rotor}}{\Re} \tag{5.1}$$

[1] extracted from [Kimbark, 1968]

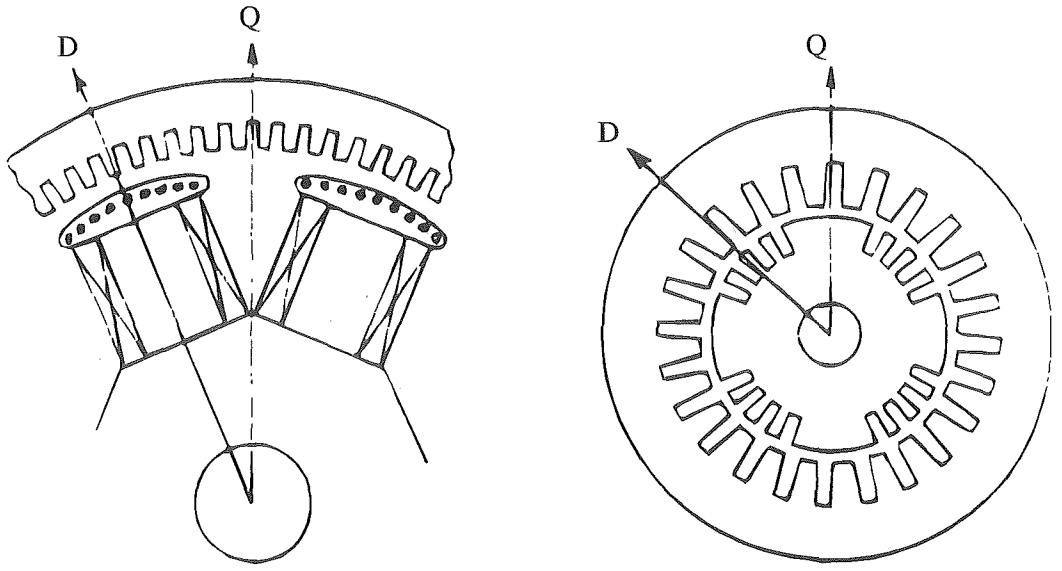


(a) Salient (b) Non Salient

**Figure 5.1** Typical Rotor Constructions

For a perfectly non–salient machine the MMFs will be sinusoidal vectors and the reluctance $\Re$ will be constant and independent of the rotor position. Consequently the flux will be fundamentally sinusoidal and undistorted under all load conditions.

Turbo generators revolve at high speed, have solid machined rotors for mechanical strength and as a consequence they are less salient in nature. The nonsalient machine, with an almost constant air gap or rotor permeance, can be simplified to a voltage source behind a reactance and suitably represented by a phasor diagram. This simplified representation was used in the preliminary studies of the series excitation.

For the salient machine the magnetic circuit reluctance is different on the D and Q axes resulting in air gap flux distortion. How much distortion occurs will depend on the rotor angle and the degree of saliency; the most common method of solution is to resolve the stator MMF into two components aligned along the two respective axes. The effect of saliency can thus be briefly summarised in the following way: as the rotor angle increases the flux density will shift to the leading/lagging edge of the rotor pole where the air gap is larger. The flux linking the stator and rotor sees an increasingly complicated reluctance as more flux is pushed into the interpole region and this results in significant flux distortion.

Hydro generators are usually salient since they revolve at lower speeds and have a greater number of pole pairs. Generally salient machines are constructed with damper or amortisseur windings. These windings improve the transient stability of the machine by opposing rotor oscillations. Even if damper circuits are not intentionally included in the rotor design, then damper action can result anyway from closed circulating current paths in the iron. For example the bolts that secure the pole pieces together in the pole faces provide such circulating current paths. The damper circuits, while of simple construction, are difficult to analyse electrically.

The exploitation of remote hydro resources will invariably employ salient pole generators.

It has been shown that over simplified representations of salient machines lead to less accurate predictions of operational performance of direct connection schemes and that a more thorough dynamic simulation analysis is required [Arrillaga *et al.*, 1991]. To begin with the theory describing a more detailed approach to accurately representing the synchronous machine is outlined that is equipped to represent the bi–lateral interactions between synchronous machines and converters.

### 5.1.2 Basic Electrical Equations

The general equation for a single winding or coil is

$$V(t) = -R.i(t) - \frac{d}{dt}\Psi(t) \tag{5.2}$$

where V(t) is the voltage induced in the winding, R the resistance and i(t) the current. $\Psi(t)$ is the flux linkage of the winding produced by the current i(t). The convention adopted to distinguish per unit (pu) from actual values will be to signify actual values with a bold type face, i.e. $R$ is a pu value and **R** is the corresponding real value.

A standard representation of the synchronous machine consists of six mutually coupled windings. There are three evenly distributed stator windings and damper winding effects are represented by lumped short circuited coils on the D and Q axes of symmetry while the field winding is considered as a concentrated coil on the D axis only to which an excitation voltage is applied. Figure(5.2)a shows this diagrammatically where the field structure is rotating at synchronous speed with respect to the fixed stator windings.

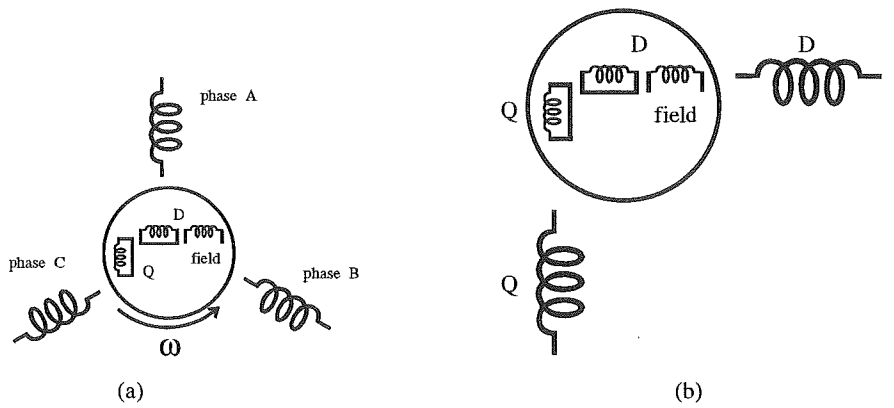


**Figure 5.2** Transformation of stator quantities to the rotor frame

Equation(5.2) can be generalised to suit the six mutually coupled machine windings i.e.

$$[V] = -[R][i] - \frac{d}{dt}[\Psi] \tag{5.3}$$

The flux linkage of the windings is defined by

$$[\Psi] = [L][i] \tag{5.4}$$

where

$$L = \begin{bmatrix} L_{aa} & L_{ab} & L_{ac} & L_{afd} & L_{akd} & L_{akq} \\ L_{ba} & L_{bb} & L_{bc} & L_{bfd} & L_{bkd} & L_{bkq} \\ L_{ca} & L_{cb} & L_{cc} & L_{cfd} & L_{ckd} & L_{ckq} \\ L_{fda} & L_{kda} & L_{kqa} & L_{ffd} & L_{fkd} & 0 \\ L_{fdb} & L_{kdb} & L_{kqb} & L_{kdf} & L_{kkd} & 0 \\ L_{fdc} & L_{kdc} & L_{kqc} & 0 & 0 & L_{kkq} \end{bmatrix} \tag{5.5}$$

and the subscripts a, b, c denote the stator quantities and f, kd, kq denote field, direct and quadrature axis damping circuit quantities respectively. There is no mutual coupling between the D and Q rotor circuits. The relative motion of the stator and the salient rotor cause the self and mutual inductances to be periodic functions of rotor position. Hence a set of differential equations is derived whose coefficients are periodic functions of rotor position, and this makes the equations awkward to solve.

For example the armature self inductances $L_{aa}$, $L_{bb}$ and $L_{cc}$ can be expressed as

$$L_{aa} = a_o + a_2 cos2\theta + a_4 cos4\theta + ... \tag{5.6}$$

where $L_{bb}$ and $L_{cc}$ are similar except $\theta$ is replaced by $(\theta - 120)$ and $(\theta - 240)$ respectively. The stator–stator mutual terms vary in a similar fashion i.e.

$$L_{bc} = -b_o + b_2 cos2\theta + b_4 cos4\theta + ... \tag{5.7}$$

and $L_{ca}$, $L_{ab}$ are given by the same expression except that $\theta$ is replaced by $(\theta - 120)$ and $(\theta - 240)$ respectively. The stator–rotor mutual terms vary as a fundamental sinusoid of rotor position.

$$L_{afd} = c_1 cos\theta + c_3 cos3\theta + ... \tag{5.8}$$

$$L_{akd} = d_1 cos\theta + d_3 cos3\theta + ... \tag{5.9}$$

$$L_{akq} = e_1 sin\theta - e_3 sin3\theta + ... \tag{5.10}$$

where again the remaining inductance terms involving b and c coils are obtained by replacing $\theta$ with $(\theta - 120)$ and $(\theta - 240)$. The inductance matrix is completely symmetrical i.e.

$$L_{afd} = L_{fda} \tag{5.11}$$

and so forth. The rotor self and mutual inductances $L_{ffd}$, $L_{fkd}$, $L_{kkd}$ and $L_{kkq}$ are constants and so are the resistances of the respective windings.

No assumptions have been made about the MMFs of any of the windings however eddy current and hysteresis losses are not included. The inductance coefficient values can be determined from the design, Fourier analysis [Rafian and Laughton, 1976] or experimental test [Concordia, 1951]. While these equations can be solved in phase variable form it is very common to transform the stator circuit to a new set of axes revolving at the same speed relative to the rotor.

### 5.1.3 Per Unit Systems

In many instances it is desirable to re–express real values of volts, amperes and ohms as fractions of defined base quantities. This normalisation process makes the values of a similar order and makes the system equations more amenable to numerical solution. Usually the base quantities are self evident i.e. base power and base voltage can be selected as the rated power and voltage of the system respectively. Base quantities of current and impedance can then be derived from these quantities by well known relations.

The principles applied to simple inductively coupled static circuits are equally applicable to synchronous machine equations. It will be seen later that in some circumstances the selection of a base quantity is completely arbitrary although there may be one choice that is particularly advantageous i.e. the choice that allows simplified equivalent circuits to be formed. A comprehensive discussion can be found by reading [Lewis, 1958] and [Anderson and Fouad, 1977]; only the main laws are summarised here.

- The system voltage equations must be exactly the same whether the equations are in pu or MKS units

- The system power equation must be exactly the same whether the equations are in pu or MKS units.

These conditions specify that all circuits have the same power and time bases.

### 5.1.4 The DQO Transformation

Transformations are important mathematical tools for the understanding and solution of electrical circuit problems. Transformations can reduce complexity and simplify the calculation sequence by redefining the quantities of interest in a domain where they are more readily determined. The new transformed variables may or may not have a physical significance. Some examples of common transformations include;

- converting branch currents to mesh currents or line voltages to phase voltages
- a three phase system to positive, negative and zero sequence components
- a matrix that diagonalises another matrix, or a mapping that relates a matrix to a vector (an eigenvalue).

One very important transformation with particular significance to synchronous machine analysis is called the DQO transformation. This method has its origins in two reaction theory first proposed by Blondel and later developed in a series of papers by [Park, 1929]. It is found that a relatively simple transformation eliminates the functions of angle from the machine equations described above.

#### 5.1.4.1 Assumptions

It is assumed that the self and mutual inductance terms of order 3 and higher in equations(5.6) to (5.10) can be neglected; a condition true for most machines except those exhibiting extreme saliency. Furthermore $a_2$ must equal $b_2$ in equations(5.6) and (5.7) which, among other things, prescribes that the stator circuit is balanced and sinusoidally distributed and that no stationary harmonic MMFs are produced by the stator. Again, nonlinear effects such as hysteresis and eddy current losses are neglected however saturation can be considered at a later stage.

#### 5.1.4.2 The Three Phase to 2 Axis transformation Matrix

The three stator windings are replaced by equivalent fictitious stator windings on the D and Q axes that are stationary with respect to the rotor as shown in Figure(5.2)b. A matrix for transforming the stator quantities $[V_s]$,$[I_s]$ and $[\Psi_s]$ to the rotor frame of reference is

$$\tau = \begin{bmatrix} cos(\theta) & cos(\theta - 120) & cos(\theta - 240) \\ sin(\theta) & sin(\theta - 120) & sin(\theta - 240) \\ \frac{1}{2} & \frac{1}{2} & \frac{1}{2} \end{bmatrix} \tag{5.12}$$

and therefore

$$\begin{bmatrix} V_d \\ V_q \\ V_0 \end{bmatrix} = \tau \begin{bmatrix} V_a \\ V_b \\ V_c \end{bmatrix}, \quad \begin{bmatrix} I_d \\ I_q \\ I_0 \end{bmatrix} = \tau \begin{bmatrix} I_a \\ I_b \\ I_c \end{bmatrix}, \quad \begin{bmatrix} \Psi_d \\ \Psi_q \\ \Psi_0 \end{bmatrix} = \tau \begin{bmatrix} \Psi_a \\ \Psi_b \\ \Psi_c \end{bmatrix} \tag{5.13}$$

and after making substitutions equation(5.3) can be written

$$[V_{dqo}] = -[R].[i_{dqo}] - \frac{d}{dt}[\Psi_{dqo}] + \omega[\Psi_{dq}] \tag{5.14}$$

where $\omega$ is the speed.

Currents in the new fictitious coils, perpendicular to each other and coincident with the respective rotor coils, produce the same MMF as the previous three coil system given that each current is scaled by $\frac{3}{2}$. Furthermore the axes are perpendicular and independent by definition so that the direct axis flux doesn't link the quadrature axis coils and vice versa, the only extra consideration being the speed voltage terms $\omega[\Psi_{dq}]$. The speed voltage terms arise from the derivative of the transformation matrix and represent the voltages induced in the stator by the revolving field poles.

#### 5.1.4.3 Zero Sequence Current

In general the three stator currents can be represented by the two phase system $I_d$ and $I_q$ however there is an implied constraint since three independent variables can not be represented by two when the inverse transformations are performed. The constraint is that the neutral point of the star connected machine is not grounded i.e. $I_a + I_b + I_c = 0$. For the delta machine there is no net voltage to cause zero sequence current to flow. If this constraint doesn't apply then the equation

$$I_o = \frac{1}{2}I_a + \frac{1}{2}I_b + \frac{1}{2}I_c \tag{5.15}$$

is required from equation(5.13) leading to the definition of zero sequence current. This instantaneous zero sequence current flows in all phases simultaneously and therefore produces no resultant air gap MMF.

#### 5.1.4.4 Flux Linkage

The per unitised equation(5.14) can be rewritten in terms of flux linkage,

$$\dot{\Psi}_d = V_d - \omega\Psi_q - R_a I_d \tag{5.16}$$

$$\dot{\Psi}_q = V_q - \omega\Psi_d - R_a I_q \tag{5.17}$$

$$\dot{\Psi}_f = V_f - R_f I_f \tag{5.18}$$

$$\dot{\Psi}_{kd} = -R_{kd} I_{kd} \tag{5.19}$$

$$\dot{\Psi}_{kq} = -R_{kq} I_{kq} \tag{5.20}$$

where it is assumed that the direct and quadrature axis damper windings are short circuited and have no external voltage sources and

$$\Psi_d = L_a I_d + L_{md}(I_d + I_{kd} + I_f) \tag{5.21}$$

and

$$\Psi_q = L_a I_q + L_{mq}(I_q + I_{kq}) \tag{5.22}$$

lead to the speed voltage terms. An implicit constraint on these equations and an essential condition for an equivalent static circuit is that there must be a reciprocity of the pu mutual inductance coefficients between stator and rotor. To achieve this a power invariant transformation can be chosen or instead a non power invariant transformation combined with a suitable per unit system can be used [Sarma, 1979].

### 5.1.5 Synchronous Machine Equations

By recalling that $\Psi = LI$ the above equations can be partitioned into separate sub matrices equations(5.23) and (5.24) for the direct and quadrature axes respectively.

$$\begin{bmatrix} V_d - \omega\Psi_q - R_a I_d \\ V_f - R_f I_f \\ -R_{kd} I_{kd} \end{bmatrix} = \begin{bmatrix} L_{md} + L_a & L_{md} & L_{md} \\ L_{md} & L_{md} + L_{kf} + L_f & L_{md} + L_{kf} \\ L_{md} & L_{md} + L_{kf} & L_{md} + L_{kf} + L_{kd} \end{bmatrix} \frac{d}{dt} \begin{bmatrix} I_d \\ I_f \\ I_{kd} \end{bmatrix} \tag{5.23}$$

$$\begin{bmatrix} V_q - \omega\Psi_d - R_a I_q \\ -R_{kq} I_{kq} \end{bmatrix} = \begin{bmatrix} L_{mq} + L_a & L_{mq} \\ L_{mq} & L_{mq} + L_{kq} \end{bmatrix} \frac{d}{dt} \begin{bmatrix} I_q \\ I_{kq} \end{bmatrix} \tag{5.24}$$

The mutually coupled circuits on each axis are combined into equivalents as illustrated in Figure(5.3) where

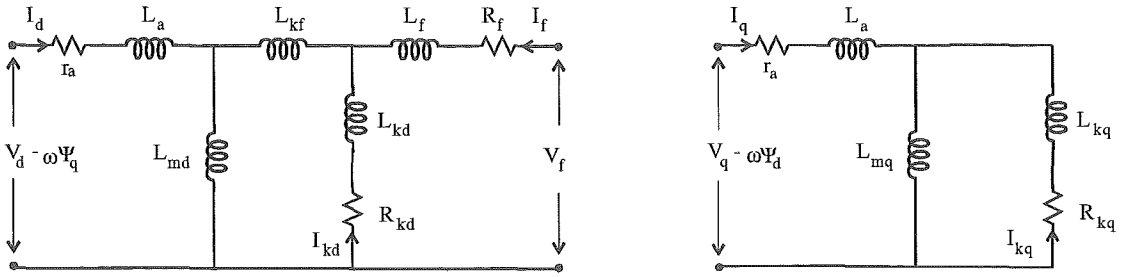


(a) Direct Axis (b) Quadrature Axis

**Figure 5.3** Circuit equivalents of D and Q axes

- $L_f, R_f$ are the field leakage inductance and resistance respectively
- $L_{kd}, R_{kd}, L_{kq}, R_{kq}$ refer to the direct and quadrature damper leakages and resistances respectively
- $R_a$ is the armature resistance
- $L_a$ is the leakage inductance
- $L_{kf}$ is the field to damper winding mutual inductance [Canay, 1969]
- $L_{md}$ and $L_{mq}$ are the direct and quadrature axis mutual or magnetising inductances.

Equations (5.23) and (5.24) are in a suitable form for integration, and via the appropriate inverse transformation the phase currents can be calculated.

## 5.2 Dynamic Series Excitation Representations

### 5.2.1 The TCS model

The synchronous machine is a direct implementation of equations(5.3) to (5.5). Usually self and mutual terms of order 3 and higher are neglected, although any number of known terms can be included. Similarly it is usual to assume $a_2 = b_2$, although this is clearly not a strict requirement. The per unitised system equations are integrated in phase variable form [Arrillaga *et al.*, 1978].

#### 5.2.1.1 Manufacturer's Data

Manufacturer's data is usually provided in DQ pu format and it is thus necessary to convert to ABC (phase) quantities. The required calculation steps and a set of typical machine data are described in Appendices C.1 and C.2 and the interesting thing is that the same equations are used for calculating the leakage inductances for the D and Q equivalent circuits in section(5.1.5). This strongly suggests that, apart from algorithmic differences, the TCS and EMTDC machine models are equivalent.

In all physical systems the mutual inductance matrix is symmetrical. On conversion to the per unit system it also makes sense that the pu mutual inductances are equal. Given that the stator base quantities are defined, then this condition can be met by judicious selection of the as yet unspecified rotor base quantities [Lewis, 1958]. Furthermore reciprocity of the pu mutual inductances allows simplified equivalent diagrams to be constructed (such as Figure(5.3)) which can aid in the understanding of the machine. If the field and damper current bases are specially chosen and the condition of equal pu mutual inductances must be satisfied, then this will entail the specification of some of the real parameters of the machine, namely $\mathbf{L_{afd}}$, $\mathbf{L_{akd}}$ and $\mathbf{L_{akq}}$.

It is common for machine data to be given in pu form and this tends to obscure the true physical characteristics and impedances of the machine. There is ambiguity because, having specified the definitive properties of the machine (i.e. rated power and rated voltage), the remaining choice of free unspecified rotor bases determines the pu impedances of the machine. Hence for a unique machine there is no unique set of pu values. A number of pu sets may be correct when defined properly in terms of the chosen rotor current bases.

#### 5.2.1.2 Series excitation machine pu values

The machine pu values of section(5.2.1.1) are not valid when the field winding is connected in series with the dc output if the respective dc circuit and rotor impedance and current bases are different. In the above, the field winding current base was specified such that the pu mutual inductances would be reciprocal enabling an equivalent circuit to be formed. However the generalised pu system doesn't demand equal pu mutual inductances and this fact will be exploited to derive a new set of machine pu impedances for the series connected machine.

Via the formulae in [Rankin, 1945a] outlined in Appendix C.3, real MKS impedance values for the generator are determined. The rotor base quantities are then respecified as the dc line quantities and new pu values of the series excited machine thereby calculated.

### 5.2.2 The EMTDC model

The use of the EMTDC simulation package [Manitoba Hydro, 1988] is advantageous as it allows a high degree of modeling flexibility. The synchronous machine model is compartmentalised into a separate subsystem enabling the state variable representation embodied by equations (5.23) and (5.24) to be implemented [Woodford *et al.*, 1983]. The input parameters are field voltage, mechanical torque and the three phase terminal voltages of the machine as shown in Figure(5.4). These voltages are integrated with time to determine the field and stator currents. The stator currents are injected from the machine model back into the rest of the network.

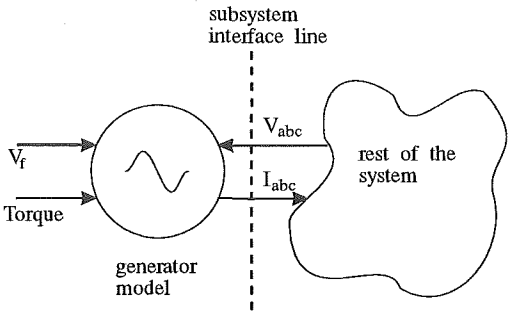


**Figure 5.4** EMTDC machine interface

To model the series excitation in EMTDC it is not possible to physically connect the machine field winding on the ground side of the converter in the manner of the series excitation. Hence the field winding in the converter subsystem is simply represented by the field self inductance as a first approximation. Voltages will be induced by the machine on the field winding but these will be small compared to the dc line voltage and are therefore neglected.

The rectifier and inverter terminal voltages which drive the change of dc current are significantly larger than those of a conventional static excitation system. It is therefore assumed that the field current and the rate of change of field current are well defined and specified by the dc link. The model was thus rewritten to allow the field current and rate change of field current as input parameters [Arrillaga *et al.*, 1993b][Arrillaga *et al.*, 1993a].

Equation(5.23) can be reformed as

$$\begin{bmatrix} V_d - \omega\Psi_q - R_a I_d \\ -R_{kd} I_{kd} \end{bmatrix} = \begin{bmatrix} L_{md} + L_a & L_{md} \\ L_{md} & L_{md} + L_{kf} + L_{kd} \end{bmatrix} \frac{d}{dt} \begin{bmatrix} I_d \\ I_{kd} \end{bmatrix} + \begin{bmatrix} L_{md} \\ L_{md} + L_{kf} \end{bmatrix} \frac{d}{dt} I_f \tag{5.25}$$

where the field voltage ($V_f$), no longer an input parameter, is given by

$$V_f = R_f I_f + \begin{bmatrix} L_{md} & L_{md} + L_{kf} + L_f & L_{md} + L_{kf} \end{bmatrix} \frac{d}{dt} \begin{bmatrix} I_d \\ I_f \\ I_{kd} \end{bmatrix} \tag{5.26}$$

The rest of the network voltages and currents are specified in kA and kV whilst the machine quantities are calculated in pu. Hence there is a mismatch of units when the dc line current is

injected into the modified machine model. In practice the values of $I_f$ and $\frac{dI_f}{dt}$ are scaled to ensure the correct nominal steady state operating point is achieved.

The assumption that the machine does not induce voltages on the field winding is however incorrect and equation(5.26) specifies this relationship explicitly. The induced voltages under fault conditions are significant and tend to increase the severity of the fault. Therefore a combination of the field self inductance

$$\mathbf{L_{ffd}} = (L_{md} + L_{kd} + L_f) \times L_b^f \tag{5.27}$$

and an induced voltage source

$$V_f' = \begin{bmatrix} L_{md} & L_{md} + L_{kf} \end{bmatrix} \frac{d}{dt} \begin{bmatrix} I_d \\ I_{kd} \end{bmatrix} \tag{5.28}$$

are used as an equivalent rotor circuit. Via the defined flux linkage bases, the pu induced voltages can be converted to kV (Appendix C.4) and included in series with the field self inductance term such as depicted in Figure(5.5).

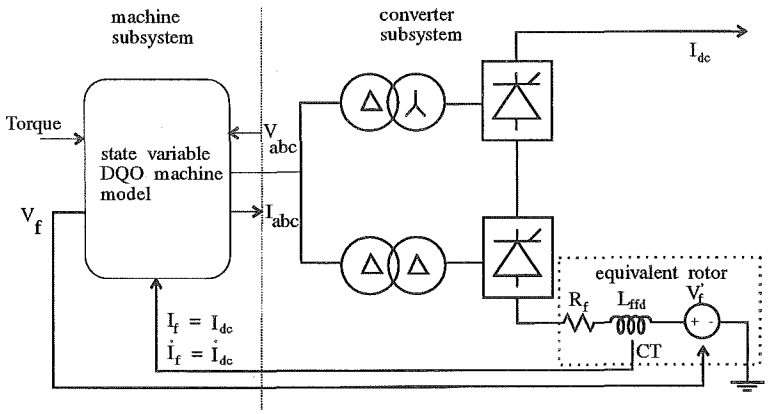


**Figure 5.5** Series excitation model in EMTDC

The quadrature axis matrix equation(5.24) need not be modified.

### 5.2.3 Comparison between TCS and EMTDC models

#### 5.2.3.1 Steady State Operation Point

The procedure described in Appendix C was implemented to derive the parameters for the respective TCS and EMTDC simulations. The same nominal operating point of 80kV dc voltage, 1kA dc current and a 10 degree firing angle were established for the specified machine twelve pulse converter system. A salient machine is used to emphasise any differences between the respective models. In both systems the machines are separately excited and the respective steady state ac current and voltage waveforms are given in Figure(5.6)a. There is an apparent discrepancy between the ac currents and this is due to a higher TCS magnetising current. The differences in the harmonic voltages are however larger and are attributed to modeling differences. To support this assertion the same simulation was run in PSCAD, the latest version of EMTDC. Compared to the previous figure, the new harmonic voltage waveform is more similar to the TCS simulation.

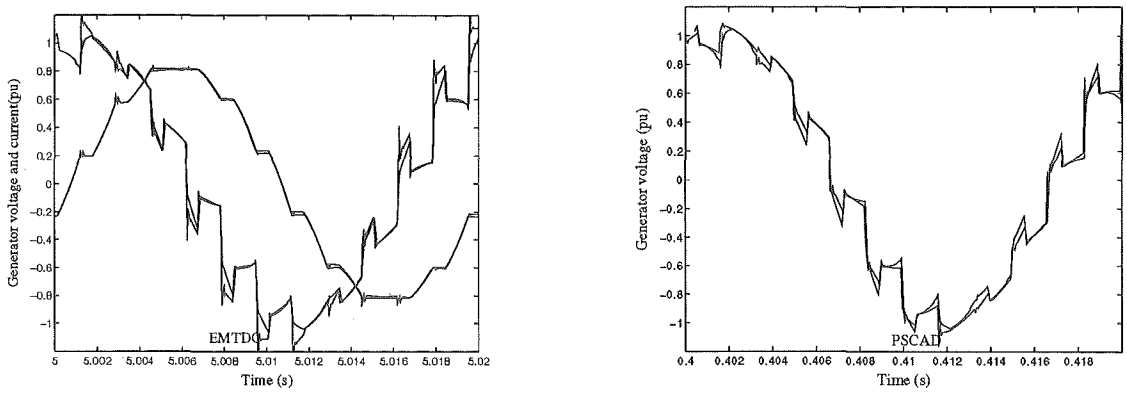


(a) EMTDC-TCS

(b) PSCAD-TCS

**Figure 5.6** Steady State Comparisons

The EMTDC synchronous machine was reconfigured in series mode. The distorted voltage and current waveforms were identical to their respective separately excited counterparts and are hence not repeated. This reflects the fact that the commutation process is governed by the subtransient parameters i.e. leakage and damper reactances, and not the field leakage which has been suppressed. As far as the series excited machine in TCS is concerned, the result of the conversion of the machine data to the new pu system led to errors. For some unexplainable reason the TCS simulation firing controllers had difficulty maintaining a correct 30 degree phase shift between the respective 6 pulse bridges. This manifested itself with characteristic 6 pulse harmonic currents flowing in the stator windings.

### 5.2.3.2 Dynamic response

In spite of the difficulty encountered with the TCS simulation, a short circuit fault was applied to the line side of the smoothing reactor in each system to gauge the similarity of each model's dynamic response. The converter firing angle was advanced to 125 degrees on detection of the current surge to reduce the line current to zero. The transient waveforms recorded for TCS and EMTDC systems are displayed in Figure(5.7). While the waveforms are not exact they are sufficiently consistent to justify the use of the EMTDC model. The peak fault currents for the TCS and EMTDC simulations were 0.697 and 0.679 pu respectively, fault duration times were 25 and 16 ms respectively. Overall it appears that the series model in EMTDC is more damped.

### 5.2.3.3 Modeling differences

There are quite distinctive algorithmic characteristics that differentiate the TCS and EMTDC simulations [Zavahir, 1992].

The EMTDC approach divides the converter and machine into separate subsystems. Machine voltages applied at one time step are integrated to calculate compensated currents that will be injected at the next solution time step and hence there is a time step delay between the subsystems. The field current is specified and the impedance looking from the machine into the dc circuit is infinite. A differentiation is performed to calculate $\frac{dI_f}{dt}$ which must also be filtered to suppress numerical noise and instability in the EMTDC series model.

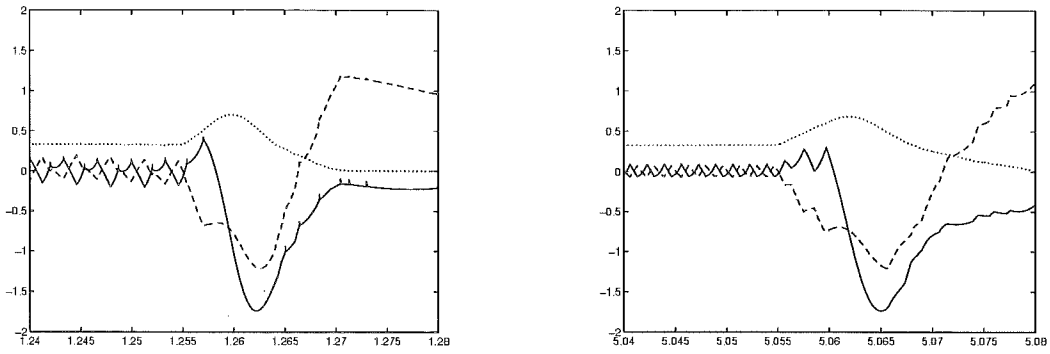

(a) TCS (b) EMTDC

**Figure 5.7** Current Waveforms $I_{dc}$=*dotted*, $I_{kd}$=*dashed*, $I_{kq}$=*solid*

On the other hand the TCS single-subsystem concept is based in pu and is the direct solution of the system differential equations with less approximations. It is directly possible to physically connect the field circuit in series with the converter provided that the machine pu system is suitably modified.

When comparing the dynamic response to the dc line fault it was found that the waveforms were dependent on the value of $\alpha$ chosen to extinguish the fault current. While exactly the same firing angle order can be implemented in each system, the valve monitoring and firing mechanisms operate differently to give different results in some cases.

## 5.3 The Dynamic behaviour of the Series Excitation

The dynamic response and stability of the system is of utmost importance especially if a new design or configuration is being implemented. In this section the dynamic responses of the series excitation are determined with the EMTDC based series excitation model. The dc line fault and current order change responses are compared to a separately excited system. The test system used is the same as that of section(4.3.2). The series–group field winding arrangement has a low effective fault impedance because the field self inductances are in parallel yet the induced field voltage is the same for the combination as illustrated in Figure(5.8).

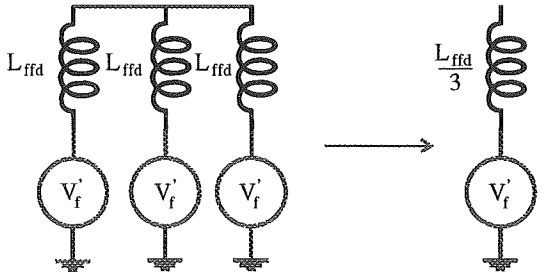


**Figure 5.8** Series–group equivalent rotor circuit

In the following comparisons the separately excited system smoothing reactance is specified

as 1.0 Henry. For the series–group system, 1.0 Henry of independent smoothing inductance will also be used.

### 5.3.1 Current order change

To quantify this effect Figures(5.9)a and (5.9)b show the response of the conventional and series excited cases to a change of current order from 0.9 to 1.0 pu. The 0.1 current order change was implemented over a 0.05 second interval. The response of the series excitation appears sluggish although in this case the power change is approximately twice that of the separately excited scheme. Note how that in Figure(5.9)b the dc line voltage has increased linearly with the dc current at the minimum firing angle order.

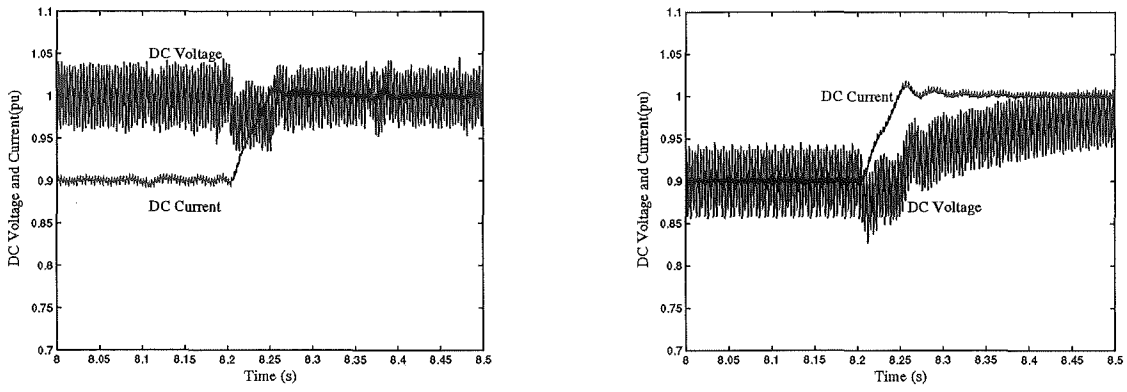


(a) Separately Excited System

(b) Series Excited System

**Figure 5.9** Dynamic Response to a change in current order

### 5.3.2 Fault Recovery

Following a dc short-circuit fault the rectifier current will rise to about two per unit, with a consequent increase in machine excitation in the case of the series connection. In the absence of any special fault controls this effect would increase substantially the severity of the fault.

However, it is standard practice in HVdc transmission to advance temporarily the firing angle into the inversion region to accelerate the collapse of the fault current by transferring the stored reactive energy to the ac side. In the series excitation scheme the fault retarding dc voltage is dependent on the dc current. Hence it must be determined if a dc line fault can be completely extinguished.

The short circuit was applied to the line side of the smoothing reactor after 8.1 seconds of dynamic simulation. Upon fault detection the rectifier firing angle was set to 115 degrees. Figures(5.10)a and (5.10)b show the dc line voltages and currents for the cases of conventional and series excitation respectively. The line current reduced to zero at times t = 8.12 and t = 8.125 seconds for the respective separately excited and series excited cases. At this point the converter is blocked to allow the line a 100ms period of deionisation after which line re–energisation takes place. The peak fault current for the series excitation was 2.35 pu compared to 2.03 pu for the

separately excited system. Without increasing the independent smoothing reactance this would increase the peak fault current rating of the thyristor valves for the series excited system.

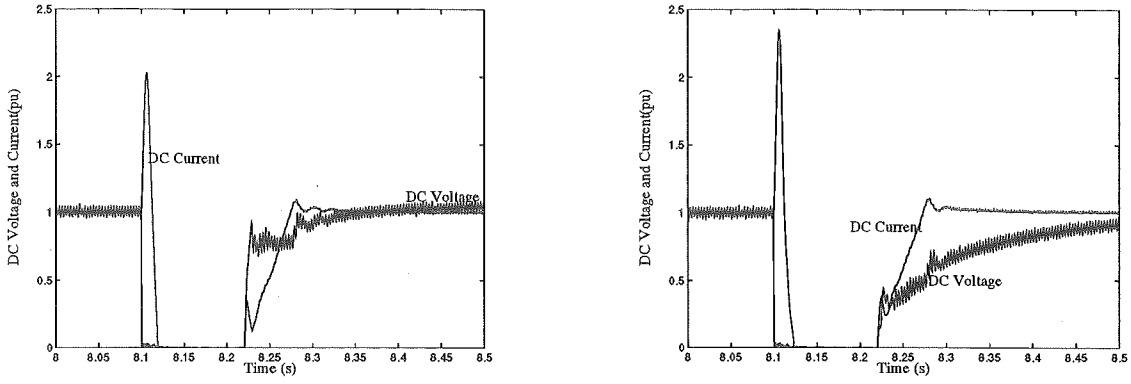


(a) Separately Excited System

(b) Series Excited System

**Figure 5.10** Response to system fault

### 5.3.3 Machine insulation requirements

Rotor field transients will occur, the worst imaginable being a a short circuit dc fault on the line side of the smoothing reactor. In practice fault transients will be governed in part by the of arc flashover characteristics plus tower and earth resistances that limit the applied transients [Kohler, 1967].

The insulation durability will depend on the applied mechanical, electrical, thermal and chemical stresses. Hence the insulation of large machines is carefully considered and utilises a variety of processes with varnishes, papers, chemical treatments and mica composites to achieve a desired insulation requirement. The abnormal operation practices of the series excitation scheme therefore makes mention of the electrical insulation aspects relevant.

There is a universal theory that insulation has a constant voltage time life expectancy. At a given overpotential there may be a total time during which failure will be resisted and it makes little difference if this time is continuous or a summation of several applications [Miner, 1941].There are two kinds of voltage transients that can cause insulation voltage pressures namely dc line faults and dc current order changes. The first is hopefully a rare occurrence yet even short large transients will age the insulations. For the multi–machine system the impedance provided by the series parallel connection of the field windings is the smaller fraction of the fault impedance. The transient voltage stresses will be shared by the field circuit and the independent smoothing reactance.

Separately excited machines will also be subject to internally generated voltages during dc line faults. For the separately excited system already investigated the internally induced voltage, which causes the field current to initially rise and then decrease, is ±40kV. The smoothing reactor bears the brunt of the dc line voltage swing however. In the series excited case the induced transient field voltage was between +60kV and -50kV and the peak voltage across each field winding was 60kV under dc fault conditions. Hence field winding voltage stresses up to 120kV could be expected in the series excited case.

## 5.4 Conclusions

A salient machine has different magnetic properties on two axes of symmetry which leads to the characteristic machine inductance matrix to be a function of rotor position. The use of simplified generator equivalents in direct connection studies that ignore stator–rotor harmonic cross coupling effects has been previously shown to be invalid.

Beginning from a description of the machine inductance matrix in phase quantities, the DQO transformation is applied to remove the functions of angle from the machine equations and allowed a neat set of differential equations in terms of new fictitious variables. This model was reconfigured to represent the dynamic behaviour of the series excited machine and implemented in the EMTDC algorithm. With regards the phase variable equations, the numerical values of many of the pu impedances are dependent upon the value of base field current. Hence from the given pu data and some assumptions, a new set of pu values were determined to suitably represent the series connection in a completely independent state variable model of the same circuit. The steady state and dynamic responses of the respective models were compared and shown to complement each other leading to the conclusion that the modified machine model is valid for representing the series excited machine.

The transient performance of the series excitation was predicted and compared with a conventional separately excited unit connection scheme. It was shown that a dc line fault could be satisfactorily cleared. The fault clearance time was marginally longer than the conventional separately excited scheme. For the separately excited and series excited systems with the same independent smoothing reactance, the induced field voltage in the series–group scheme significantly increased the severity of the fault which resulted in a higher peak fault current. Moreover under dc fault conditions the field voltage stress is approximately three times that of the conventionally excited scheme.

# Chapter 6

# THE ACCELERATED STEADY STATE

## 6.1 Introduction

The thesis thus far has concentrated on issues relating to the direct connection. Before a scheme will be built computer dynamic simulation studies will play an important role in the design phase to determine the optimum parameters. There are various simulation packages that are capable of analysing directly connected machine and converter interactions however the drawback has always been the excessive amount of computer and engineering time required to perform the simulation runs. Moreover as the numbers and ratings of power electronic devices in the power system increase it is necessary to model the converter in detail to consider the effects of asymmetry and nonideal smoothing. Presently dynamic simulation is the only means of achieving this. Having justified the use of dynamic simulation, it is desirable to maximise the efficiency and reduce the cost.

Simulation programmes integrate nonlinear differential equations where a direct analytical solution is not possible. A good review paper is [Skelboe, 1982] that discusses aspects of time domain steady state analysis. Power electronic circuits are by and large reactive and well suited to analysis by 1st order differential equations, the solutions and properties of which are well known. The equations are referred to as 'stiff' if they have a wide range of time constants. Start up transients take many cycles to decay. The normal solution method is to integrate until the steady state is reached which can be very time consuming. For these cases fast steady state techniques aim to find a starting point or initial condition whereby the steady state starts directly.

A History of Fast Steady State Techniques

The first accelerated steady state method was proposed by [Aprille and Trick, 1972] and this paper has become somewhat of a landmark. A dc power supply circuit and a frequency doubler were analysed containing the nonlinear elements of a diode and transistor respectively. Instead of looking for a solution directly they formulated a two–point boundary value problem. This was followed [Aprille, JR and Trick, 1972] by a paper concerning the solution of the periodic state of non–linear oscillators where the period of oscillation, $T$, was unknown *a priori*. In this case $T$ was incorporated as an unknown in the solution vector. Further work [Colon and Trick, 1973] looked at the analysis of large signal electronic circuits.

[Trick *et al.*, 1975] dwelt in detail on the computation of the Jacobian and introduced the idea of the sensitivity circuit. This approach logically justified the concept of the Jacobian and gave it some physical interpretation. Furthermore they showed how to extend the sensitivity analysis for

circuits that contained inductor cutsets and capacitor loops.

[Zein, 1980] showed that the steady state formulation could be generalised to handle a mixture of algebraic–differential quantities. The solution state vector, normally containing state variables capacitor voltage and inductor current (and possibly the period itself), could also be a vector containing algebraic components regardless of the formulation used. [El-Bidweihy and Al-Badwaihy, 1982] applied a steady state formulation to a single phase naturally commutated rectifier bridge. This was a valuable contribution because it concentrated on the significance of correctly calculating the valve extinction angle derivative contribution to the Jacobian.

Two important papers appeared four years later [Grötzbach and Von Lutz, 1986] and [Verghese *et al.*, 1986]. The first presented a unified method of modeling rectifier controlled dc supplies and gave a comprehensive mathematical description of the incorporation of controller dynamics in the operation of the 3 phase line commutated 6 pulse bridge. The latter contribution although along a similar vein was developed independently and treated power electronic circuits as cyclically switched systems. Both contributions comment in detail on the solution of closed loop system equations and the associated small signal model.

[Luciano and Strollo, 1990] developed the principles contained in these two last mentioned works to perform the analysis of a Buck converter where the controller circuitry was explicitly modeled in detail and included with the switching power network. The turn–on and turn–off and regulatory control of the transistor was governed by algebraic relations. A Chebyshev series was used to compute the state transition matrix, and the change of topology instants were solved with a simple algebraic equation so that no step by step numerical integration was necessary. In a similar manner the converter analysis of [Ooi *et al.*, 1980] iteratively solved for the next topology change instants although the state transition matrix was calculated in an entirely different fashion. Three phase symmetry and the repetition pattern of the converter were used to minimise computation time. These methods assume piecewise linearity over each conduction interval and they appear to provide very efficient solutions.

The methods surveyed so far have considered systems exclusively dealing with traditional state variable analysis. [Usaola and Mayordomo, 1990] converted and applied the same principles to an EMTP [Dommel, 1969] formulation. Instead of capacitor voltages and inductor currents as state variables, the new state variables were the history term current sources. In terms of power system analysis this was a significant step given the wide spread use of EMTP techniques. Because the solution efficiency reduced for large systems it was proposed to divide the circuit into linear and nonlinear components and represent them in the frequency and time domains respectively [Usaola, 1990]. In a similar manner the applications to harmonic balance techniques have also been exploited [Van Den Eijnde and Schoukens, 1990] [Ushida *et al.*, 1992]. [Perkins *et al.*, 1993] followed with their own different initialisation procedure for the EMTP algorithm based on sensitivity circuit analysis [Trick *et al.*, 1975].

The drawback of what has been published so far (with the exception of [Verghese *et al.*, 1986]) is that the systems presented tend to be simplified and/or the programmes tailored for specific cases. Previous works have assumed undisturbed and conventional operation of the converter i.e. 3 phase symmetrical commutating voltages and a regular valve firing pattern [Ooi *et al.*, 1980] [El-Bidweihy and Al-Badwaihy, 1982]. Balanced operation does lead to simplifications that have

been well and truly pointed out if steady state analysis is the primary goal. The goal of this chapter is to introduce more flexibility and consider the rapid steady state of combinations of components not yet reported upon, particularly HVdc converters and synchronous machines.

## 6.2 The steady state problem

### 6.2.1 Aspects of Differential Equation solutions

The following section illustrates how initial conditions lead to a solution consisting of two parts: steady state and transient. The system state equations can be expressed in the form

$$\dot{x} = Ax + Bu \tag{6.1}$$

where $x$ is the state variable vector, $u$ is the independent periodic source vector and $A$ and $B$ are coefficient matrices. In general $A$ and $B$ can be functions of time however at this stage they will be constant to simplify the explanation, furthermore similar results are obtained if equation(6.1) is generalised with discrete time varying systems of equations.

The solution set has two parts, steady state and transient components, also known as the complementary function and particular integral respectively. Solving the homogeneous equation gives the complementary function or transient part

$$x = ke^{At} \tag{6.2}$$

and $k$ is determined from the initial conditions. If the eigenvalues of $A$ have negative real parts then the system will be stable. The 'stiffness' of the equations will be determined by how close the eigenvalues lie to the imaginary axis or how much damping there is in the system. The particular integral will be determined by the forcing function $Bu$. Hence the total solution is:

$$x = ke^{At} + F(Bu) \tag{6.3}$$

At time zero there exists some initial condition $x(0)$ and hence the integration constant can be calculated.

$$k = x(0) - F(Bu) \tag{6.4}$$

If $x(0) \neq F(Bu)$ then $k$ will be non zero and there exists a transient component to the solution of equation(6.3). If, on the other hand, $x(0)$ is the solution then $k$ is zero, i.e. $x(0)$ is the steady state solution.

As an example consider the circuit of Figure(6.1)a where V is a dc voltage source and where the steady state operating point is to be determined. DC circuit analysis yields the solution immediately however the most general implementation of the circuit is expressed using Kirchhoff's voltage law to give the following expression.

$$V - i.R - L.\frac{di}{dt} = 0 \tag{6.5}$$

By way of the Laplace transform an expression for the current as a function $i(t)$ of time can therefore be determined where i(0) is the initial current flowing through the inductance

$$i(t) = \frac{V}{R} + \left[i(0) - \frac{V}{R}\right] \exp^{-\frac{L}{R}t} \tag{6.6}$$

If the initial condition,

$$i(0) = \frac{V}{R} \tag{6.7}$$

is chosen then the final steady state solution is determined immediately because

$$i(t) = \frac{V}{R} = constant \tag{6.8}$$

For any other value of $i(0)$ there will be a transient component in the solution as illustrated in Figure(6.1)b. Curve (i) represents choice of the correct initial condition whereas curve (ii) represents the time response for $i(0) = 0$.

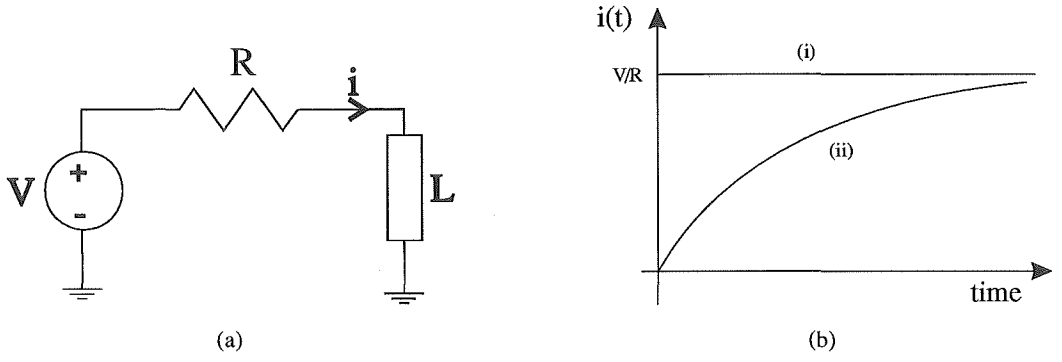


**Figure 6.1** The time response of an R L circuit

### 6.2.2 State Variable Analysis

The "state of the network" is the minimal amount of information necessary at any time to characterise completely the possible future behaviour of the network. State variable analysis leads to a set of first order differential equations, the properties and solutions of which have been comprehensively studied and are suitable for solution by digital computer. Moreover they are readily applicable to time varying and non linear systems [DeRusso *et al.*, 1967][Karni, 1986].

In many applications it is most common to select inductor current and capacitor voltage as the state variables. However the most general and unified approach is to assign inductor flux and capacitor charge as the state variables i.e.

$$V_l = \frac{d}{dt}(\Phi_l(t)) = \frac{dL}{dt} i_l(t) + L\frac{di_l(t)}{dt} \tag{6.9}$$

and

$$i_c = \frac{d}{dt}(Q_c(t)) \tag{6.10}$$

The basic component relations can be combined with network connection relations to derive the standard expression

$$\dot{x} = Ax + Bu \tag{6.11}$$

Linear systems can be solved in closed form in a straight forward manner provided the state variables are independent. For nonlinear systems the equations must be integrated by a numerical method appropriate to the solution. For power system analysis the trapezoidal method has been shown to have good stability and accuracy. Matrix and vector analysis can be used to handle large numbers of variables however the limitation is that the computation becomes slow as the systems of equations become large.

### 6.2.3 The Newton–Raphson iteration formula

Consider a generalised system of differential equations

$$\dot{x} = f(x, t) \tag{6.12}$$

It is known *a priori* that the solution is some periodic function $q$ of period $T$. The problem is to find the initial state such that integrating equation(6.12) over $[0, T]$ gives the periodic function, i.e. $x(0) = x(T)$. This is essentially the two-point boundary value problem postulated by Aprille and Trick and can be considered as a mapping

$$x(0) = M(x(0)) \tag{6.13}$$

where

$$M(x(0)) = \int_0^T f(x, \xi)d\xi + x(0) \tag{6.14}$$

Normal contraction mapping techniques or 'brute force' methods integrate the system equations until the steady state solution is reached. In other words the finishing point of each integration cycle is used as the next starting vector of the new iteration. In this procedure a correction term to be added to the initial state vector is calculated as a function of the residuum of the initial and final state vectors and the mapping derivative over the period. Hence a Newton iteration for the above equation is defined by

$$x_0^{v+1} = x_0^v - [I - M'(x_0^v)]^{-1}[x_0^v - M(x_0^v)] \tag{6.15}$$

where $I$ is the identity matrix, $x_0^v$ is the initial state vector for the $v$th iterate, $x_0^{v+1}$ is the new state estimate and

$$M'(x_0^v) = \frac{\delta x_T}{\delta x_0} \tag{6.16}$$

It is thus necessary to calculate the derivative of the mapping with respect to the initial condition $x_0^v$ along the trajectory $[0, T]$. The term $(I - M'(x_0^v))$ is commonly called the Jacobian (J) or sensitivity matrix. How J is calculated for fixed topology and then switching networks will be discussed in the following sections but first the continuous time case of equation(6.3) is considered.

### 6.2.4 The State Transition Matrix

By substituting equation(6.4) into (6.3) and rearranging yields

$$x = e^{At}x(0) + F(Bu)(I - e^{At}) \tag{6.17}$$

where $e^{At}$ is called the State Transition Matrix (STM) [DeRusso *et al.*, 1967]. To calculate the Jacobian for the purposes of fast steady state techniques the partial derivative of equation(6.17) with respect to $x(0)$ must be computed. This partial derivative is in fact $e^{At}$, the STM of the system.

Consider again the simple linear R–L system embodied by the equation

$$\frac{di}{dt} = -\frac{R}{L}.i + \frac{V}{L} \tag{6.18}$$

The state transition matrix of the system by definition is $e^{-\frac{R}{L}t}$ and hence assuming the initial condition, $i(0) = 0$, then the current after an arbitrary time, $t_o$ will be

$$i(t_o) = \frac{V}{R} - \frac{V}{R}\exp^{-\frac{L}{R}t_o} \tag{6.19}$$

which is also the state vector difference. For the dc solution the period $\frac{1}{t_0}$ is arbitrary. Equation(6.15) can now be used to derive a new estimate of the state vector, i.e.

$$i_o^{new} = \frac{V}{R}.\frac{(1 - \exp^{-\frac{L}{R}t_o})}{(1 - \exp^{-\frac{L}{R}t_o})} = \frac{V}{R} \tag{6.20}$$

The true steady state solution has been determined in one iteration because the system is linear. This trivial example is a precursor to the solution of much more sophisticated sets of equations.

### 6.2.5 Sensitivity Circuit Analysis

An alternative way of deriving the Jacobian of the system is via a sensitivity analysis. Each state variable is individually perturbed by a small amount, $\delta x_o$, and the corresponding change of the state variables at the end of the period $\delta x_T$ is recorded. Hence columns of sensitivities for each state variable can be calculated consisting of the variations divided by the initial perturbation. If there are $N$ state variables this would suggest that $N + 1$ separate cycles of dynamic simulation would be required to build up a Jacobian and it is subject to the hazards of numerical differentiation. Alternatively for a system of $N$ state variables a set of $N$ sensitivity circuits can be derived and solved concurrently with the network solution [Trick *et al.*, 1975] [Perkins *et al.*, 1993] to calculate the Jacobian.

### 6.2.6 The Jacobian of a Discrete State Variable System

For nonlinear equations that cannot be solved in closed form the state equations can be accurately integrated with good stability by the trapezoidal method of equation(6.21)

$$x_{t+h} = x_t + \frac{h}{2}(\dot{x}_t + \dot{x}_{t+h}) \tag{6.21}$$

where $x_t$,$\dot{x}_t$ and $x_{t+h}$,$\dot{x}_{t+h}$ are the discrete state vectors and their derivatives at time $t$ and $t+h$ respectively. The integration step length is $h$. For one integration time step the following equations are true.

$$\dot{x_t} = Ax_t + Bu_t \tag{6.22}$$

$$\dot{x}_{t+h} = Ax_{t+h} + Bu_{t+h} \tag{6.23}$$

By combining equations(6.21), (6.22) and (6.23) an expression results such that the new state vector ($x_{t+h}$) is written as a function of the previous state vector ($x_t$) and source terms.

$$x_{t+h} = \frac{I + \frac{hA}{2}}{I - \frac{hA}{2}}.x_t + \frac{\frac{hB}{2}}{I - \frac{hA}{2}}(u_t + u_{t+h}) \tag{6.24}$$

The term

$$\phi_1 = \frac{I + \frac{hA}{2}}{I - \frac{hA}{2}} \tag{6.25}$$

is the STM for the interval $[t, t+h]$, and letting the source vector term be denoted $f_1$, then

$$x_{t+h} = \phi_1.x_t + f_1 \tag{6.26}$$

If a cycle of integration steps are carried out then

$$x_{t+T} = \Phi.x_t + F \tag{6.27}$$

where

$$\Phi = \phi_{t+T}.\phi_{t+T-h}....\phi_1 \tag{6.28}$$

and $F$ is the collection of forcing functions. $x_{t+T}$ is thus expressed in terms of the initial state vector $x_t$ and the source terms and therefore $\Phi$ is the system mapping derivative of equation(6.16) and hence

$$J = I - \Phi \tag{6.29}$$

It has therefore been shown how the Jacobian can be analytically evaluated for a state variable system with trapezoidal integration. This Jacobian is directly applicable to fixed topology linear and nonlinear solutions. Moreover it is valid for switched circuit analysis if the switching moments are known and independent of the system state variables. In the class of systems to be studied this is a restriction that we will seek to remove by extending the Jacobian to include the sensitivity of the switching instants to the state variables.

### 6.2.7 Switched Network Modeling

Converters can be modeled as periodically switched networks for which the fundamental period of operation is divided into a number of sub intervals. For the *vth* sub interval the topology is constant and the system can be represented by the linear time invariant system of differential state and algebraic switching equations below

$$\dot{x}_v = f_v(x_v, u, t) \tag{6.30}$$

$$g_{v+1}(x_v, u, t_{v+1}) \tag{6.31}$$

The algebraic equation $g_{v+1}$ contains the conditions that determine when a switching instant occurs. Whether or not the STM over two adjoining subintervals, $[t_o, t_2]$, can be expressed as

$$\frac{\delta x(t_2)}{\delta x(t_0)} = \frac{\delta x(t_2)}{\delta x(t_1)} \frac{\delta x(t_1)}{\delta x(t_0)} \tag{6.32}$$

i.e. the product of the state transition matrices for each sub interval

$$\Phi(t_2, t_1)\Phi(t_1, t_0) \tag{6.33}$$

will depend on the nature of the switching instant [Bedrosian and Vlach, 1992].

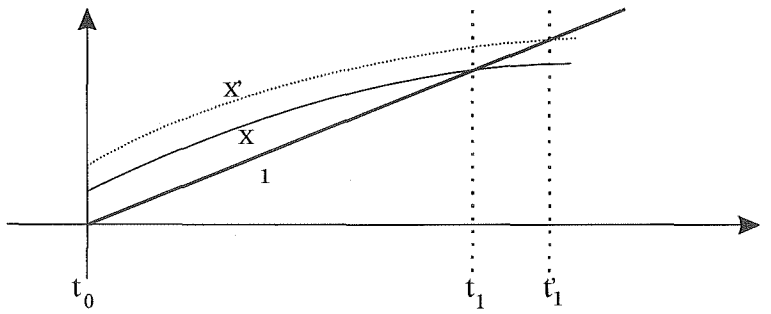


(a) Valve firing

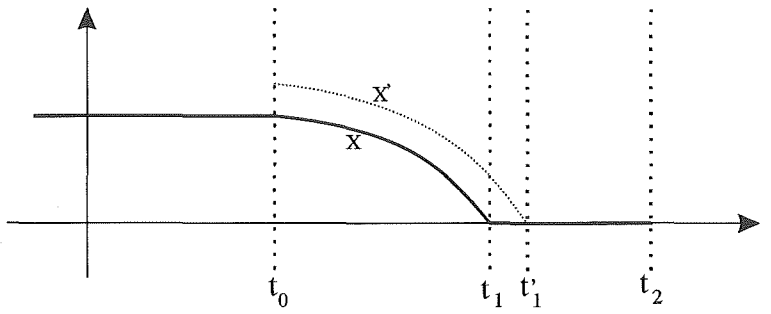


(b) Valve extinction

**Figure 6.2** Sensitivity calculations at switching instants

For many classes of closed loop circuits, in particular the case of the line commutated static converter, the switching moments depend on the state variables at the start of each cycle. There are two types of transition or switching; those directly controlled by external control action and those indirectly or implicitly controlled. To understand the extent of applicability of equation(6.32) for calculating the sensitivity over a switching interval two illustrative examples will be considered.

Figure(6.2)a illustrates the turn on switching instant, $t_1$, of a thyristor. Curve 1 is a ramp function that is compared to a control state variable signal (x) that has also been perturbed from its initial value (x'). The intersections with the ramp function determine the switching instants $t_1$

and $t_1'$ respectively. Clearly a small change in the initial condition at $t_0$ affects the value of x at the respective switching instants. Therefore a variation of x at the switching instant ($\delta x(t_1)$) for a variation of the initial condition ($\delta x(t_0)$) exist and the partial derivatives of equation(6.32) are defined.

In Figure(6.2)b, the end of a commutation period depends on a zero current condition which occurs at $t_1$ and $t_1'$ for unperturbed and perturbed initial conditions respectively. The value of x at the switching instants is the same i.e. $x(t_1) = x(t_1') = 0$ and hence $\delta x(t_1) = 0$. As a consequence the partial derivatives in equation(6.32)

$$\frac{\delta x(t_1)}{\delta x(t_0)} = 0 \tag{6.34}$$

and

$$\frac{\delta x(t_2)}{\delta x(t_1)} = \infty \tag{6.35}$$

is undefined.

For valve extinctions it transpires that it is much more appropriate to calculate, via the chain rule, the sensitivity of the switching instant $t_1$ to variations in the initial conditions i.e.

$$\frac{\delta x(t_2)}{\delta x(t_0)} = \frac{\delta x(t_2)}{\delta x(t_1^+)} \left[ \frac{\delta x(t_1^+)}{\delta t_1} \frac{\delta t_1}{\delta x(t_1^-)} \right] \frac{\delta x(t_1^-)}{\delta x(t_0)} \tag{6.36}$$

The sensitivity at the switching instant expressed in terms of the functions $f$ and $g$ is stated without proof [Grötzbach and Von Lutz, 1986] as

$$\left[ \frac{\delta x(t_1^+)}{\delta t_1} \frac{\delta t_1}{\delta x(t_1^-)} \right] = (I - \Delta f_{v-1} H_v^T) \tag{6.37}$$

where

$$\Delta f_{v-1} = -f_v + f_{v-1} \tag{6.38}$$

and

$$H_v^T = \left( \frac{\delta g_v}{\delta x_{v-1}} \cdot \frac{\delta x_{v-1}}{\delta t_v} + \frac{\delta g_v}{\delta u} \cdot \frac{du}{dt_v} + \frac{\delta g_v}{\delta t_v} \right)^{-1} \cdot \frac{\delta g_v}{\delta x_{v-1}} \tag{6.39}$$

Therefore a complete Jacobian is computed by combining the state transition matrices for each sub interval and the necessary sensitivity matrices at each switching instant. For example, assuming that $t_0$ is the beginning of the period then the cumulative state transition matrix up to point $t_2$ is

$$\Phi(t_2, t_1) = \Phi(t_2, t_1)(I - \Delta f_0 H_1^T)\Phi(t_1, t_0) \tag{6.40}$$

Having outlined the theory required to calculate the Jacobian and its application to systems of differential and algebraic equations, the following section discusses the application of these techniques to the TCS programme.

## 6.3 The Transient Converter Simulation (TCS) Programme

State variable analysis is a popular choice for modeling dynamic converter-machine interactions [Kitchin, 1981],[Arrillaga *et al.*, 1978]. The TCS algorithm employs state variable analysis that is particularly suitable for modeling systems that include 6 or 12 pulse line commutated converters. Other components can be represented such as synchronous machines, filters, transformers, and transmission lines. The integration method is trapezoidal however a variable step length is used to more accurately predict converter switching performance. The phase variable format allows simplistic modeling of unbalanced circuits and easily permits nonlinear effects such as saturation or system disturbances to be included.

The aim is to use TCS to evaluate the operating characteristics of a full twelve pulse Unit connected HVdc system, i.e. representing generators, converters, transmission line, inverter and associated controls. The derivation of capability charts or harmonic studies are too time consuming and impractical when a large variance of component parameters needs to be considered. An approximate initial state can be programmed into the TCS programme from a load flow however as yet no systematic mathematical initialisation approach has yet been incorporated. Various methods can used, for example capacitor voltages can be set to line voltage and the synchronous machine damper winding resistances can be artificially increased to temporarily reduce the machine time constants until the steady state is reached. In spite of these practices however, simulation times are still long.

Given the prominence of the direct connection, it is important that improved means of initialising TCS are sought.

### 6.3.1 The TCS Formulation

The network can contains $n$ nodes interconnecting $l$ inductive branches, $r$ resistive branches and $c$ capacitive branches subject to the following restrictions.

At least one end of each capacitive branch (or subnetwork) is the common reference point of the system.

At least one end of each resistive branch (or subnetwork) is the common reference or a node also having a capacitive connection.

At least one end of each inductive branch (or subnetwork) is the common reference or a node having a resistive or capacitive connection.

The following nodal matrix equation applies,

$$K_{nl}.I_l + K_{nr}.I_r + K_{nc}.I_c = 0 \tag{6.41}$$

where I are the branch current vectors and $K_{ny}$ are the branch node incidence matrices defined such that

$$K_{ny} = \left\{ \begin{array}{l} \text{1 if node } n \text{ is the sending end of branch } y \\ \text{-1 if node } n \text{ is the receiving end of branch } y \\ \text{0 if node } n \text{ is not connected to branch } y \end{array} \right\} \tag{6.42}$$

Three types of nodes are considered, i.e.

$\alpha$ nodes : with at least one capacitive branch
$\beta$ nodes : with at least one resistive branch but no capacitive branches
$\gamma$ nodes : with only inductive branches

Some examples of the typical types of nodes formed in TCS are shown in Figure(6.3).

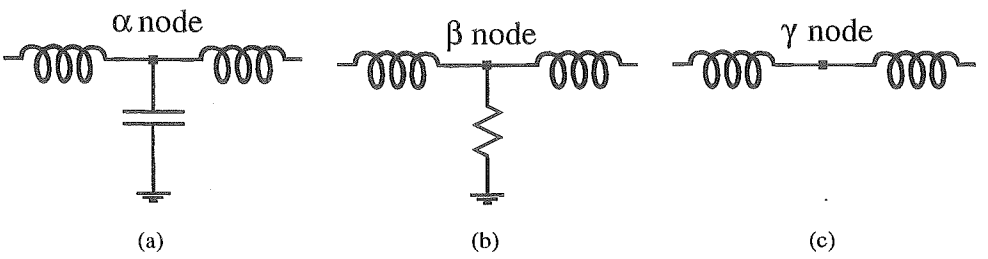


**Figure 6.3** Examples of different node types

Partitioning equation(6.41) according to the restrictions and rearranging:

$$K_{\gamma l}.I_l = 0 \tag{6.43}$$

or

$$K_{\gamma l}.\rho I_l = 0 \tag{6.44}$$

$$K_{\beta r}.I_r + K_{\beta l}.I_l = 0 \tag{6.45}$$

$$K_{\alpha c}.I_c + K_{\alpha r}.I_r + K_{\alpha l}.I_l = 0 \tag{6.46}$$

The following branch equations can be written as matrix expressions for each branch type.

- Inductive branches

$$E_l - L_l.\rho I_l - R_l.I_l + K^t_{l\alpha}.V_\alpha + K^t_{l\beta}.V_\beta + K^t_{l\gamma}.V_\gamma = 0 \tag{6.47}$$

- Resistive branches

$$- R_r.I_r + K^t_{r\alpha}.V_\alpha + K^t_{r\beta}.V_\beta = 0 \tag{6.48}$$

- Capacitive branches

$$C_c\rho(K^t_{c\alpha}V_\alpha) = I_c \tag{6.49}$$

Multiplying through by $K_{\alpha c}$ and substituting equation(6.46) gives

$$K_{\alpha c}C_c\rho(K^t_{c\alpha}V_\alpha) = -K_{\alpha r}I_r - K_{\alpha l}I_l \tag{6.50}$$

Equations(6.47) and (6.49) are integrated to assess the system performance. The dependent vectors $V_\alpha$, $V_\beta$, $V_\gamma$ and $I_r$ are listed below but not derived. It is convenient and practical to use the

inductor flux $\Psi_l$ and charge at a node $Q_\alpha$ as the state variables. The magnitude of the derivatives are of the same order and this improves the numerical stability. It is also the most general form otherwise it would be difficult to account for the sinusoidally varying inductance terms of the synchronous machine. The state space equations are

$$\rho\Psi_l = E_l - R_l I_l + K_{l\alpha}^t.V_\alpha + K_{l\beta}^t.V_\beta + K_{l\gamma}^t.V_\gamma \tag{6.51}$$

$$\rho Q_\alpha = -K_{\alpha r}.I_r - K_{\alpha l}.I_l \tag{6.52}$$

and the dependent variables are interrelated by the following equations:

$$I_l = L_l^{-1}\Psi_l \tag{6.53}$$

$$V_\alpha = C_\alpha^{-1}Q_\alpha \tag{6.54}$$

$$V_\beta = -R_\beta(K_{\beta l}I_l + K_{\beta r}R_r^{-1}K_{r\alpha}^t V_\alpha) \tag{6.55}$$

$$V_\gamma = -L_\gamma K_{\gamma l}L_l^{-1}(E_l - R_l I_l - \rho L_l I_l + K_{r\alpha}^t V_\alpha + K_{l\beta}^t.V_\beta) \tag{6.56}$$

$$I_r = R_r^{-1}(K_{r\alpha}^t V_\alpha + K_{r\beta}^t.V_\beta) \tag{6.57}$$

It is possible to eliminate the dependent vectors from the formulation to simplify the expressions however having them easily accessible allows monitoring of node voltages and branch currents. Furthermore if the dependent equations are eliminated then some matrix sparsity will be lost. The equations as they stand employ simple matrix additions and subtractions when connection matrices are multiplied to vectors. If the dependent quantities are removed then the integration process will require multiplication of non integer values.

### 6.3.2 Controller Implementation

The method used in TCS allows for control simulation by means of user defined block diagrams. The basic elementary functions (integrators, limiters, summers etc) which form the control diagram are read in from a data file [Sankar, 1991]. The controller differential equations are decoupled from the main system but form part of the iterative integration loop. Moreover as they are not physically connected to the power components the controller state variables are not included in the TCS formulation described so far.

### 6.3.3 Converter Operation

At each integration step converter valve voltages and currents are monitored enabling the conduction state can be updated. Converter switching is achieved by modifying the gamma node to branch connection matrix $K_{\gamma l}$. The secondary windings of the converter transformer are rearranged to represent the different conduction states. Figure(6.4) shows an example of two conduction modes of a six pulse bridge circuit.

Equi–distant pulse control is used to minimise non characteristic harmonics. The converter controller model is based on the phase locked oscillator principle that does not depend on the ac voltage waveform for firing angle calculation. Consequently valve firings are predictable in

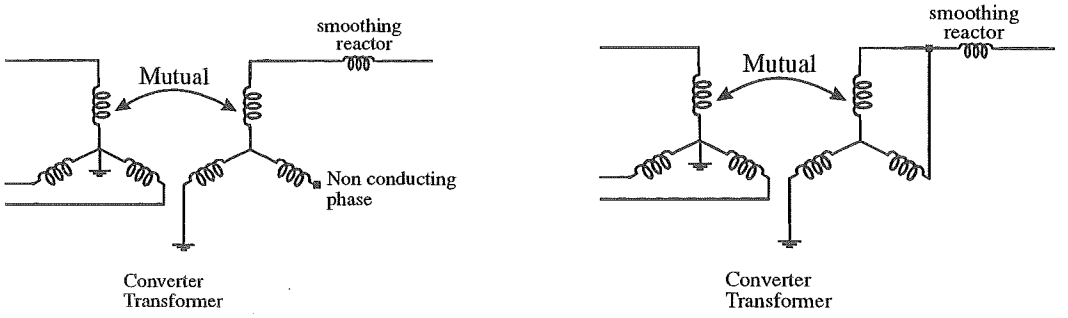


**Figure 6.4** Two specific conduction intervals

advance and the simulation time step can be adjusted to correspond with the switching time. Valve extinction events are not predictable in advance and are thus detected after they have occurred. The state equations are then interpolated back to pinpoint the true valve extinction instant.

### 6.3.4 Calculation of the TCS Jacobian Matrix

The most straightforward manner of calculating the system Jacobian is by rearranging the equations of the formulation into the form of equation(6.1). This involves the substitution of the dependent equations (6.53) to (6.57) into matrix equations (6.51) and (6.52). The substitutions and rearrangements are performed to yield:

$$\begin{bmatrix} \dot{\Psi}_l \\ Q_\alpha \end{bmatrix} = \begin{bmatrix} A_{ll} & A_{l\alpha} \\ A_{\alpha l} & A_{\alpha\alpha} \end{bmatrix} \begin{bmatrix} \Psi_l \\ Q_\alpha \end{bmatrix} + \begin{bmatrix} B_{ll} \\ 0 \end{bmatrix} \begin{bmatrix} u_l \\ 0 \end{bmatrix} \tag{6.58}$$

where

$$A_{ll} = -[I + \kappa][R_l L_l^{-1} + K_{l\beta}^t R_\beta K_{\beta l} L_l^{-1}] - \kappa(\rho L_l) L_l^{-1} \tag{6.59}$$

$$A_{l\alpha} = [I + \kappa][K_{l\alpha}^t C_\alpha^{-1} + K_{l\beta}^t R_\beta K_{\beta r} R_r^{-1} K_{r\alpha}^t C_\alpha^{-1}] \tag{6.60}$$

$$A_{\alpha l} = -K_{\alpha l} L_l^{-1} + K_{\alpha r} R_r^{-1} K_{r\beta}^t R_\beta K_{\beta l} L_l^{-1} \tag{6.61}$$

$$A_{\alpha\alpha} = -K_{\alpha r} R_r^{-1} [I - K_{r\beta}^t R_\beta K_{\beta r} R_r^{-1}] K_{r\alpha}^t C_\alpha^{-1} \tag{6.62}$$

$$B_{ll} = I + \kappa \tag{6.63}$$

$$\kappa = -K_{l\gamma}^t L_\gamma K_{\gamma l} L_l^{-1} \tag{6.64}$$

Thus equations (6.59) to (6.62) represent the $A$ matrix of equation(6.24) and therefore the state transition matrix for each step can be calculated with equation(6.25) which in due course leads to the evaluation of the Jacobian after the inclusion of the sensitivities at the switching instants.

While the terms of this $A$ matrix appear complicated they can be evaluated in a straightforward manner with a series of sparse matrix operations. Moreover many of the terms disappear if there are no $\beta$ or $\alpha$ nodes (something likely in direct connection studies) which greatly simplifies the calculations. For example the 6–pulse converter circuit of Figure(6.5), has no $\alpha$ nodes and the system equations reduce to

$$\dot{\Psi}_l = A_{ll}\Psi_l + B_{ll}u_l \tag{6.65}$$

where

$$A_{ll} = -[I + \kappa][R_l L_l^{-1} + K_{l\beta}^t R_\beta K_{\beta l} L_l^{-1}] \tag{6.66}$$

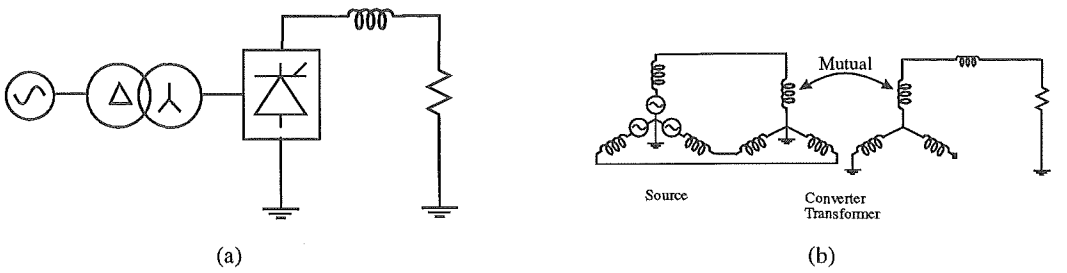


**Figure 6.5** TCS representation of source and converter unit

### 6.3.5 The Steady State Procedure

The Jacobian is calculated in a subroutine added into the conventional simulation programme. A flow diagram of the procedure to calculate the state transition matrix on $[0, T]$ for the initial state vector $x_0^v$ is described in Figure(6.6). The actual integration of the system equations for each time step is not elaborated on here but a full explanation can be found in [Arrillaga *et al.*, 1984].

The minimum computation at each time step is $N^2$ multiplications to update the Jacobian when no switching or step width changes take place. Circuit topology changes will entail the recalculation of the $A$ matrix and consequently a maximum number of Jacobian calculations. The presence of a synchronous machine requires $A$ to be re–evaluated at each time step however the calculations can be minimised by recomputing only the varying portion of the STM matrix.

#### 6.3.5.1 Steady State Convergence Tolerance

The steady state convergence criterion is defined such that $\Delta < \epsilon$ where $\epsilon$ is an arbitrarily specified error tolerance for steady state and

$$\Delta = max\left(\frac{|x_n^0 - x_n^T|}{|x_n^0|}\right)_{n=1}^{n=N} \tag{6.67}$$

is the maximum relative difference of the initial and final state variables. This criterion led to problems however because in some instances a particular state variable would have a numerically small value at the end of each cycle. The relative difference would then not give a true indication of the proximity to the steady state solution.

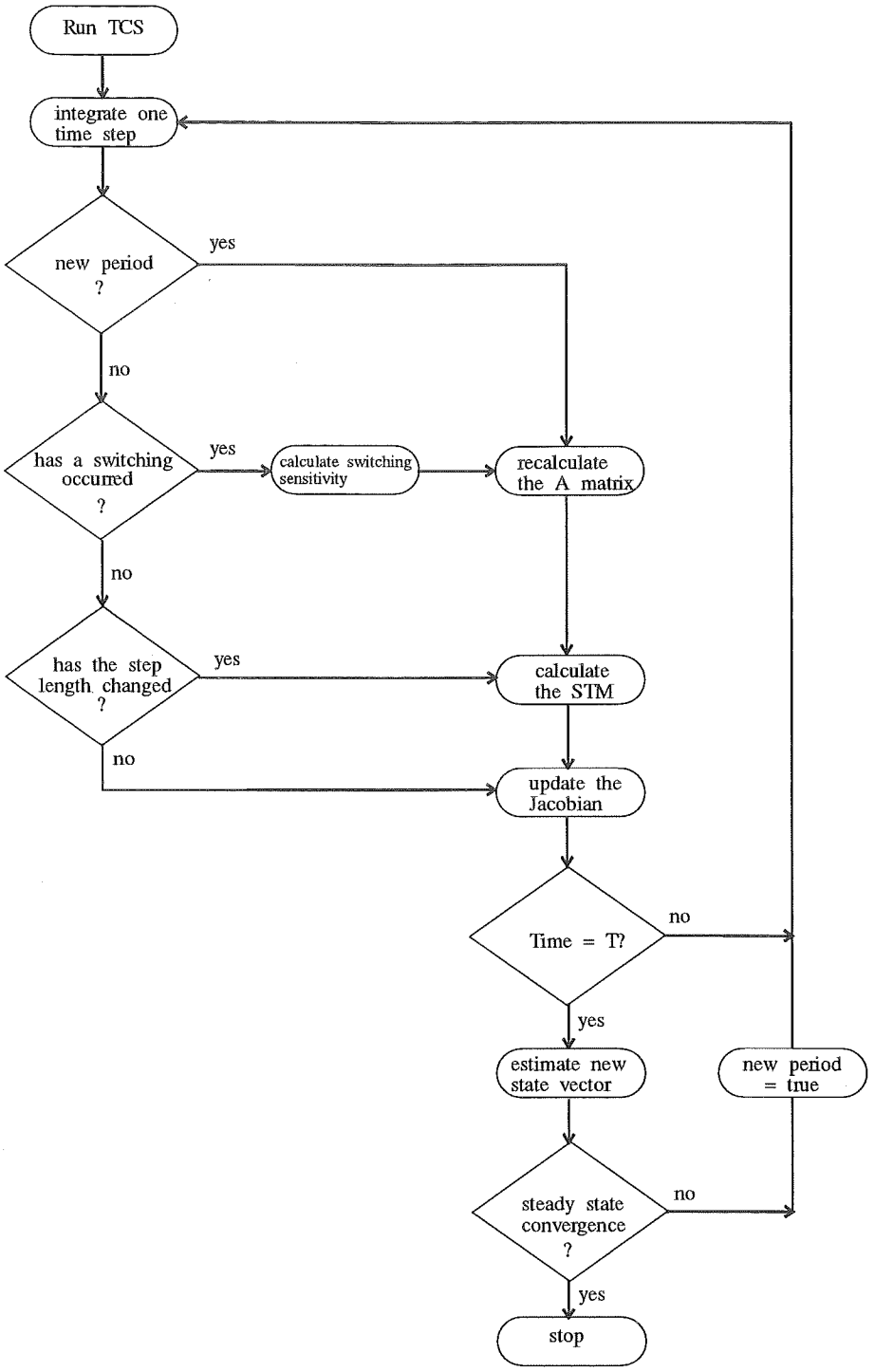


**Figure 6.6** Description of Jacobian Calculation

Instead a slightly less stringent condition is applied to determine if the steady state has been reached. $\Delta$ is defined such that

$$\Delta = \frac{1}{N} \sum_{n=1}^{n=N} |x^O(n) - x^T(n)| \tag{6.68}$$

i.e. the average state vector difference is the measure used to determine proximity to the solution.

### 6.3.6 Fixed topology networks

Once a set of equations has been integrated from [0,T] and the STM $\Phi$ calculated, it becomes necessary to evaluate

$$J^{-1} = (I - \Phi)^{-1}. \tag{6.69}$$

For this to be possible there is a requirement that $J$ and consequently $A$ must have linearly independent rows or columns which is equivalent to saying that the state variables of the system are independent.

This need can be easily shown by considering some simple matrix properties. Each state transition matrix for each time step can be approximated i.e.

$$\phi_1 = \frac{I + \frac{hA}{2}}{I - \frac{hA}{2}} \simeq I + hA \tag{6.70}$$

If the time step is fixed for the moment then over one period, the product of all the state transition matrices will be of the form

$$I + f(hA) \tag{6.71}$$

Hence the inverse of $J$ is effectively the inverse of $(I - (I + f(hA)))$ or the inverse of $f(hA)$. Because $A$ is a matrix of rank less than dimension then $f(hA)$ is also of rank less than dimension and therefore cannot be inverted. Problems arise where $\gamma$ nodes are present since by definition they only have inductive connections and hence there exist inductive cut-sets. Therefore if the circuit has $\gamma$ nodes then $J$ is not immediately invertible because the state variable set of fluxes is not minimised.

A dependent state variable can be expressed as a linear combination of the set of independent state variables. Therefore the Identity matrix at the inversion stage can be modified to take account of any dependencies arising from $\gamma$ nodes. If $I'$ is the modified identity matrix [Grötzbach and von Lutz, 1985] then this leads to $(I' - \Phi)$ being invertible and a new state vector can be estimated.

It is interesting to note that the flux state variable dependence problem could be eliminated if very small capacitances could be used to convert otherwise $\gamma$ nodes to $\alpha$ nodes. In doing so there is no possibility of forming all capacitor loops because the charge at a node is the true state variable [Joosten *et al.*, 1985]. While it is possible to introduce capacitive connections at the system bus bars, it is not readily feasible to replace the internal converter $\gamma$ nodes. In any case the conventional state variable convergence would be significantly affected by the introduction of very small capacitive elements.

### 6.3.7 6–pulse Converter with constant current control

A constant firing angle order combined with equi–distant firing pulses makes the valve turn on events completely external and independent of the system state variables. However the inclusion of CCC allows greater flexibility in the specification of the system operating point and the transient

stability of the initialisation for some systems will be enhanced. Therefore the valve turn on events are now system dependent.

#### 6.3.7.1 Controller Dynamics

As explained in section(6.3.2) the controller state variables are decoupled from the main system equations although they form part of the iterative integration loop. However, for the study of more general systems with closed loop dynamic control the controller state variables must be included as part of the Jacobian solution. One way of including the controller dynamics is to introduce extra components into the power circuit to represent these controller state variables. In this way their sensitivities are automatically and simply included when the system Jacobian is evaluated.

TCS is not adequately configured to achieve the inclusion of the control componentry and hence the controller dynamics that can be implemented will be crude and possibly limit the applicability of these techniques to larger systems. The six pulse circuit of Figure(6.5) is augmented to include an approximate proportional–integral (PI) controller to give a combined circuit illustrated in Figure(6.7)a. The firing angle controller dynamics are thus represented by an R–L branch in parallel with the dc resistive load. The scaled inductor flux, $\Psi_{cd}$, becomes the converter firing angle control signal i.e. $\alpha = k\Psi_{cd}$.

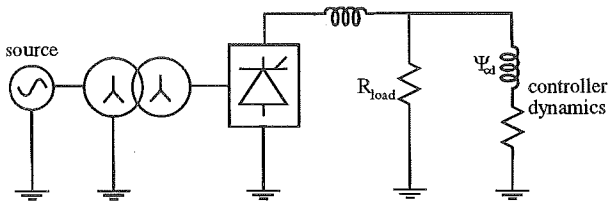


(a) circuit diagram

| | | |
|---|---|---|
| Source | $R_s$ | 0.0001pu |
| | $V_s$ | 1.5 pu |
| | $X_s$ | 0.01 pu |
| Transformer | leakage | 11.5 % |
| | MVA | 187.5 |
| Converter | reactor | 30 pu |
| | $R_{load}$ | 3.0 pu |
| Controller | $X_c$ | 4.25 pu |
| | $R_c$ | 10.0 pu |
| | $\alpha$ | $6.9\Psi_{cd}$ |

(b) circuit values

**Figure 6.7** Explicit Controller Modeling

If the desired controller blocks cannot be implemented in the conventional TCS circuit diagram then the only alternative is to calculate the Jacobian in the normal way and then add additional rows and columns to it for the control state variable sensitivities. An extra routine is then needed to calculate the control state variable sensitivities which could be quite a complex task. The advantage of the former method is that the control state variables are automatically included without extra burden, although some flexibility is lost.

#### 6.3.7.2 Explicit switching equations

For the reasons explained in section(6.2.7) no switching sensitivities are required in addition to the normal STM from one interval to the next for valve switch on events.

The switching equations for valve extinction can be determined by considering the commutating circuit in Figure(6.8) where the out going and in coming currents flow in coils c3 and c5 respectively. The control condition or switching equation, $g_{v+1}(x_v, u, t_{v+1})$, for this particular valve current extinction is

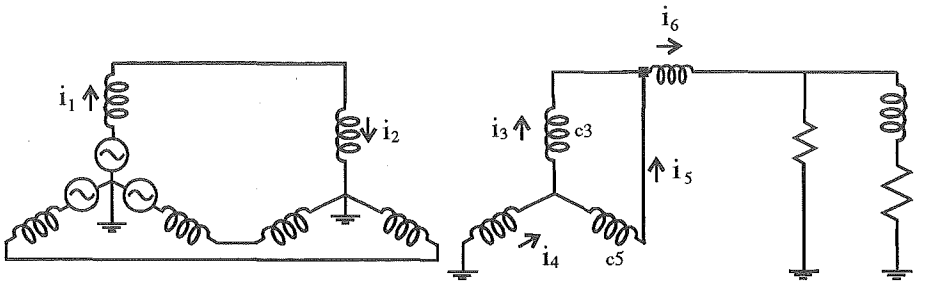


**Figure 6.8** TCS state variable dependence

$$i_3 = 0 \tag{6.72}$$

Conversely other conditions exist that equally well define the end of the commutation period, namely

$$-i_4 = i_5 \tag{6.73}$$

and

$$i_5 = i_6 \tag{6.74}$$

It turns out that the last two conditions are not necessary because by combining them yields the equation

$$-i_4 = i_6 \tag{6.75}$$

which is true throughout the commutation period and is therefore not a control condition that governs switching.

Apart from the control condition $i_3 = 0$ two other valid conditions exist indirectly due to state variable dependence, namely $i_1 = 0$ and $i_2 = 0$. These three relations must be converted to expressions for the system fluxes before the terms of equation(6.39) and subsequently the sensitivity matrix at the switching instant are calculated. In summary, for this valve extinction the components of $g_{v+1}(x_v, u, t_{v+1})$ are

$$i_1 = l_1^{-1}\Psi_1 = 0 \tag{6.76}$$

$$i_2 = l_{22}^{-1}\Psi_2 + l_{23}^{-1}\Psi_3 = 0 \tag{6.77}$$

$$i_3 = l_{32}^{-1}\Psi_2 + l_{33}^{-1}\Psi_3 = 0 \tag{6.78}$$

where the $l_n^{-1}$ terms are members of the system inverse inductance matrix and $\Psi_n$ are the fluxes of each branch. A similar methodology is used to assemble the five other sets of valve extinction switching equations.

#### 6.3.7.3 An approximate inverse Jacobian

The previous section has emphasised the care that is required to determine switching equations complicated by state variable dependence. Moreover with the particular converter switching method of TCS (i.e. as explained in section(6.3.3), the flux state variable dependence changes from one conduction interval to the next. The required $J^{-1}$ cannot be calculated, instead an approximation is sought via a matrix binomial expansion

$$J^{-1} = (I - \Phi)^{-1} = I + \Phi + \Phi^2 + \Phi^3 + ... + \Phi^n \tag{6.79}$$

The equations are arbitrarily initialised at zero and integrated for three cycles to establish a regular valve conduction pattern. The next cycle of integration is then performed and $\Phi$ is computed simultaneously. By estimating $J^{-1}$ from equation(6.79) the new initial state vector is then calculated and used for the next cycle of integration and so forth.

#### 6.3.7.4 Steady State Convergence

Table(6.1) contains a sample of results showing the reduction in simulation times in seconds for the specified steady state accuracy compared to normal integration method. The recomputation of J during every cycle is time consuming and at best only a slight reduction (75 to 58 seconds with 5 terms) in computing time can be achieved for a specified tolerance of 0.001. Moreover at the lower tolerance the use of more Jacobian terms actually consumes more computing time since the solution is being continually *overstepped.* Thus the longer steady state time is not a reflection on the amount of time required for the Jacobian calculation rather a reflection on the manner of the convergence. The use of 6 or more terms for this particular system resulted in a gradual divergence of the solution.

| no. terms of $J^{-1}$ | steady state tolerance | |
|---|---|---|
| | 0.005 | 0.001 |
| 2 | 4.6 | 105.0 |
| 3 | 8.5 | 76.0 |
| 4 | 16.0 | 69.0 |
| 5 | 40.0 | 58.0 |
| normal integration | 3.0 | 75.0 |

**Table 6.1** Reduced simulation times (seconds)

Figure(6.9) is a graphic illustration of the method of convergence to the solution for the dc current and shows the results of using the approximate inverse with 3 and 5 terms of the series. Only the fourth cycle and onwards is shown for clarity. While it appears the use of 3 terms rapidly

achieves a steady state solution, the convergence to the specified error tolerance is more efficient with a larger number of terms.

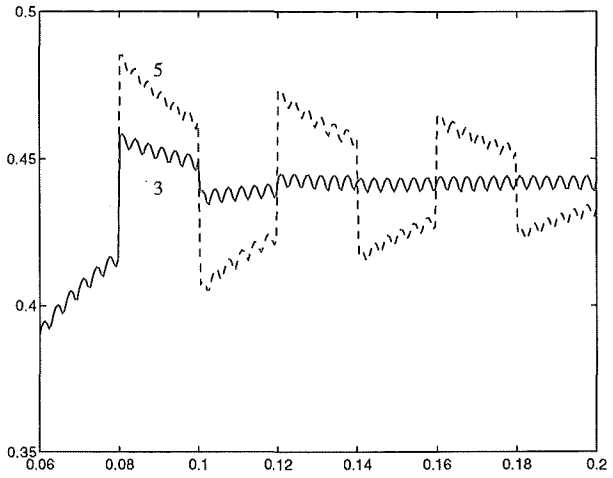


**Figure 6.9** Convergence behaviour of approximate inverse

### 6.3.7.5 Further Computational Efficiency gains

To further reduce the steady state convergence time it was decided to calculate $J^{-1}$ only on the 3rd cycle and use it on subsequent cycles to converge to the solution. This resulted in a more significant reduction in computing speed as shown in table(6.2) without compromising accuracy. For a tolerance of 0.001 a reduction from 75 to 17.6 seconds (a fourfold reduction) was achieved.

| no. terms of $J^{-1}$ | steady state tolerance | |
|---|---|---|
| | 0.005 | 0.001 |
| 2 | 3.4 | 33.5 |
| 3 | 3.8 | 28.4 |
| 4 | 5.5 | 23.0 |
| 5 | 10.6 | 17.6 |
| normal integration | 3.0 | 75.0 |

**Table 6.2** Reduced simulation times, Jacobian calculated only on third cycle

Computation of the Jacobian matrix is very time consuming and ways of reducing the necessary calculations must be exploited. For the 6 pulse converter there are twelve distinct topologies of which 6 are unique. Therefore it is only necessary to calculate the Jacobian for half the cycle. Most of the complexity of the Jacobian calculation comes from the switching sensitivities. It was concluded however that the inclusion of these terms was vital for convergence to the correct steady state solution.

## 6.4 The Electromagnetic Transient Programme (EMTP) Formulation

The EMTP formulation is well known [Dommel, 1969] [Dommel (Editor), 1986] and hence only a brief outline will follow. Capacitors and inductors are represented as discrete Norton equivalents, thus an electrical system can be resolved into a resistive network with voltage and current sources. Figure(6.10) illustrates the conversion of L,C elements to the equivalent resistance and paralleled history term current source.

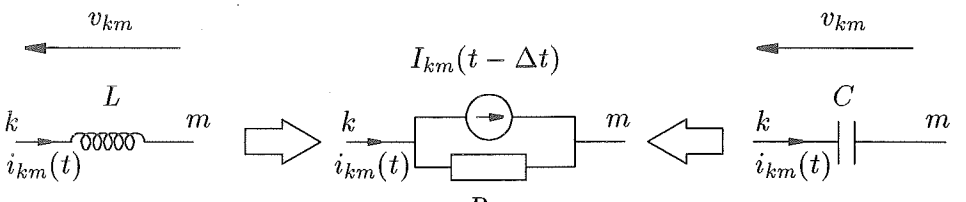


**Figure 6.10** Discretisation of L,C elements using trapezoidal integration method

Nodal analysis is employed and the node voltages are used as the state variables. The branch currents of each component are expressed as functions of the node voltages. A system of network equations can be formed

$$[G][v(t)] = [i(t)] - [I(t-\Delta t)] \tag{6.80}$$

where
$[G]$ is an $n \times n$ symmetrical nodal conductance matrix
$v(t)$ is a vector of nodal voltages
$i(t)$ is a vector of current sources
$I(t-\Delta t)$ is the vector of known history terms.

Furthermore equation(6.80) can be partitioned for systems with known and unknown voltage sources and hence a set simultaneous equations of the form

$$[G][V] = [I] \tag{6.81}$$

can be solved for where $[V]$ is the set of unknown voltages. Compared to state variable techniques the method of solution is very efficient. The presence of transmission lines in particular allows the system to be segregated into a number of smaller subsystems. Moreover many detailed models (e.g. synchronous machine) are interfaced via compensation methods which do not increase the system order.

### 6.4.1 Existing methods of initialising the steady state

The primary purpose of EMTP based packages is transient or dynamic analysis and hence steady state algorithms are usually added in an ad–hoc fashion.

Even so, the writers of EMTP have been active in searching for steady state solutions and means of initialising transient simulations. The nonlinear components are replaced by current sources that contain fundamental and harmonic components. The network is then linear and hence the voltages can easily be determined. The complete solution is then found with two iterative loops. "Power Flow" iterations are used to obtain an approximate fundamental frequency solution. The "Distortion" iterations take harmonics into account. The voltages found from the power flow are used to estimate the flux of the nonlinear element which is then related point by point to the current. Known harmonic sources from converters are used also though it is not clear whether these are fixed injections or continually updated. >From the harmonic current vector the voltage harmonics are straightforwardly evaluated. There are unavoidable discrepancies between this method and the transient simulation that cause small errors when then iterative method is used to initialise the transient solution.

### 6.4.2 The FASST programme

The FASST programme [Usaola and Mayordomo, 1990] is based on the EMTP solution procedure and a steady state initialisation algorithm is incorporated. Instead of the node voltages, the history current sources $I_n(t-\Delta t)$ are treated as the state variables. As in previous sections the final state vector is expressed as a function of the initial state vector and using a Newton algorithm the steady state history current source terms are solved for

$$I^T = \Phi I^0 + F \tag{6.82}$$

where $I_n^0$ and $I_n^T$ are the state variable vectors at the beginning and end of the period respectively. The $\Phi$ matrix is a product of the nodal impedance $Z_n$ and nodal conductance $G_n$ matrices.

The harmonic analysis for a large system combines time and frequency domain techniques [Usaola, 1990]. Solution efficiency reduces as the number of state variables increases (as with conventional state variable approaches) and hence to improve efficiency only the nonlinear elements are modeled in the time domain and the linear circuit is represented in the frequency domain. Newton–Raphson iterations determine the time domain steady state response and are also used for the harmonic balance between time and frequency domains.

### 6.4.3 Newton–Raphson techniques applied to EMTP Algorithms

Two variants of the Newton–Raphson technique have been applied to EMTP type algorithms. In the work of [Perkins *et al.*, 1993] only the analysis of a saturating inductance is presented and it is difficult to judge how easily the sensitivity circuit approach could be extended for example to switching systems. As far as the work of [Usaola and Mayordomo, 1990] is concerned the calculation of the conductance matrix is part of the EMTP solution and therefore imposes no computational overhead as far as the steady state algorithm is concerned. The necessity of evaluating the nodal impedance matrix $Z_n$ does impose constraints both in terms of numerical accuracy, stability and computation time and becomes less practical for large systems. Furthermore at this stage modeling of controller dynamics has not been included.

For EMTP based programmes the calculation of a system Jacobian is complicated by a number of factors. The separation of networks into subsystems would make it much more

difficult to calculate the cross sensitivities of state variables in different subsystems. Non standard user defined subroutines are allowed thereby putting the onus on the user to fully understand the Jacobian calculation in all its subtleties. The EMTDC programme in particular has been developed to a high level of sophistication that allows the combination and interconnection of a diverse range of components. In particular there is now an extensive library of control componentry and a steady state algorithm using the techniques already described would have to take into account the state variables of a potentially highly nonlinear control structure.

## 6.5 Conclusions

The fact that computer dynamic simulation programmes require prohibitive amounts of computing time has stimulated research into seeking means of improving the steady state solution efficiency. The basis, theory and application of Newton–Raphson numerical techniques to state of the art dynamic simulation algorithms has been outlined in this chapter.

A steady state algorithm was developed and incorporated into an existing simulation package TCS. The prime limitation relates to overcoming the state variable dependence inherent in the system of equations which poses difficulties in the inversion of the Jacobian. Furthermore the automatic calculation of valve extinction sensitivities requires more research. The solution of fixed topology networks presents no problems because the state variable dependence can be taken into account. While this is encouraging, the analysis of these types of circuits is trivial and not worth mentioning because the switched network problem is of greater importance.

For systems containing converters the Jacobian could not be fully inverted and therefore a binomial approximation was used instead. With this approximation the convergence of the iterates was slow however a clear and significant reduction in the steady state convergence times was demonstrated. The inclusion of control systems is desirable to fix the steady state operating point as well as provide start up transient stability. The controller state variables must therefore be included in the Jacobian and therefore as part of the iterative solution. Although the control and power network equations are decoupled, this can be best achieved by incorporating controller componentry in the power network. The explicit representation of controller dynamics in this fashion for the TCS programme (and many other programmes) will restrict the controller complexity and ultimately the size of the system to be simulated.

For systems having mutually coupled circuits, such as transformers and synchronous machines, the elements of the characteristic system matrices will be in general non zero with few opportunities to exploit matrix sparsity. As the dimension of the system increases then so the efficiency of the steady state procedure will reduce because the number of Jacobian calculations is proportional to the square of the number of state variables. While the TCS numerical integration is economical, the Jacobian calculation is less efficient because there is a non minimal set of state variables.

In systems where a very small time step is required and many iterations needed at each integration time step to satisfy state variable convergence tolerances, then fast steady state techniques will be hugely beneficial as the additional Jacobian calculation time is small compared to one cycle of integration time. In systems such as these even an approximate initialisation procedure would be beneficial.

While Newton–Raphson algorithms have been successfully applied in the past to EMTP based formulations, the implementation of general algorithms is limited by circuit complexity.

# Chapter 7
# CONCLUSIONS

Direct Connection Studies

Direct connection schemes are attractive alternatives for the rectifying end of conventional HVdc transmission systems when the generators exclusively supply the HVdc converters. Significant cost savings are realised by removing the filters, transformer banks and associated switchyards. The lower number of components should improve the reliability and reduce the costs. Furthermore the frequency of generation is no longer tied and hence may be used to optimise the conversion of water to electrical energy.

Of the direct connection schemes, the unit connection is the simplest although it requires a higher number of converter transformers and valve groups. On the other hand the group connection, while needing synchronous generation and machine circuit breakers, has only one converter group and subsequently superior efficiency and reactive power characteristics at reduced power settings.

The first direct connection harmonic test results have been presented. The measured harmonic current levels were below specified generator ratings. Dynamic simulation models accurately predicted the levels of harmonic currents although the harmonic voltages were sensitive to the machine subtransient parameters. It is recommended that specialised harmonic measurement equipment (such as CHART) be available for future tests.

The Series Excitation

A novel extension of the direct connection principle has been proposed where the dc current is fed back in series to provide the excitation of the generators. Further simplification and cost savings are achieved by removing expensive excitation systems, controls and by reducing the size of the smoothing reactor. In the absence of separate excitation systems the rectifier station is controlled entirely by the converter.

This arrangement was shown to provide natural field forcing to aid inverter transient stability although it suffered from reduced efficiency at lower power settings because the levels of excitation naturally decrease with the dc current. However because the dc line current typically exceeds the machine excitation requirement, a new field winding arrangement for multiple machines, called the series–group connection, was developed to boost the dc voltage at low power levels.

In the test system examined the series–group arrangement had a better transmission efficiency than the unit connection in the low to mid power range as well as a reduced peak inverter

reactive power consumption. To improve the series–group voltage profile further, a modified field saturation characteristic was employed allowing the dc voltage to be maintained at the nominal level. This achieved significant gains in efficiency and a reduction of inverter reactive power demand at the expense of higher valve and rotor costs.

The main operational disadvantage of the series–group arrangement relates to the complete removal of a machine from service. Under an outage condition the link capability is reduced because a healthy paired machine must also be removed to ensure equal current sharing between the remaining field windings.

A modified version of the EMTDC machine model was proposed to investigate the dynamic responses of the series excitation. This new model was complemented by the results from an independent state variable dynamic simulation programme. It was demonstrated that the series excitation could successfully clear a dc line fault. The fault impedance of the machine field circuit will be a fraction of the usual converter smoothing reactance. Therefore a measure of independent smoothing inductance is still needed. Even so, the induced field voltage significantly increases the severity of the fault resulting in higher peak fault currents.

Efficient dynamic simulation initialisation procedures

Dynamic simulation is becoming an increasingly used design tool to analyse the steady state and transient behaviour of complex systems. Even though computer speed and storage capabilities are continually advancing, the initialisation of the system equations to achieve a steady state response or as a precursor to a transient (i.e fault) study is very time consuming. The most common form of initialisation process, is simply to integrate the system equations until all start up transients have decayed.

Fast steady state techniques have previously been applied to traditional state variable formulations. The cases studied have been rather specific and the wider application of these techniques will be limited by a number of factors. Conventional state variable techniques are only efficient for small systems. The integration and Jacobian calculation becomes slow as the number of state variables increases.

The application of the Newton–Raphson technique to speed the determination of the steady state for differential equation analysis has been discussed with a view to switched network modeling. The technique was applied to the TCS programme with the aim to reduce simulation times for direct connection studies. Due to inductor flux state variable dependence (an integral feature of the TCS algorithm) that could not be eliminated, only an approximate estimate of the inverse Jacobian could be computed. This approximation led to marginally faster steady state convergence compared to conventional brute force integration.

The use of Newton–Raphson techniques for EMTP algorithms has been discussed and given serious consideration. EMTP techniques are very efficient solvers for large systems especially when the network can be divided into smaller decoupled sub systems. However computation of the system Jacobian is complicated indeed due to the need to determine cross sensitivities of state variables in different subsystems. Moreover the proliferation of user defined componentry complicates the goal of applying a generalised steady state algorithm for EMTP techniques.

Suggestions for future work

A more complete understanding and appreciation of the behaviour of the directly connected synchronous machine must be attained. Dynamic simulation models typically have a simplified rotor circuit representation that may not be sufficient to fully assess directly connected generator losses. On the other hand finite element analysis is an excessively time consuming means of evaluating damper current flows, although it is undoubtably the most accurate. A comprehensive representation of the salient synchronous machine, accounting for resistively coupled multiple damper circuits, can be found in [Rankin, 1945b]. The circuit parameters are derived from the physical construction of the field poles.

This model was intended to be implemented on network analysers but there is no reason why it couldn't be incorporated into an EMTDC type simulation package. Moreover a laboratory test system could be constructed where the field is stationary with respect to a rotating stator. In this way individual damper bar currents could be measured and compared to theoretical results. This in turn may lead to conclusions regarding the necessity of finite element techniques.

The continuation of harmonic tests at Benmore provides an exciting opportunity to collect more direct connection data. The availability of the CHART system would be beneficial in two respects. Firstly CHART would be field tested, and experience in this application may point to areas of improvement. The automatic collection of the harmonic waveforms would be a vast improvement on the previous field tests where some difficulties were experienced in capturing and analysing the harmonic data.

Other methods of provided the excitation of direct connection schemes, such as extracting a dc ripple voltage, should be investigated. A steady state analysis of such an arrangement has already been proposed however dynamic simulation would be required to ascertain the transient performance. To this end the modified machine model of section(5.2.2) could be readily applied to such a situation.

# REFERENCES


[Adkins and Harley 1975]
Adkins, B. and Harley, R.G. *The General Theory of A.C Machines: Application to Practical Problems*, Chapman and Hall London.

[Anderson and Fouad 1977]
Anderson, P.M. and Fouad, A.A. *Power System Control and Stability*, Vol. 1, The Iowa State University Press, Ames, Iowa USA.

[Aprille and Trick 1972]
Aprille, T.J. and Trick, T.N. "Steady State Analysis of Nonlinear Circuits with Periodic Inputs," *Proceedings of the IEEE*, Vol. 60, No. 1, January, pp. 108–114.

[Aprille, JR and Trick 1972]
Aprille, JR, T.J. and Trick, T.N. "A computer Algorithm to Determine the Steady–State Response of Nonlinear Oscillators," *IEEE Transactions on Circuits and Systems*, Vol. 19, No. 4, July, pp. 354–359.

[Arrillaga 1983]
Arrillaga, J. *High Voltage Direct Current Transmission*, Peter Peregrinus, London.

[Arrillaga *et al.* 1977]
Arrillaga, J., Al-Khashali, H.J. and Campos-Barros, J.G. "General formulation for dynamic studies in power systems including static convertors," *Proceedings of the IEE*, Vol. 124, No. 11, November, pp. 1047–1051.

[Arrillaga *et al.* 1978]
Arrillaga, J., Campos Barros, J.G. and Al-Khashali, H.J. "Dynamic Modelling of Single Generators Connected to HVDC Convertors," *IEEE Transactions on Power Apparatus and Systems*, Vol. 97, No. 4, July, pp. 1018–1029.

[Arrillaga *et al.* 1984]
Arrillaga, J., Arnold, C.P. and Harker, B.J. *Computer Modelling of Electrical Power Systems*, John Wiley and Sons, New York.

[Arrillaga *et al.* 1991]
Arrillaga, J., Sankar, S., Watson, N.R. and Arnold, C.P. "Operational Capability of generator–HVDC Convertor units," *IEEE Transactions on Power Delivery*, Vol. 6, No. 3, July, pp. 1171–1176.

[Arrillaga *et al.* 1992]
Arrillaga, J., Sankar, S., Arnold, C.P. and Watson, N.R. "Characteristics of unit-connected

HVDC generator convertors operating at variable speeds," *Proceedings of the IEE, Part C*, Vol. 139, No. 3, May, pp. 295–299.

[Arrillaga *et al.* 1993a]
Arrillaga, J., Macdonald, S., Watson, N.R. and Watson, S. "Direct Connection of Series Self–Excited Generators and HVDC Converters,", IEEE Winter Power Meeting, Columbus, Ohio, February.

[Arrillaga *et al.* 1993b]
Arrillaga, J., Macdonald, S., Watson, N.R. and Watson, S. "Series Self-Excited HVDC Generation," *Proceedings of the IEE, Pt C*, Vol. 140, No. 2, March, pp. 141–146.

[Arrillaga *et al.* 1993c]
Arrillaga, J., Camacho, J.R., Macdonald, S.J. and Arnold, C.P. "Operating characteristics of unit and group connected generator–HVDC converter schemes," *Proceedings of the IEE, Part C*, Vol. 140, No. 6, November, pp. 503–508.

[Bedrosian and Vlach 1992]
Bedrosian, D.G. and Vlach, J. "An Accelerated Steady State Method for Networks with Internally Controlled Switches," *IEEE Transactions on Circuits and Systems*, Vol. 39, No. 7, July, pp. 520–530.

[Bowles 1981]
Bowles, J.P. "Multiterminal HVDC Transmission Systems Incorporating Diode Rectifier Stations," *IEEE Transactions On Power Apparatus and Systems*, Vol. 100, No. 4, April, pp. 1674–1678.

[Calverley *et al.* 1973]
Calverley, T.E., Ottaway, C.H. and Tufnell, D.H.A. "Concept of a Unit Generator Converter Transmission System," *IEE Conference on High Voltage dc and ac Transmission, London.*

[Canay 1969]
Canay, I.M. "Calculation of rotor quantities and exact equivalent diagrams of the synchronous machine," *IEEE Transactions on Power Apparatus and Systems*, Vol. 88, No. 7, July, pp. 1114–1120.

[CIGRE Joint Working Group 11/14-09 1993]
CIGRE Joint Working Group 11/14-09 "HVdc Unit Connected Generators," *ELECTRA*, Vol. 149, August.

[Colon and Trick 1973]
Colon, F.R. and Trick, T.N. "Fast Periodic Steady–State Analysis for Large–Signal Electronic Circuits," *Journal of Solid-State Circuits*, Vol. 8, No. 4, August, pp. 260–269.

[Concordia 1951]
Concordia, C. *Synchronous Machines Theory and Performance*, John Wiley and Sons Inc, New York.

[DeRusso *et al.* 1967]
DeRusso, Roy and Close *State Variables for Engineers*, John Wiley and Sons NY.

[Dommel 1969]
Dommel, H.W. "Digital Computer Solution of Electromagnetic Transients in Single and Multiphase Networks," *IEEE Transactions on Power Apparatus and Systems*, Vol. 88, No. 4, April, pp. 388–395.

[Dommel (Editor) 1986]
Dommel (Editor), H.W. *Electromagnetic Transients Program Reference Manual*, BPA, Portland, Oregan, USA.

[El-Bidweihy and Al-Badwaihy 1982]
El-Bidweihy, E.A. and Al-Badwaihy, K. "Steady State Analysis of Static Power Convertors," *IEEE Trans on Industry Applications*, Vol. 18, No. 4, July, pp. 405–410.

[Grötzbach and von Lutz 1985]
Grötzbach, M. and von Lutz, R. "Evaluation of Converter Harmonics in Power Systems by a Direct and Analytically based State Variable Approach," *Proceedings of the EPE*, Vol. 1, pp. 2.153–2.158.

[Grötzbach and Von Lutz 1986]
Grötzbach, M. and Von Lutz, R. "Unified Modeling of Rectifier–Controlled DC-Power Supplies," *IEEE Transactions on Power Electronics*, Vol. 1, No. 2, April, pp. 90–100.

[Hungsasutra and Mathur 1989]
Hungsasutra, S. and Mathur, R.M. "Unit Connected Generator with Diode Valve Rectifier Scheme," *IEEE Transactions on Power Systems*, Vol. 4, No. 2, May, pp. 538–543.

[Ingram 1988]
Ingram, L. "A Practical Design for an Integrated HVDC Unit Connected Hydro Electric Power Station," *Transactions of the IEEE*, Vol. 3, No. 4, October, pp. 1615–1621.

[Jaquet 1986]
Jaquet, M. "The Pan Jia Kou Pumped Storage Station, Part I: Hydraulic Equipment,", 4th ASME International Hydro Power Fluid Machinery Symposium, December.

[Joosten *et al.* 1985]
Joosten, A.P.B., Arnold, C.P. and Arrillaga, J. "State Variable Dependence in State Space Analysis of Electric Power Systems," *Modelling Simulation and Control, A, AMSE Press*, Vol. 2, No. 3, pp. 51–63.

[Karni 1986]
Karni, S. *Analysis of Electrical Networks*, John Wiley and Sons.

[Kettleborough *et al.* 1983]
Kettleborough, J.G., Smith, I.R. and Fanthome, B.A. "Simulation of a dedicated aircraft generator supplying a heavy rectified load," *Proceedings of the IEE, Part B*, Vol. 139, No. 6, November, pp. 431–435.

[Kimbark 1968]
Kimbark, E.W. *Power System Stability: Synchronous Machines*, Dover Publications, New York.

[Kitchin 1981]
Kitchin, R.H. "New method for digital-computer evaluation of converter harmonics in power systems using state–variable analysis," *Proceedings of the IEE, Part C*, Vol. 128, No. 4, July, pp. 196–207.

[Kohler 1967]
Kohler, A. "Earth Fault clearing on HVDC Transmission Line with special consideration of the properties of the DC Arc in free air," *IEEE Transactions on Power Apparatus and Systems*, pp. 298–304.

[Lewis 1958]
Lewis, W.A. "A Basic Analysis of Synchronous Machines–Part 1," *American Institute of Electrical Engineers*, Vol. 77, August, pp. 436–455.

[Long *et al.* 1990]
Long, W.F., Reeve, J., McNichol, J.R., Holland, M.S., Taisne, J.P., LeMay, J. and Lorden, D.J. "Application Aspects of Multiterminal DC Power Transmission," *IEEE Trans. on Power Delivery*, Vol. 5, No. 4, pp. 2084–2087.

[Luciano and Strollo 1990]
Luciano, A.M. and Strollo, A.G.M. "A Fast Time–Domain Algorithm for the Simulation of Switching Power Converters," *IEEE Transactions on Power Electronics*, Vol. 5, No. 3, July, pp. 363–370.

[Manitoba HVdDC Research Centre 1994]
Manitoba HVdDC Research Centre "PSCAD Manuals,", January.

[Manitoba Hydro 1988]
Manitoba Hydro *The EMTDC Users Manual*, Canada.

[Miller 1992]
Miller, A.J.V. "Multichannel Continuous Harmonic Analysis in Real Time," *IEEE Transactions on Power Delivery*, Vol. 7, No. 4, October, pp. 1813–1819.

[Miner 1941]
Miner, D.F. *Insulation of Electrical Apparatus*, McGraw Hill Book Company Inc, New York, 1st ed.

[Naidu and Mathur 1989]
Naidu, M. and Mathur, R.M. "Evaluation of Unit Connected, Variable Speed, Hydropower Station for HVDC Power Transmission," *IEEE Transactions on Power Systems*, Vol. 4, No. 2, May, pp. 668–676.

[O'Brien 1993]
O'Brien, M.T. "Letter regarding the Operational Capabilities of the Benmore Generators,", March.

[Ooi *et al.* 1980]
Ooi, B.T., Menemenlis, N. and Nakra, H.L. "Fast Steady State solution for HVDC Analysis," *IEEE Transactions on Power Apparatus and Systems*, Vol. 99, No. 6, November, pp. 2453–2459.

[Park 1929]
Park, R.H. "Two–Reaction Theory of Synchronous Machines - Generalized Method of Analysis - Part I," *AIEE Transactions*, Vol. 48, pp. 716–727.

[Perkins *et al.* 1993]
Perkins, B.K., Marti, J.R. and Dommel, H.W. "Nonlinear Elements in the EMTP: Steady–State Initialization," *IEEE Summer Power Meeting, Seattle, USA.*

[Rafian and Laughton 1976]
Rafian, M. and Laughton, M.A. "Determination of synchronous–machine phase–co–ordinate parameters," *Proc IEE*, Vol. 123, No. 8, August, pp. 818–824.

[Rankin 1945a]
Rankin, A.W. "Per–Unit Impedances of Synchronous Machines," *American Institute of Electrical Engineers*, Vol. 64, August, pp. 569–573.

[Rankin 1945b]
Rankin, A.W. "The Direct and Quadrature–Axis Equivalent Circuits of the Synchronous Machine," *American Institute of Electrical Engineers*, Vol. 64, December, pp. 861–868.

[Salgado *et al.* 1986]
Salgado, E., Lima, A.G.G., Pilotto, L.A.S., Szechtman, M., Guarini, A.P. and Roitman, M. "Technical and Economic Aspects of the use of HVDC Converters as Reactive Power Controllers,", International Conference on Large High Voltage Electric Systems. Proceedings of the 31st session, group 14 , paper 06 Paris.

[Sankar 1991]
Sankar, S. *Dynamic Simulation of AC/DC Systems with reference to Converter Control and Unit Connection*, PhD thesis, University of Canterbury.

[Sarma 1979]
Sarma, M.S. *Synchronous Machines (Their Theory, Stability, and Excitation Systems)*, Gordon and Breach Science Publishers, New York.

[Skelboe 1982]
Skelboe, S. "Time–Domain Steady–State Analysis of Nonlinear Electrical Systems," *Proceedings of the IEEE*, Vol. 70, No. 10, October, pp. 1210–1227.

[Sudhoff and Wasynczuk 1993]
Sudhoff, S.D. and Wasynczuk, O. "Analysis and Average–Value Modeling of Line–Commutated Converter–Synchronous Machine Systems," *IEEE Transactions on Energy Conversion*, Vol. 8, No. 1, March, pp. 92–99.

[Trick *et al.* 1975]
Trick, T.N., Colon, F.R. and Fan, S.P. "Computation of Capacitor Voltage and Inductor Sensitivities with Respect to Initial Conditions for the Steady–State Analysis of Nonlinear Periodic Circuits," *IEEE Transactions on Circuits and Systems*, Vol. 22, No. 5, May, pp. 391–396.

[Uhlman 1975]
Uhlman, E. *Power Transmission by Direct Current*, Springer–Verlag.

[Usaola 1990]
Usaola, J. *Regimen permanente de sistemas electricos de potencia con elementos no lineales mediante un procedimiento hibrido de analisis en los dominios del tiempo y de la frecuencia*, PhD thesis, Universidad Politecnica de Madrid.

[Usaola and Mayordomo 1990]
Usaola, J. and Mayordomo, J.G. "Fast Steady State Technique for Harmonic Analysis," *ICHIPS conference Budapest*, October.

[Ushida *et al.* 1992]
Ushida, A., Adachi, T. and Chua, L.O. "Steady–State Analysis of Nonlinear Circuits Based on Hybrid Methods," *IEEE Transactions on Circuits and Systems*, Vol. 39, No. 8, August, pp. 649–661.

[Van Den Eijnde and Schoukens 1990]
Van Den Eijnde, E. and Schoukens, J. "Steady State Analysis of a Periodically Excited Nonlinear System," *IEEE Transactions on Circuits and Systems*, Vol. 37, No. 2, February, pp. 232–241.

[Verghese *et al.* 1986]
Verghese, G.C., Elbuluk, M.E. and Kassakian, J.G. "A General Approach to Sampled–Data Modeling for Power Electronic Circuits," *IEEE Transactions on Power Electronics*, Vol. 1, No. 2, April, pp. 76–88.

[Woodford *et al.* 1983]
Woodford, D.A., Gole, A.M. and Menzies, R.W. "Digital Simulation of DC Links and AC Machines," *IEEE Transactions on Power Apparatus and Systems*, Vol. 102, No. 6, June, pp. 1616–1623.

[Yikang He and Yaoming Wang 1990]
Yikang He and Yaoming Wang "The State–Space Analysis of Excitation Regulation of Self–Controlled Synchronous Motor with Constant Margin–Angle Control," *IEEE Transactions on Power Electronics*, Vol. 5, No. 3, July, pp. 269–275.

[Zavahir 1992]
Zavahir, J.M. *Interfacing State Variable HVDC Models with Electromagnetic Transient Simulation Programs*, PhD thesis, University of Canterbury.

[Zein 1980]
Zein, D.A. "On the Periodic Steady–State Problem by the Newton Method," *IEEE Transactions on Circuits and Systems*, Vol. 27, No. 12, December, pp. 1263–1268.

# Appendix A

# BENMORE TERMINAL DATA

Generators

| | | | |
|---|---|---|---|
| Rating | | 112.5 | MVA |
| Voltage | | 16.0 | kV |
| Direct axis reactance | $X_d$ | 1.168 | pu |
| Direct axis transient reactance | $X'_d$ | 0.264 | pu |
| Direct axis subtransient reactance | $X''_d$ | 0.174 | pu |
| Quadrature axis reactance | $X_q$ | 0.672 | pu |
| Quadrature axis subtransient reactance | $X''_q$ | 0.19 | pu |
| Direct axis transient open circuit time constant | $T'_{do}$ | 8.7 | seconds |
| Direct axis subtransient open circuit time constant | $T''_{do}$ | 0.087 | seconds |
| Quadrature axis subtransient open circuit time constant | $T''_{qo}$ | 0.132 | seconds |
| Armature leakage reactance | $X_l$ | 0.15 | pu |
| Armature resistance | $R_a$ | 0.0042 | pu |

Note: $X''_q$, $T''_{do}$ and $X_l$ are estimated values.

Converter Transformers

| | |
|---|---|
| Type | Delta–Wye and Delta–Delta |
| Rating | 187.5 MVA |
| Voltage | 16–110 kV |
| Leakage | 11.2 and 11.5 % respectively |
| Tap | ± 2.5 % |

Transmission Line

| | |
|---|---|
| Nominal Voltage | 270kV |
| Nominal Current | 2kA |
| Resistance | 5.93 Ohms |

# Appendix B

# SERIES EXCITATION SYSTEM DATA

Generator

| | | | |
|---|---|---|---|
| Rating | | 90 | MW |
| Terminal Voltage | | 13.8 | kV |
| Direct-axis reactance | $X_d$ | 1.18 | pu |
| Direct-axis damper reactance | $X_{kd}$ | 1.24 | pu |
| Quadrature-axis reactance | $X_q$ | 1.05 | pu |
| Quadrature-axis damper reactance | $X_{kq}$ | 1.05 | pu |
| Field Reactance | $X_f$ | 1.27 | pu |
| Direct-axis damper resistance | $R_{kd}$ | 0.021 | pu |
| Direct-axis sub-transient reactance | $X_d''$ | 0.145 | pu |
| Quadrature axis damper resistance | $R_{kq}$ | 0.036 | pu |
| Quadrature axis sub-transient reactance | $X_q''$ | 0.145 | pu |
| Field resistance | $R_f$ | 0.00068 | pu |
| Armature leakage reactance | $X_l$ | 0.075 | pu |
| Armature resistance | $R_a$ | 0.0035 | pu |
| Direct-axis open circuit time constant | $T_{do}$ | 0.042 | s |

Excitation characteristic

| | |
|---|---|
| $k_f = 20.75V/A$ | (linear part) |
| $k_f^s = 0.5V/A$ | (saturated part) |
| $I_{sat} = 1kA$ | (knee point) |

Converter:

| | |
|---|---|
| Type | 12 pulse |
| Nominal Current | $I_{dc} = 1kA$ |
| Nominal Voltage | $V_{dc} = 40kV$ |

Converter Transformers:

| | |
|---|---|
| Rating | 50 MVA |
| Reactance | $x_t = 5percent$ |
| Voltage | $13.8/30.36kV$ |

# Appendix C

# DATA PREPARATION

A salient generator based on that used by [Sankar, 1991] is given below in Appendix C.1, a more comprehensive collection of data can be found in [Anderson and Fouad, 1977]. The value of $X_d''$ was increased from 0.2 to 0.3 to ensure the existance of a direct axis damper circuit. This data can be directly entered into the EMTDC algorithm. The equivalent TCS generator data is calculated in Appendix C.2 and from further assumptions the series excited pu values are determined in Appendix (C.3). To differentiate fron pu values, real quantities such as Henrys will be depicted in a bold type face.

## C.1 Salient Machine parameters

| | | | |
|---|---|---|---|
| Rating | | 100 | MVA |
| Voltage | | 13.8 | kV |
| Direct axis reactance | $X_d$ | 1.2 | pu |
| Direct axis transient reactance | $X_d'$ | 0.3667 | pu |
| Direct axis subtransient reactance | $X_d''$ | 0.3 | pu |
| Direct axis transient open circuit time constant | $T_{do}'$ | 7.64 | s |
| Direct axis subtransient open circuit time constant | $T_{do}''$ | 0.0633 | s |
| Quadrature axis reactance | $X_q$ | 0.8 | pu |
| Quadrature axis subtransient reactance | $X_q''$ | 0.367 | pu |
| Quadrature axis subtransient open circuit time constant | $T_{qo}''$ | 0.132 | s |
| Leakage reactance | $X_l$ | 0.2 | pu |
| Armature resistance | $R_a$ | 0.005 | pu |
| Zero sequence reactance | $X_0$ | 0.05 | pu |
| Field current that gives rated open circuit voltage | | 0.5 | kA |

The same transformers as in Appendix A were used in the series excitation comparison between TCS and EMTDC.

## C.2 The TCS Machine Inductance Matrix.

TCS represents the stator of the machine as a set of sinusoidally varying self and mutual inductance parameters. Since the frequency is normalised to one, values of inductance and impedance become

equal and there is not need to differentiate between them further. The stator self, mutual and 2nd harmonic terms are determined from the manufacturer's DQO data with the transformation

$$\begin{bmatrix} a_o \\ b_o \\ a_2 \end{bmatrix} = \begin{bmatrix} 1/3 & 1/3 & 1/3 \\ 1/6 & 1/6 & -2/6 \\ 1/3 & -1/3 & 0 \end{bmatrix} \begin{bmatrix} X_d \\ X_q \\ X_o \end{bmatrix} \tag{C.1}$$

where the machine coefficient inductance terms $a_0$,$b_o$ and $a_2$ $(= b_2)$ have already been mentioned in section(5.1.2). The stator–rotor mutual coupling terms $X_{md}$ and $X_{mq}$ are straightforwardly calculated as

$$X_{md} = X_d - X_l \tag{C.2}$$

$$X_{mq} = X_q - X_l \tag{C.3}$$

The rotor inductances are determined from the transient and subtransient time constants of the machine as given by the equations in [Adkins and Harley, 1975]. For example equations (C.4) to (C.6) can be used to calculate $X_f$, $X_{kd}$ and $X_{kq}$ respectively. It is assumed that $L_{kf} = 0$.

$$X'_d = X_l + \frac{X_{md}X_f}{X_{md} + X_f} \tag{C.4}$$

$$X''_d = X_l + \frac{1}{\frac{1}{X_{md}} + \frac{1}{X_{kd}} + \frac{1}{X_f}} \tag{C.5}$$

$$X''_q = X_l + \frac{1}{\frac{1}{X_{mq}} + \frac{1}{X_{kq}}} \tag{C.6}$$

The field and respective damper resistances, $R_f$, $R_{kd}$ and $R_{kq}$, can be computed from the time constant equations (C.7) to (C.9).

$$T'_{do} = \frac{1}{\mathbf{100\pi R_f}}(X_f + X_{md}) \tag{C.7}$$

$$T''_{do} = \frac{1}{\mathbf{100\pi R_{kd}}}(X_{kd} + \frac{X_{md}X_f}{X_{md} + X_f}) \tag{C.8}$$

$$T''_{qo} = \frac{1}{\mathbf{100\pi R_{kq}}}(X_{kq} + X_{mq}) \tag{C.9}$$

The rotor reactances and resistances must be scaled down by a factor of two thirds to compensate for the rationalisation done to the stator and hence the symmetrical machine matrix to be entered into the TCS programme is of the form

$$\left[\begin{array}{c|ccc|ccc} R_a & a_o & b_o & b_o & \frac{2}{3}X_{md} & \frac{2}{3}X_{md} & \frac{2}{3}X_{mq} \\ R_a & & a_o & b_o & \frac{2}{3}X_{md} & \frac{2}{3}X_{md} & \frac{2}{3}X_{mq} \\ R_a & & & a_o & \frac{2}{3}X_{md} & \frac{2}{3}X_{md} & \frac{2}{3}X_{mq} \\ \hline \frac{2}{3}R_{ffd} & & & & \frac{2}{3}(X_{md} + X_f) & \frac{2}{3}X_{md} & 0 \\ \frac{2}{3}R_{kkd} & & & & & \frac{2}{3}(X_{md} + X_{kd}) & 0 \\ \frac{2}{3}R_{kkq} & & & & & & \frac{2}{3}(X_{mq} + X_{kq}) \end{array}\right] \tag{C.10}$$

and hence using equations(C.1) to (C.9) the pu inductance matrix with the winding resistances in the left most column is

$$\left[\begin{array}{c|ccc|ccc} 0.005 & 0.68333 & 0.31667 & 0.31667 & 0.66667 & 0.66667 & 0.4 \\ 0.005 & & 0.68333 & 0.31667 & 0.66667 & 0.66667 & 0.4 \\ 0.005 & & & 0.68333 & 0.66667 & 0.66667 & 0.4 \\ \hline 3.33e-4 & & & & 0.8 & 0.66667 & 0 \\ 0.0123 & & & & & 0.8 & 0 \\ 0.0133 & & & & & & 0.554 \end{array}\right] \tag{C.11}$$

## C.3 Conversion to Series Excitation pu system

The stator and rotor bases are known from the assumptions used to derive the conventional pu system suitable for equivalent circuits. These bases are now used to covert the pu values back to real values and upon reselection of the new rotor bases the new series excitation pu values are found.

$\mathbf{L_{afd}}$ is determined from the field current required to induce peak open circuit phase to neutral voltage i.e.

$$\frac{\sqrt{2}\times 13.8}{\sqrt{3}} = \mathbf{I_f.100\pi.L_{afd}.\sin(100\pi t)} \tag{C.12}$$

however because of the inaccessability of the damper circuits, $\mathbf{L_{akd}}$ and $\mathbf{L_{akq}}$ can not be determined in a similar fashion. A general rule of thumb is to equate these terms to one tenth of $\mathbf{L_{afd}}$. Hence from equation(C.12)

$$\mathbf{L_{afd}} = 36mH \tag{C.13}$$

and

$$\mathbf{L_{akd}} = \mathbf{L_{akq}} = 3.6mH \tag{C.14}$$

The following formulae [Rankin, 1945a] can be used to derive the unknown inductance quantities.

$$X_{afd} = \frac{3}{2}\frac{\mathbf{L_{afd}}}{L_b^s}\left(\frac{I_b^f}{\frac{3}{2}I_b^s}\right) \tag{C.15}$$

$$X_{akd} = \frac{3}{2}\frac{\mathbf{L_{akd}}}{L_b^s}\left(\frac{I_b^{kd}}{\frac{3}{2}I_b^s}\right) \tag{C.16}$$

$$X_{ffd} = \frac{3}{2}\frac{\mathbf{L_{ffd}}}{L_b^s}\left(\frac{I_b^f}{\frac{3}{2}I_b^s}\right)^2 \tag{C.17}$$

$$X_{kkd} = \frac{3}{2}\frac{\mathbf{L_{kkd}}}{L_b^s}\left(\frac{I_b^{kd}}{\frac{3}{2}I_b^s}\right)^2 \tag{C.18}$$

$$X_{kfd} = \frac{3}{2}\frac{\mathbf{L_{kfd}}}{L_b^s}\left(\frac{I_b^{kd}.I_b^f}{(\frac{3}{2}I_b^s)^2}\right) \tag{C.19}$$

$$R_{ffd} = \frac{3}{2}\frac{\mathbf{R_{ffd}}}{Z_b^s}\left(\frac{I_b^f}{\frac{3}{2}I_b^s}\right)^2 \tag{C.20}$$

$$R_{kkd} = \frac{3}{2}\frac{\mathbf{R_{kkd}}}{Z_b^s}\left(\frac{I_b^{kd}}{\frac{3}{2}I_b^s}\right)^2 \tag{C.21}$$

The stator base values need no special explanation because the stator voltage and power bases $V_b^s$ and $P_b^s$ respectively are well defined and other base quantities are determined from them. In this instance $P_b^s$ is the base phase power and $V_b^s$ is the base peak phase to neutral voltage. Following then,

$$I_b^s = \frac{P_b^s}{V_b^s} \tag{C.22}$$

$$Z_b^s = \frac{V_b^s}{I_b^s} \tag{C.23}$$

$$L_b^s = \frac{Z_b^s}{\omega_b} \tag{C.24}$$

For the test system used in section(5.2) the initial base values on a $\frac{100}{3}MVA$ power base and transformers with taps of 2.2 are as follows,

| | | |
|---|---|---|
| $P_b^f$ = 33.33 MW | $P_b^s$ = 33.33 MW | $P_b^{dc}$ = 33.33 MW |
| $I_b^f$ = 0.2733 kA | $I_b^s$ = 2.958 kA | $I_b^{dc}$ = 1.3445 kA |
| $V_b^f$ = 122.0 kV | $V_b^s$ = 11.268 kV | $V_b^{dc}$ = 24.79 kV |
| $Z_b^f$ = 446.2 Ohms | $Z_b^s$ = 3.809 Ohms | $Z_b^{dc}$ = 18.4378 Ohms |
| $L_b^f$ = 1.42 H | $L_b^s$ = 12.12 mH | $L_b^{dc}$ = 58.69 mH |

If desired similar equations can be used to calculate the new pu values for the quadrature axis by replacing "d" in equations(C.15) to (C.21) with "q". Consideration of the direct axis damper is only necessary with respect to its mutual coupling with the field winding i.e. equation(C.19). There is no special need to reselect base currents for the damper circuits.

Summary of steps required to change the machine pu system

The pu values on the left hand side of equations(C.15) to (C.21) are known from equation(C.11).

- determine $I_b^s$ from equation(C.15) because $\mathbf{L_{afd}}$ is known.
- Similarly with $I_b^{kd}$ in equation(C.16).
- These base values are then used in equations(C.17) to (C.21) to calculate the real values $\mathbf{L_{ffd}}$, $\mathbf{L_{kkd}}$, $\mathbf{L_{kfd}}$, $\mathbf{R_{ffd}}$ and $\mathbf{R_{kkd}}$.
- Reselect the field current base such that $I_b^f = I_b^{dc}$ and then to recalculate the pu values affected by $I_b^f$ i.e. equations(C.15),(C.17),(C.19) and (C.20).

With this method the series excitation pu values, with the winding resistances being in the left most column, are

$$\left[\begin{array}{c|ccc|ccc} 0.005 & 0.68333 & 0.31667 & 0.31667 & 3.2797 & 0.66667 & 0.4 \\ 0.005 & & 0.68333 & 0.31667 & 3.2797 & 0.66667 & 0.4 \\ 0.005 & & & 0.68333 & 3.2797 & 0.66667 & 0.4 \\ \hline 0.00807 & & & & 19.362 & 3.2797 & 0 \\ 0.0123 & & & & & 0.8 & 0 \\ 0.0133 & & & & & & 0.554 \end{array}\right] \tag{C.25}$$

## C.4 Conversion of pu Series Excitation values to real values

In the procedure described in Appendix C.3, the conversion of machine pu values to a desired base yields real machine quantities such as $L_{ffd}$, $I_b^{kd}$ and $R_{ffd}$ which can be used to construct the equivalent rotor circuit.

Firstly $L_{ffd}$ from Appendix C.2 is 1.2 pu therefore

$$\mathbf{L_{ffd}} = 1.2 \times L_b^f \tag{C.26}$$

Finally

$$V_f' = \frac{3}{2}.100\pi.(X_{akd}.L_b^{kd}.I_b^{kd}.\frac{dI_{kd}}{dt} + X_{md}.L_b^s.I_b^s.\frac{dI_d}{dt}) \tag{C.27}$$

# Appendix D

# PUBLISHED PAPERS

# Series self-excited HVDC generation

J. Arrillaga, DSc, FIEE
S. MacDonald, BE
N.R. Watson, PhD
S. Watson, PhD

*Indexing terms: Power conversion, Unit connection, HVDC transmission*

**Abstract:** A new concept in HVDC generation simplifies the design of unit-connected generator–convertor plant. The generator exciter winding is connected in series with the output of the HVDC convertor and takes the place of the conventional smoothing reactor. As the existing steady-state AC–DC formulation is not directly applicable to the series connection a new algorithm is developed to simulate its performance. The results of the simulation show that series excitation is less efficient at low power levels but extends the temporary power conversion capability of the unit connection and permits fast fault clearances.

## 1 Introduction

The possibility of connecting generating units directly to static convertors for use in HVDC transmission has been discussed frequently in the past two decades, its main attraction being the elimination of the generator transformer and convertor filters [1–4]. Serious attempts are under way to assess the cost effectiveness of the unit connection for particular applications. As well as cost savings, the unit connection permits considerable simplification of the generator and/or convertor controls. Some proposals have gone as far as suggesting a total elimination of the convertor controls by using diode rectification [5].

The other extreme, that is a complete elimination of the generator excitation control, is considered in this paper. The motivation for the proposal comes from the traditional series DC machine. By performing the commutations statically, incorporating a transformer between the rotating machine and the commutating switches and feeding the exciter in series with the rectified output, it is possible to create what could be referred to as a high-voltage series-excited DC generator. The characteristics of the proposed alternative and its operational capability are described in this paper.

## 2 System configuration and energisation

The proposed configuration for the series excited unit-connected generator convertor group is illustrated in Fig. 1. The generator rotor windings, connected in series on the ground side of the convertor, take the place of the smoothing reactor. In the absence of the conventional separate excitation the operation of the unit connection is then controlled by the convertor.

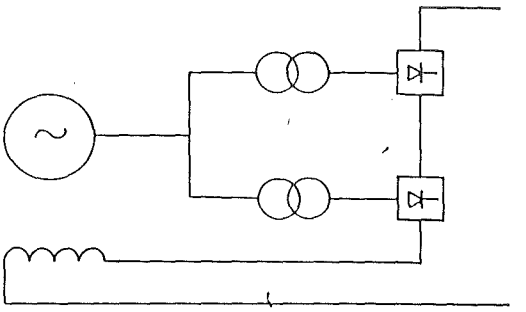

**Fig. 1** *Basic series-excited unit-connected HVDC generation*

A bipolar scheme with one generator per pole is illustrated in Fig. 2 and the scheme can be extended to several generators in series or parallel per pole. For the rectifiers to start delivering power to the link, the generators require exciting current. If the DC link is already supplying power via other connected generator–convertor units the incoming set will immediately receive excitation current. In the absence of other operating units the DC link will be energised by the receiving end convertors, which will temporarily operate in the rectification mode via normal constant-current control action.

A three set of quick isolators per unit will be required to permit the connection and disconnection of individual excitation units without interruption of the main DC line current.

## 3 Steady-state simulation

### 3.1 Synchronous generator

The internal EMF behind the synchronous reactance of the series excited generator is proportional to the direct current, i.e.

$$E = K_f I_d \tag{1}$$

To incorporate the effect of machine saturation $K_f$ is represented by a piece-wise linear function, as described in the Appendix under generator data.

For a cylindrical rotor machine the following relations apply, based on the phasor diagram of Fig. 3,

$$E \cos \xi = E'' \cos \phi$$

$$E \sin \xi = E'' \sin \phi + I(x - x'')$$

where $x = x_d$ is the direct-axis synchronous reactance. Squaring and adding the equations yields

$$E^2 = [E'' \cos \phi]^2 + [E'' \sin \phi + I(x - x'')]^2 \tag{2}$$

Paper 9148C (P7), first received 26th March and in revised form 21st August 1992

The authors are with the Department of Electrical and Electronic Engineering, University of Canterbury, Christchurch, New Zealand

### 3.2 AC–DC conversion

With reference to Fig. 4, the mean direct voltage of an HVDC convertor can be described by

$$V_d = \frac{3\sqrt{2}}{\pi} E_c \cos\alpha - \frac{3x_c}{\pi} I_d \tag{3}$$

where $E_c$ is the commutating voltage, $x_c$ is the commutation reactance, and $\alpha$ the firing angle. However, in the absence of filters at the convertor terminals, the commutations (which are brief phase to phase short circuits) are controlled by generator subtransient behaviour. Therefore the commutation reactance (in ohms) results from the addition of generator subtransient ($x''$) and transformer leakage ($x_t$) reactances. Also, the commutating voltage to be used in eqn. 3 is the machine's load dependent internal EMF behind subtransient reactance $E''$.

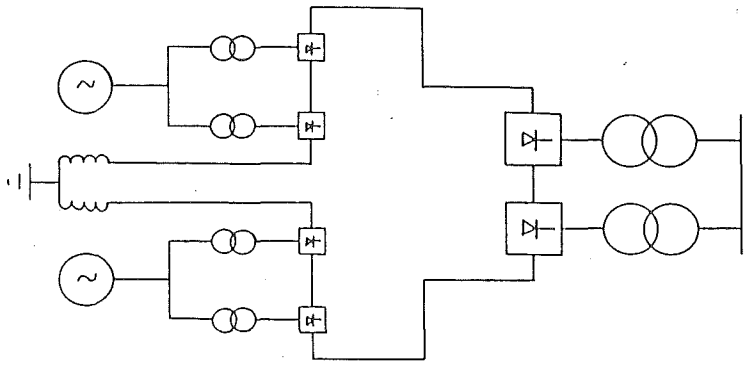

**Fig. 2** *Bipolar series-excited scheme*

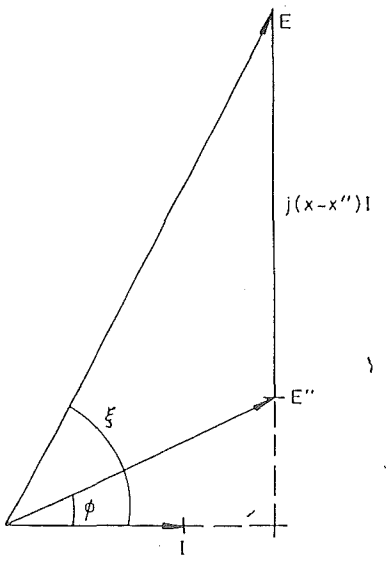


**Fig. 3** *Phasor diagram of synchronous generator*

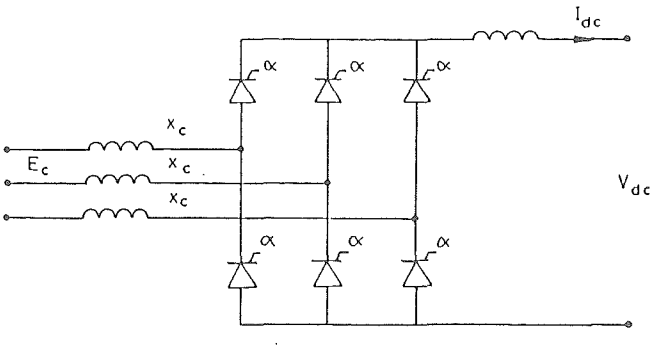


**Fig. 4** *Convertor bridge*

In the steady-state formulation the machine is assumed to be perfectly nonsalient and the direct current perfectly smooth. With these approximations, conventional theory leads to the following expressions

$$I = \frac{\sqrt{6}}{\pi} I_d \tag{4}$$

$$\cos\phi = \tfrac{1}{2}[\cos\alpha + \cos(\alpha + u)] \tag{5}$$

where $u$ is the commutation angle

$$I_d = \frac{E''}{\sqrt{(2)x_c}} [\cos\alpha - \cos(\alpha + u)] \tag{6}$$

$$V_d = \frac{3\sqrt{2}}{\pi} E'' \cos\alpha - \frac{3x_c}{\pi} I_d \tag{7}$$

### 3.3 Iterative solution

Eight variables have been identified in the steady-state formulation: $V_d$, $I_d$, $E$, $E''$, $I$, $\alpha$, $u$, $\phi$. As there are only six (eqns. 1, 2, 4–7), two of the variables must be specified. The obvious ones to derive the nominal operating point are $\alpha_{min}$ and $I_{d_N}$. Moreover, the set of nonlinear eqns. 1–7 requires an iterative solution. If an initial value of the output voltage $V_d$ is selected the solution proceeds as follows:

(i) derive $E$ from eqn. 1 which represents the separately excited open-circuit characteristic
(ii) derive $I$ from eqn. 4
(iii) derive $E''$ from eqn. 7
(iv) derive $u$ from eqn. 6
(v) derive $\phi$ from eqn. 5
(vi) derive $E$ from eqn. 3 and with it $\Delta E$
(vii) use the error ($\Delta E$) to correct the chosen value of $V_d$ and repeat the iteration cycle from (iii).

The same formulation is applicable to the separately excited machine except that in this case the internal EMF E is independent from the direct current.

### 3.4 Applicability of steady-state formulation

Two main constraints restrict the applicability of the preceding formulation. One relates to the variation of machine subtransient reactance around the air gap, which makes the fixed reactance formulation invalid for salient-pole machines. In approximate feasibility studies, such as the present work, the use of an average value $(x_d'' + x_q'')/2$ is often acceptable.

The second constraint relates to simultaneous commutating regions in the two bridges of a twelve-pulse convertor. This has the effect of increasing the commutation reactance, which makes the present AC–DC formulation

inapplicable. The effect of this restriction has been analysed with reference to the test system described in the appendix and the results are plotted in Fig. 5. The continuous line shows the maximum voltage achievable by the series connection for each operating current, while the dotted line indicates the $\alpha$ required to keep the commutation angle at 30°.

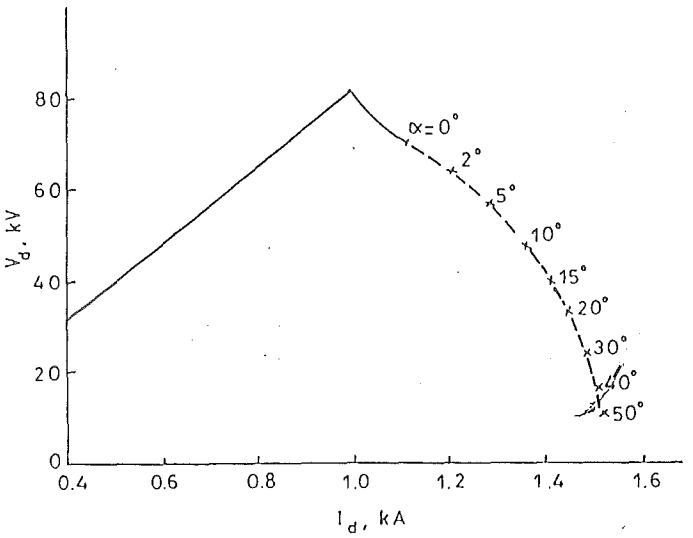


**Fig. 5** *Maximum voltage characteristics derived from steady-state formulation*

Operation beyond the region of applicability of the steady-state formulation requires time-domain simulation, also used in later Sections to assess the dynamic and transient response of the series connection.

## 4 Basic characteristics

Fig. 6 shows the derivation of the nominal operating point A for three rectifier alternatives, i.e. the conventional configuration (i), a separately-excited unit connection (ii), and the proposed series-excited unit connection (iii). All of them share the same constant-current control characteristic (iv) and inverter characteristics (broken line).

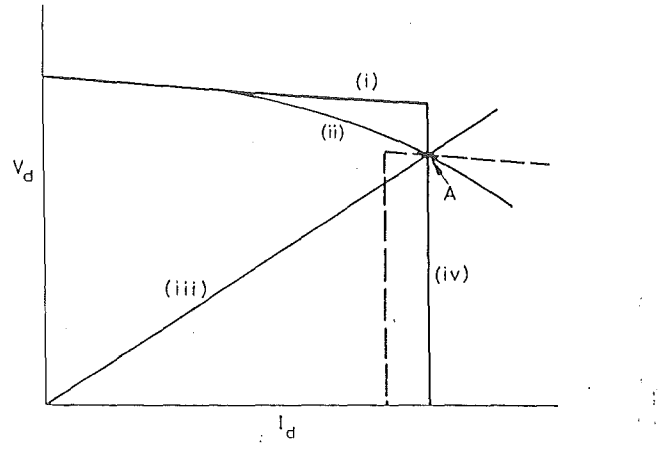


**Fig. 6** *Operating point derived from conventional and unit-connected schemes*

(i) conventional configuration
(ii) separate excitation unit connection
(iii) series excitation unit connection
(iv) constant-current control characteristic
---- inverter characteristic

Curves (i) and (ii) represent eqns. 3 and 7, respectively, while curve (iii) results from the iterative solution of the complete set of equations, i.e. including eqn. 1.

In Fig. 7 the conventional characteristics have been left out to simplify the description of the series connection. If the inverter voltage increases the rectifier reduces its firing angle until it reaches the $\alpha_{min}$ limit (point B in Fig. 7).

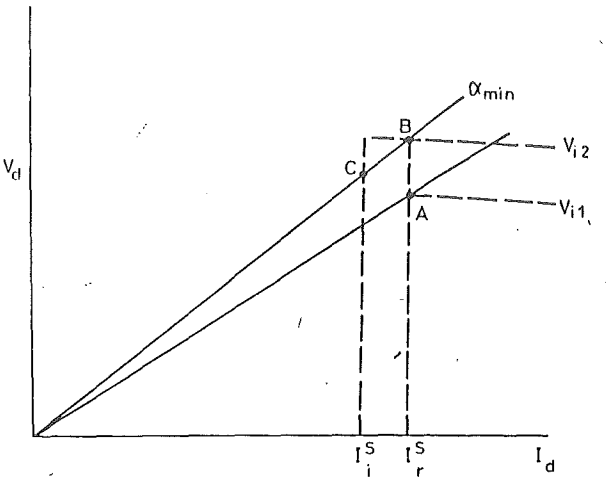


**Fig. 7** *Steady-state characteristics of series unit connection*

If the inverter voltage increases beyond $V_{i2}$ the direct current reduces and at point C the current control is transferred to the inverter (i.e. current setting $I_i^s$).

The series unit connection is seen to have a very large positive voltage regulation (slope) as compared with the relatively small negative slope of the conventional scheme. This effect should simplify the changeover of current control from the inverter to the rectifier as there is no alternative crossing in the transition region (a problem earlier encountered in conventional schemes with weak systems at the receiving end). Inverter voltage reductions will reverse the sequence, i.e. going from operating point C to B to A.

Similar reasoning for the case of constant power control, leads to the characteristics of Fig. 8. For a specified power $P_R^s$ the operating point A is under rectifier constant power control. Inverter voltage increases will take the operating point to B, beyond which point the rectifier loses controllability. The current then drops

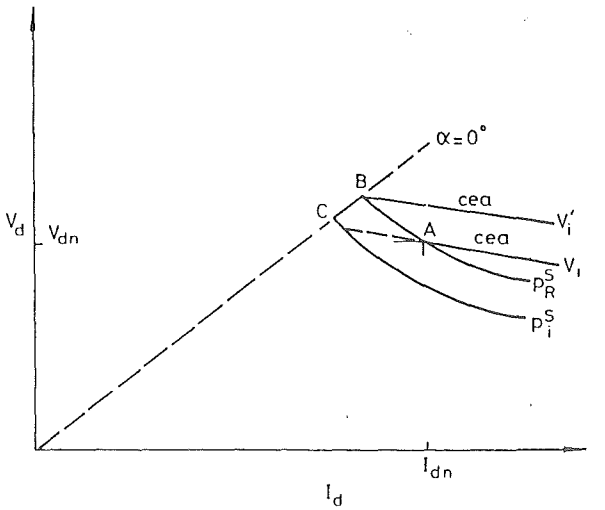


**Fig. 8** *Operating point derived from constant power and constant extinction angle characteristics*

along the $\alpha_{min}$ characteristic until the power margin setting is reached (at point C) and will remain there under inverter constant power control ($P_i^s$).

## 5 Test comparisons

A typical 90 MVA generator is used for the comparison between the conventional and series excited unit-connection schemes. Details of the generator, transformers and convertors are given in the Appendix. In the comparisons that follow the characteristics in the regions where the commutation overlap exceeds 30° have been derived using time-domain simulation [8].

### 5.1 Operating range

Optimum transmission efficiency is achieved when the direct voltage can be kept constant for the complete range of specified power levels. Series excitation can not maintain the nominal voltage at low powers because the machine EMF reduces with the current. This effect is illustrated in Fig. 9, where a nominal operating point (A)

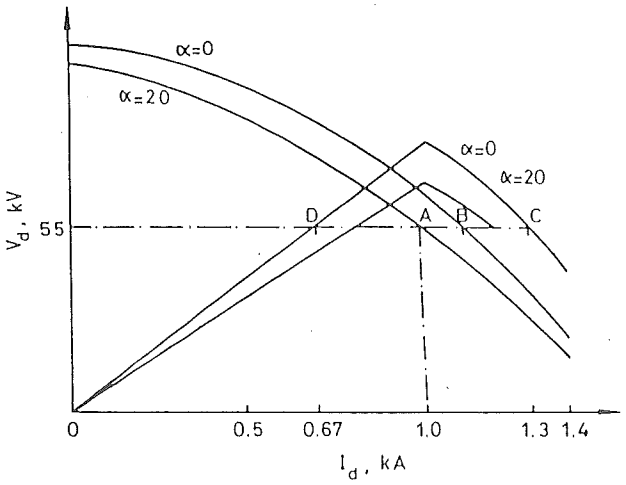


**Fig. 9** *Operating points derived from constant current and constant extinction angle characteristics*

is selected which for the separate excitation case provides 55 kV and 1 kA at a firing angle of 20°. Using series excitation, point D (at $\alpha = 0°$) marks the lower current limit (670 A) of operation at full efficiency.

In theory, the separately excited scheme can maintain full voltage down to zero current but in practice power transmission at such power levels are unlikely to use all the generators and therefore the separately excited unit scheme will also operate at lower than optimal transmission efficiencies.

Extending the power range beyond the nominal operating point presents no problem to the series connection because the excitation increases proportionally with the load. There is, however, a limit (point C) beyond which the commutation voltage drop increases faster than the current and the output power decreases; this limit occurs at 1.3 kA (or 75 MW) in the test system. Under constant excitation the separately excited scheme meets the minimum $\alpha$ characteristic at point B, which corresponds with 61 MW. The separately excited scheme could also be made to operate at point C by providing extra excitation; however, apart from the higher rating of the static exciter, such extended range would require to operate the excitation rectifiers at very large firing angles most of the time.

### 5.2 Temporary overload capability

Compared with conventional generation/HVDC transmission schemes the unit connection alternative has very limited power conversion capability [6] owing to the large commutation reactance of the unit connection, which reduces the rectified voltage at large currents.

To improve the transient stability margins at the inverter end it is important to provide some extra temporary conversion capability at the rectifier for a few cycles following fault clearance. However, to be effective, the implementation of the extra current setting must be fast acting (i.e. by firing angle rather than excitation control). Assume, to illustrate the effect, that no excitation change takes place immediately after fault clearance, the $\alpha = 0$ characteristics in Fig. 10 give an indication of

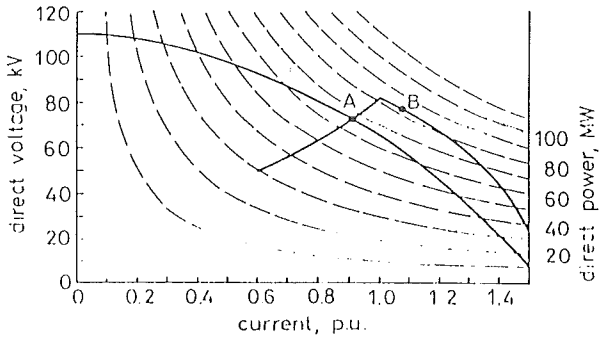


**Fig. 10** *Temporary capability charts*

the relative maximum temporary capabilities of the conventional and series alternatives.

In each case the power curve tangent to the maximum voltage characteristic determines the unrestricted power conversion capability. These are 66 MW (point A) and 83 MW (point B) for the conventional and series configurations, respectively, or an increase of 25% in favour of the last-mentioned. This increase will be lower in practice if fast-acting field forcing control is used with the separate excitation.

### 5.3 Dynamic response

With series excited generators the smoothing inductance will be larger than in a conventional separately excited system. For example, the respective series and conventional smoothing inductances may typically be 2 and 0.3 Henries, and this will affect the dynamic response of the link to a change in conditions.

To quantify this effect Figs. 11 and 12 show the response of the conventional and series excited cases to a

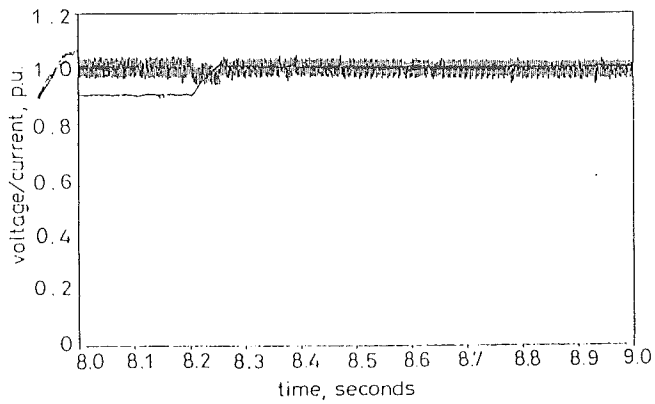


**Fig. 11** *Dynamic response to change of current order in separately excited system*

change of current order from 0.9 to 1.0 p.u. The difference in dynamic responses is seen to be very small.

### 5.4 Fault recovery

Following a DC short-circuit fault the rectifier current will rise to about two per unit, with a consequent

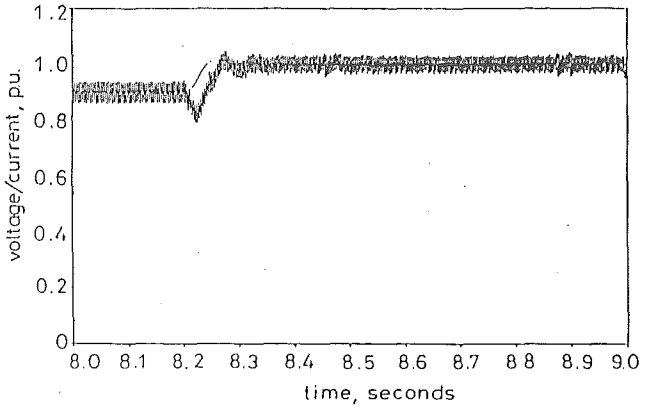


**Fig. 12** *Dynamic response to change of current order in series excited system*

increase in machine excitation in the case of the series connection. In the absence of any special fault controls this effect would increase substantially the severity of the fault. However, it is standard practice in HVDC transmission to advance temporarily the firing angle into the inversion region to accelerate the collapse of the fault current by transferring the stored reactive energy to the AC side.

A comparison of dynamic performances following DC short circuits was carried out using the EMTDC simulation algorithm. Figs. 13 and 14 show the DC line volt-

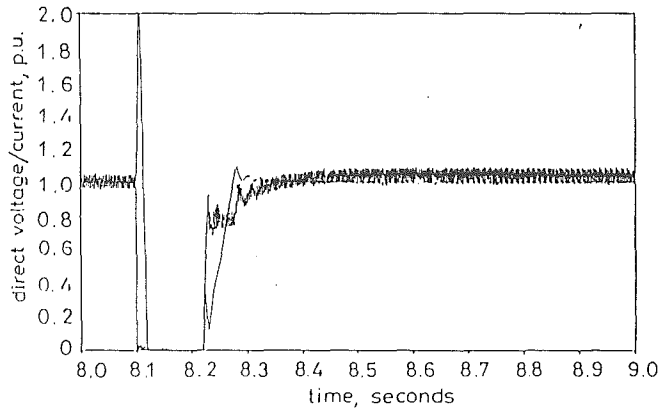


**Fig. 13** *Simulated performance of separate excitation scheme following a DC line short-circuit*

ages and currents for the cases of conventional and series excitation, respectively.

The short circuit was applied to the line side of the smoothing reactor after 8.1 seconds of dynamic simulation. Upon fault detection the rectifier firing angle was set to 115°. The figures show that the line current reduced to zero at times $t = 8.12$ and $t = 8.16$ seconds for the respective cases. At this point the converter is blocked to allow the line a 100 ms period of deionisation.

Although the reactive energy transfer, before convertor blocking, is slower the difference is only a small proportion of the total interruption time (the deionisation time could, in practice, be as long as 200 ms). Figs. 13 and 14 show a considerable reduction in the peak fault current of the series connection alternative. However, those results have been obtained with a linear excitation characteristic; in practice, the difference will be smaller due to saturation.

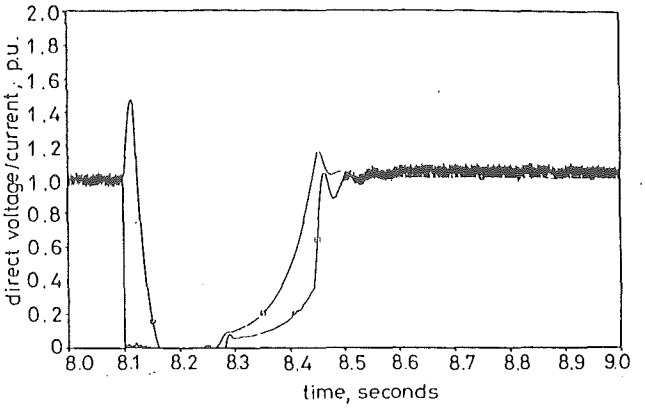


**Fig. 14** *Simulated performance of series excited scheme following a DC line short-circuit*

## 6 Conclusions

In line with the main unit-connection purpose, the new scheme permits further simplification of the generator and convertor plant and considerable cost savings. It eliminates entirely the need for large battery storage, excitation controllers and smoothing reactors. A steady-state formulation has been developed which combines generator phasor diagrams with the convertor-equations in an iterative model, which has been validated, and complemented, by time-domain simulation.

Using a conventional 90 MVA generator as a reference the theoretical models have predicted that series excitation extends the region of fast temporary power conversion capability, which should help to maintain transient stability at the inverter end. It has also been shown that the series excitation scheme can clear DC faults as effectively as the conventional excitation case.

The simulated results are sufficiently encouraging for the series excited proposal to be given serious consideration as a possible contender in future unit-connected schemes.

## 7 References


1 CALVERLEY, T.E., OTTAWAY, C.H., and TUFNELL, D.H.A.: 'Concepts of a unit generator convertor transmission system'. IEE conference on High voltage DC and AC transmission, London, 1973, pp. 53–59

2 KRISHNAYYA, P.C.S.: 'A review of unit generator-converter connections for HVDC transmission'. IEEE/CSEE joint conference on High voltage transmission systems, Beijing, China, 1987

3 KANNGIESSER, K.W.: 'Unit connection of generator and converter to be integrated in HVDC or HVAC energy transmission'. International symposium on HVDC technology, Rio de Janeiro, Brazil, 1983

4 NAIDU, M., and MATHUR, R.M.: 'Evaluation of unit connected, variable speed, hydropower station for HVDC power transmission', *Trans. IEEE*, 1989, **PWRS-4**, (2), pp. 668–676

5 BOWLES, J.P.: 'Multiterminal HVDC transmission systems incorporating diode rectifier stations', *Trans. IEEE*, 1981, **PAS-100**, (4), pp. 1674–1678

6 ARRILLAGA, J.: 'High voltage direct current transmission' (IEE Power Engineering Series 6, Peter Peregrinus, London, 1983)

7 ARRILLAGA, J., SANKAR, S., WATSON, N.R., and ARNOLD, C.P.: 'Operational capability of generator-HVDC convertor units', *Trans. IEEE*, 1991, **PD-6**, pp. 1171–1176

8 ARRILLAGA, J., ARNOLD, C.P., and HARKER, B.J.: 'Computer modelling of electrical power systems' (Wiley, London, 1983)

## 8 Appendix

### 8.1 Test system data

*Generator*

| | |
|---|---|
| Rating | 90 MVA |
| Terminal voltage | 13.8 kV |
| Direct-axis reactance | $x_d = 1.18$ |
| Direct-axis damper reactance | $x_s = 1.24$ |
| Quadrature-axis reactance | $x_q = 1.05$ |
| Quadrature-axis damper reactance | $x_t = 1.05$ |
| Field reactance | $x_f = 1.27$ |
| Direct-axis damper resistance | $r_s = 0.021$ |
| Direct-axis subtransient reactance | $x_d'' = 0.145$ |
| Quadrature axis damper resistance | $r_t = 0.036$ |
| Quadrature axis subtransient reactance | $x_q'' = 0.145$ |
| Field resistance | $r_f = 0.00068$ |
| Leakage reactance | $x_l = 0.075$ |
| Armature resistance | $r_a = 0.0035$ |
| Direct-axis open-circuit time constant | $T_{do} = 0.042$ s |
| Excitation characteristic | $K_f = 20.75$ V/A (linear part) |
| | $K_f = 0.5$ V/A (saturated part |
| | knee point = 1 kA |

*Convertor*

Type 12 pulse
Nominal current $I_d = 1$ kA
Nominal voltage $V_d = 40$ kV

*Convertor transformers*

Rating 50 MVA
Reactance $x_t = 5\%$
Voltage 13.8/30.36 kV

# DIRECT CONNECTION OF SERIES SELF-EXCITED GENERATORS AND HVDC CONVERTERS

J. Arrillaga FIEEE | S.J. Macdonald Non-Member | N.R. Watson MIEEE | S. Watson Non-Member

University of Canterbury, Christchurch, New Zealand.

Abstract - An alternative and simpler solution is proposed for the direct connection of generators to HVdc converters. The generator exciter windings are connected in series with the output of the HVdc converter and take the place of the conventional smoothing reactor. Existing steady state and time domain simulation programs are modified to represent the behaviour of the series direct connection scheme. It is shown that series excitation extends naturally the power transmission capability and permits fast fault clearances.

Keywords - HVdc Transmission, Direct Connection.

## INTRODUCTION

The unit connection of generators to HVdc converters is being given serious consideration on account of the simplicity of its design [1][2][3][4].

As an alternative to the unit connection concept serious consideration is also being given to group connected generators and HVdc Converters. Much of the design simplicity of the unit connected schemes also applies to the group connection and particulary the elimination of generator transformers and ac filters.

The main advantages of the group connection are a considerable reduction in the number of converter groups and greater flexibility of operation with the optimal number of generators in service for a particular loading condition.

The possibility of reducing the level of controllability is one of the main attractions of the direct connection.

In an attempt to simplify further the design of generator-converter plant, this paper investigates the possibility of using uncontrolled series self excitation for the generating units, thus relying entirely on converter firing control.

## PROPOSED CONFIGURATION

Figure 1 shows the proposed alternative to the conventional direct connection of generators to HVdc converters. The series excitation concept can be used with the unit connection (Figure 1(a)) and with group connection (Figure 1(b)). The exciter windings, connected in series with the converter output, provide enough smoothing inductance and no further inductors are required. Moreover these windings can be connected on the ground side of the converter to reduce insulation costs.

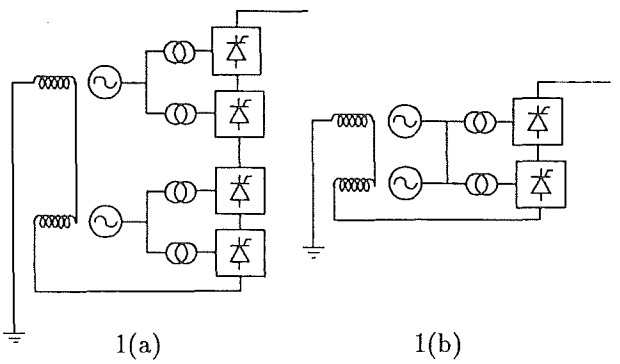


Figure 1: Basic Series Excited direct-connected HVdc generation

Thus in the absence of the conventional separate excitation, the operation of the direct connected scheme is entirely controlled by the converter.

## ENERGISATION AND BLOCKING

For the rectifiers to start delivering power to the link, the generators require exciting current. If the dc link is already supplying power via other connected generator-converter units the incoming set will imediately receive excitation current. In the absence of other operating units the dc link will be energised by the receiving end converters, which will temporarily operate in the rectification mode via normal constant current control action.

Converter blocking (in the series connected alternative) presents no special problem with respect to the

separate excitation alternative, both cases requiring a by-pass path if a group is to be disconnected. In the series excitation case a three set of quick isolators is needed; the first, to connect a resistor in parallel with the exciter winding, the second to by pass this winding and the third to remove it from service without the interruption of the main dc line current. The isolators and resistor constitute the only additional requirement of the generator. The field winding current will be considerably smoother than in the conventional static exciter and should reduce the harmonic rating of the rotor.

## SIMULATION REQUIREMENTS

In conventional schemes the converter bus voltage to which the converters are connected is used as the comutating voltage and the reactance between that bus and the converter (normally the transformer leakage) is used as the commutation reactance. In a direct connected scheme, without filters at the converter terminals, the commutations (which are brief phase to phase short-circuits) are controlled by the generator emf behind the subtransient reactance ($E''$).

A steady state formulation which takes into account the non-linear variation of the commutating voltage with the load is given in Appendix A. However the applicability of this formulation to the direct connection is restricted for two reasons.

One of them relates to the variation of machine subtransient reactance around the air gap, which makes the fixed reactance formulation invalid for salient pole machines. In approximate feasibility studies, such as the present work, the use of an average value, $(x_d'' + x_q'')/2$ is often acceptable.

The second constraint relates to simultaneous commutating regions in the two bridges of a twelve pulse converter. When the commutation angle exceeds 30 degrees, a condition likely to occur due to the large commutation reactance of the direct connection, then the formulation does not apply.

Operation beyond the region of applicability of the steady state formulation , requires time domain simulation. The latter is also required to assess the series connection dynamic and transient responses.

The Manitoba EMTDC package [7] is used for this purpose with a modified synchronous machine presentation to accommodate series excitation. The algorithmic modification is explained in Appendix B.

## STEADY STATE CHARACTERISTICS

A typical output characteristic of a direct connected machine is shown in Figure 2 (curve $V_{r1}$). Under nominal operating conditions the rectifier is on constant power ($P_{ds}$) or current ($I_r{}^s$) control and the intersection between this line and the inverter extinction angle control characteristic ($V_{i1}$) determines the operating point (point A).

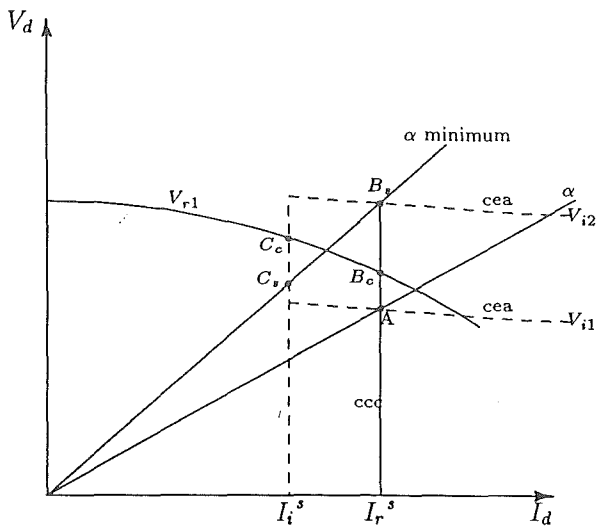


Figure 2: Operating Points derived from constant current and constant extinction angle characteristics

To simplify the explanation the operating point has been assumed to occur in the linear part of the excitation characteristic. When the inverter ac voltage increases, the rectifier constant current control reduces the firing angle until it reaches the alfa minimum limit(point $B_c$ in the figure for the conventional and $B_s$ for the series unit connections respectively).

If the inverter voltage increases beyond $v_{i2}$ the dc current control transfers to the inverter (i.e. current setting $I_i{}^s$), with a new operating point at $C_c$ (for the conventional) or $C_s$ (for the series connection).

The series unit connection is seen to have a very large positive voltage regulation as compared with the relatively small negative slope of the conventional scheme. This effect should simplify the change over of current control from the inverter to the rectifier as there is no alternative crossing in the transition region ( a problem earlier encountered in conventional schemes with weak systems at the receiving end). Inverter voltage reductions will reverse the sequence, i.e. going from operating point $C_s$ to $B_s$ to A.

For optimum transmission efficiency the dc voltage should be kept constant for a full range of power variation. However with series excitation it is not possible to maintain the nominal voltage at low power levels because the excitation reduces, and hence the machine emfs, with line current. This is illustrated in Figure 3, where the nominal operating point (A) is obtained with the rectifier on constant power ($P_{ds}$) and the inverter on constant extinction angle (CEA) control. However, when the range of rectifier firing angle control has been used, the output voltage will reduce linearly following the minimum $\alpha$ characteristic.

If a lower power setting (say $\frac{P_{ds}}{2}$) is used, the new operating point is $A'$, with the inverter in control of the power. In order to maintain high turbine efficiency at

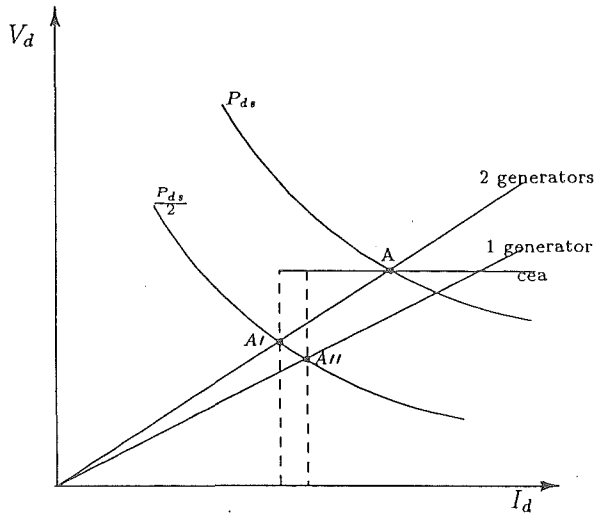


Figure 3: Operating Points derived from constant power and constant extinction angle characteristics

lower powers the number of generators in service should be reduced. However this alternative is impractical with the unit connected alternative, because the voltage reduces in proportion to the number of generators. When applied to the group connection, the use of fewer generators increased slightly the commutation reactance and thus the voltage regulation, i.e. the operating point moves from $A'$ to $A''$. This effect partly offsets the benefit of a higher turbine efficiency. Apart from lower transmission efficiences, operating at points $A'$ or $A''$ transfers the power control to the inverter and thus increases it's reactive power requirements.

In theory the separately excited scheme can maintain full voltage down to zero current but in practice power transmission at such power levels is unlikely to use all the generators and therefore the separately excited unit scheme will also operate at lower than optimal transmission efficiences.

Extending the power range beyond the nominal rating point presents no problem to the series connection because the excitation increases proportionally with the load.

## DUAL EXCITATION ARRANGEMENT

Normally the nominal dc currents used in HVdc schemes will exceed the generator excitation requirement. This suggests the alternative connection illustrated in Figure 4 for a four machine group connected scheme. It is a two stage arrangement which permits halving the number of machines without reducing the common bus voltage. Information for the generators, transformers and converters of the test system are given in Appendix C.

The resulting steady state characteristic, illustrated in Figure 5, shows an obvious improvement over the previous configuration. Below point B, which determines the limit of rectifier constant current control, the dc voltage begins to fall down the path of the minimum $\alpha$ characteristic. At point C, when the dc current reduces to half the nominal rating, two generators are disconnected (e.g. $G_3$ and $G_4$ or $G_1$ and $G_2$) such that each remaining rotor receives the full dc current.

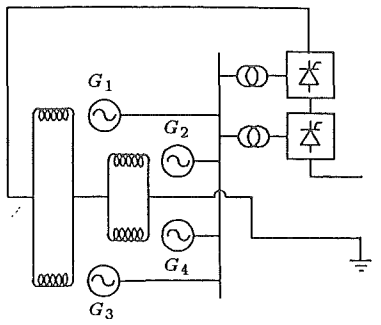


Figure 4: Alternative field winding connection

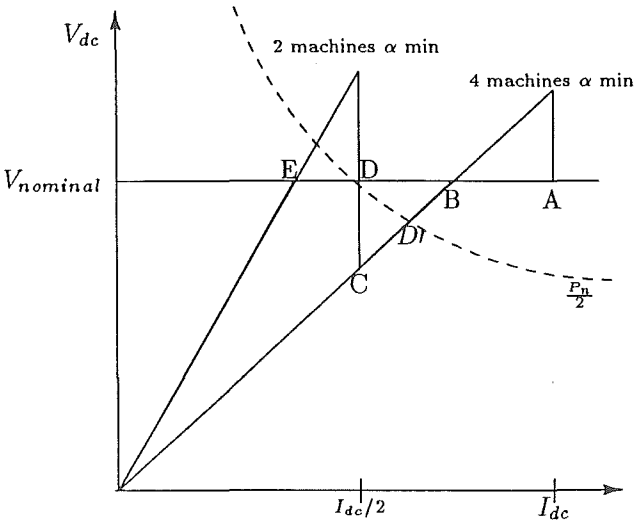


Figure 5: Maximum Voltage Characteristics derived from the steady state formulation

However there is no need to continue down the linear characteristic below $D'$ because the same power setting (shown in the dotted line) can be obtained more efficiently by halving the number of machines at that point, i.e. transfering the operation to point D. The new configuration (at point D) returns the power control to the rectifier end, which will initially operate at a large firing angle; further power reductions will use the available firing angle and at point E power control will again transfer to the inverter end. From this point the voltage output will reduce linearly with the dc current. However in this region the current levels are too low to be of any practical consequence.

## TEMPORARY OVERLOAD CAPABILITY

As compared with conventional generation/HVdc transmission schemes the direct connection alternative is restricted in overload capability [5] due to a large commutation reactance which reduces the rectifier voltage at large currents.

On the other hand, improved transient stability margins at the inverter end require the provision of extra temporary conversion capability at the rectifier for a few cycles following fault clearance.

The conventional system can only achieve such extra power if the exciter is designed with fast acting field forcing capability, i.e with firing angle reserve, and therefore operating inefficiently at steady state rated powers. Because the dc current is also the excitation current in the proposed series connection, field forcing occurs naturally following the increased power setting in the link.

## DYNAMIC RESPONSE

With series excited generators the smoothing inductance will be larger than in a conventional separately excited system. For example, the respective series and conventional smoothing inductances may typically be 2 and 0.5 Henries, and this will affect the dynamic response of the link to a change in conditions. To quantify this effect Figures 6 and 7 show the response of the conventional and series excited cases to a change of current order from 0.9 to 1.0 p.u. The difference in dynamic responses is seen to be very small.

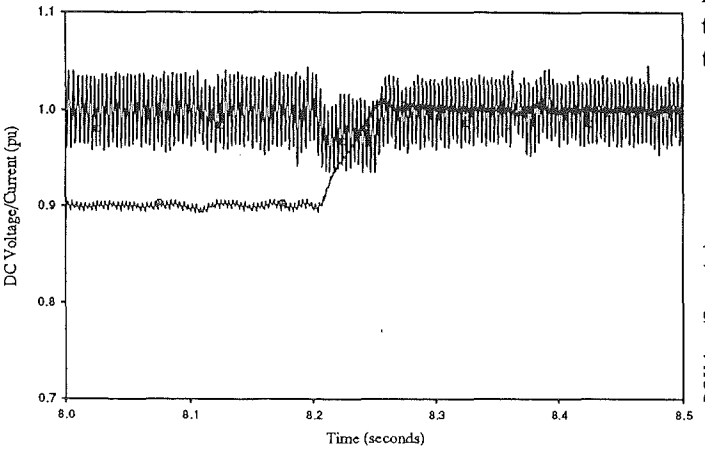


Figure 6: Dynamic Response to a Change of Current Order in a Separately Excited System

## FAULT RECOVERY

Following a dc short-circuit fault the rectifier current will rise to about two per unit, with a consequent increase in machine excitation in the case of the series connection. In the absence of any special fault controls this effect would increase substantially the severity of the fault.

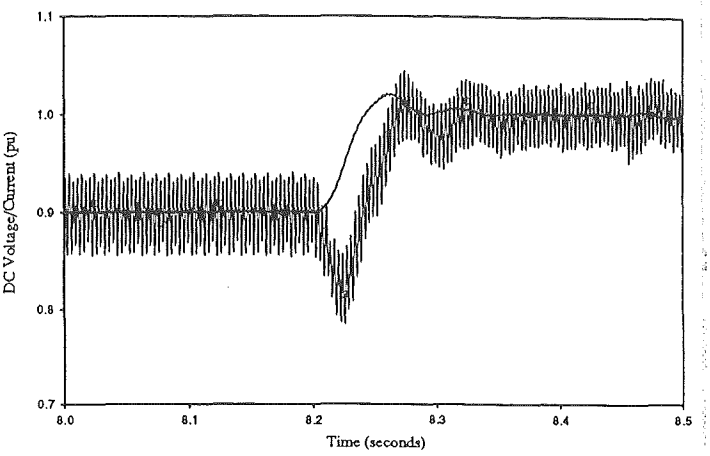


Figure 7: Dynamic Response to a Change of Current Order in a Series Excited System

However, it is standard practice in HVdc transmission to advance temporarily the firing angle into the inversion region to accelerate the collapse of the fault current by transfering the stored reactive energy to the ac side.

A comparison of dynamic performances following dc short circuits was carried out using the EMTDC simulation algorithm. Figures 8 amd 9 show the dc line voltages and currents for the cases of conventional and series excitation respectively.

The short circuit was applied to the line side of the smoothing reactor after 8.1 seconds of dynamic simulation. Upon fault detection the rectifier firing angle was set to 115 degrees. The figures show that the line current reduced to zero at times t = 8.12 and t = 8.16 seconds for the respective cases. At this point the converter is blocked to allow the line a 100ms period of deionisation.

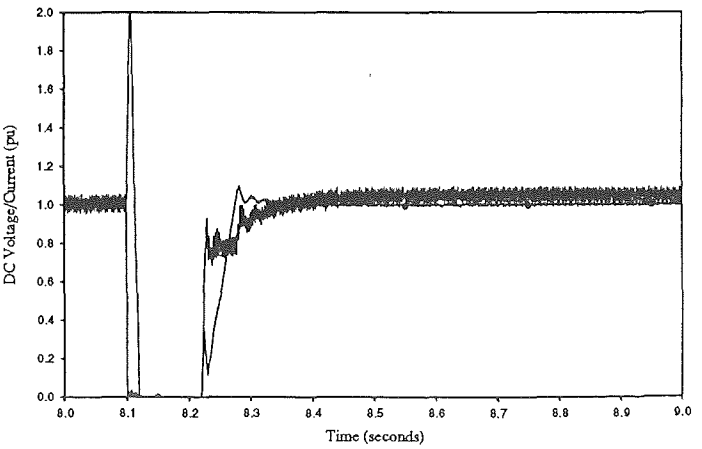


Figure 8: Conventional System Fault

Although the reactive energy transfer, before converter blocking, is slower the difference is only a small proportion of the total interruption time (the deionisation time could, in practice, be as long as 200ms). On the other hand the series connection exhibits a significant reduction in the peak fault current from 2.0 to 1.46 pu with a corre-

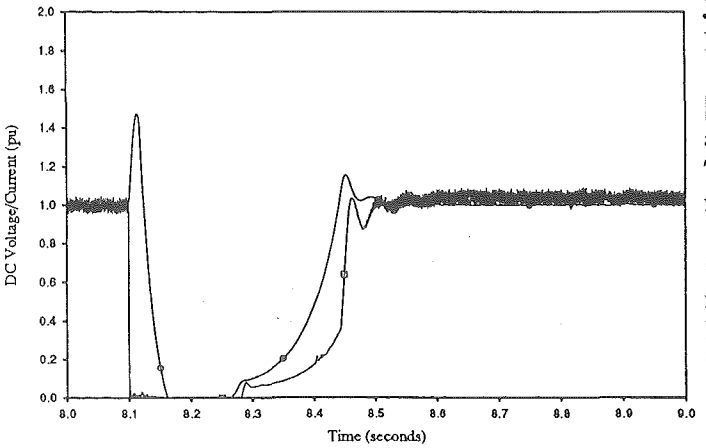


Figure 9: Series Connected System Fault

sponding reduction in thyristor dc line fault peak current rating.

## CONCLUSIONS

A new concept of direct-connected HVdc generation has been proposed based on the use of series self excitation of synchronous generators, which provides further simplification of the generator and converter plant. It eliminates entirely the need for excitation controllers and smoothing reactors.

A steady state formulation has been developed to model series excitation which combines generator phasor diagrams with the converter equations in an iterative model; this model has been validated and complemented by time domain simulation.

The simulation predicts that the series excitation is less efficient at low powers, but provides natural field forcing following temporary increases in the power setting. This is expected to improve the transient stability at the inverter end.

The loss of one degree of controllability (i.e. the excitation) has practically no effect on the rectifier speed of response to changing conditions or to dc faults. Moreover the series excited scheme reduces substantially the dc line fault current peak.

## ACKNOWLEDGMENTS

The authors wish to acknowledge the financial assistance provided by TRANSPOWER N.Z. to carry out this investigation.

## REFERENCES

[1] T.E. Calverley, C.H. Ottaway and D.H.A Tufnell, "Concepts of a Unit Generator Converter Transmission System", IEE Conference on High Voltage dc and ac Transmission, London, 1973.

[2] P.C.S. Krishnayya, "Review of unit generator converter connections for HVdc transmission",IEEE/CSEE Joint Conference on High Voltage Transmission Systems, Beijing, China, 1987.

[3] K.W. Kanngiesser, "Unit Connection of Generator and Converter to be integrated in HVdc or HVac Energy Transmission", International Symposium on HVdc Technology, Rio de Janeiro, Brazil, 1983.

[4] M. Niadu and R.M. Mathur, "Evaluation of unit connected, Variable speed, Hydropower Station for HVdc Power Transmission", IEEE Transaction on Power Systems, vol. 4, no. 1, pp.668-676, May,1989.

[5] J. Arrillaga, S. Sankar, N.R. Watson and C.P. Arnold, "Operational Capability of Generator-HVdc Converter units", IEEE Transactions on Power Delivery, vol. 6, no. 3, pp. 1171-76, July, 1991.

[6] J. Arrillaga, "High Voltage Direct Current Transmission", IEE Power Engineering Series 6, Peter Peregrinus, London, 1983.

[7] EMTDC Users Manual - Manitoba HVdc Research Centre, 1988.

[8] B. Adkins and R.G. Harley, "The General Theory of Alternating Current Machines", Chapman and Hall, London, 1975.

## APPENDIX A: Steady State Formulation

In the case of the series excited machine driven at a constant speed the generator emf is proportional to the dc current, i.e.

$$E = K_f . I_d \tag{1}$$

With reference to the phasor diagram of Figure 10 the commutating voltage (i.e. $E''$), assuming a symmetrical rotor, is implicitly specified by the equation

$$E^2 = [E''.cos(\phi)]^2 + [E''.sin(\phi) + I.(x - x'')]^2 \tag{2}$$

The dc voltage output of a two bridge configuration becomes

$$V_d = 2\left[\frac{3\sqrt{2}}{\pi} E''.r.cos\alpha - \frac{3}{\pi}.X_c.I_d\right] \tag{3}$$

where

- $\alpha$ is the firing angle
- $\mu$ is the commutation angle
- r is the transformer ratio

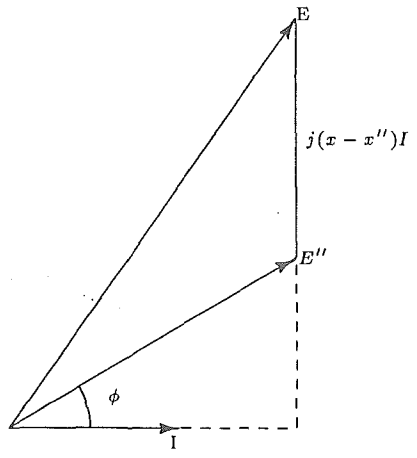


Figure 10: Phasor diagram of the synchronous generator

- $X_c = x'' + 2X_t$ for the unit connection
- $X_t$ is the transformer leakage reactance
- $X_c = \left(\frac{x''}{n_s}\right) + \left(\frac{2X_t}{n}\right)$ for the group connection
- $n$ is the total number of generators
- $n_s$ is the number of generators in service.

From conventional theory [6] the following equations can be added

$$I = \frac{\sqrt{6}}{\pi} I_d \tag{4}$$

$$cos(\phi) = \frac{1}{2}[cos(\alpha) + cos(\alpha + \mu)] \tag{5}$$

$$I_d = r.\frac{E''}{\sqrt{2}}.\frac{n_s}{x'' + n_s X_t}[cos(\alpha) - cos(\alpha + \mu)] \tag{6}$$

Equations 1 to 6 together with control specifications can be used in an iterative solution to derive the eight variables identified in the formulation, i.e. $V_d, I_d, E, E'', I, \alpha, \mu, \phi$.

## APPENDIX B: Modelling the Series Connected Generator in EMTDC

In EMTDC the synchronous machine is modelled in state variable form using generalised machine theory [7][8]. The equivalent circuit for the direct axis of the synchronous machine is illustrated in figure(11)

where

- $L_f, R_f$ are the field winding quantities

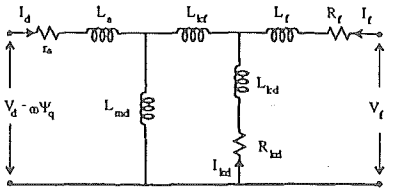


Figure 11: The Conventional and Direct Connection Characteristics

- $L_{kd}, R_{kd}$ refer to the damper winding
- $R_a$ is the armature resistance
- $L_a$ is the leakage inductance
- $L_{kf}$ is the field to damper winding mutual inductance
- $L_{md}$ is the direct axis mutual inductance

and from which equation(7) results.

$$\begin{bmatrix} V_d - \nu\Psi_Q - r_a i_d \\ V_f - R_f i_f \\ -r_{kd} i_{kd} \end{bmatrix} =$$

$$\begin{bmatrix} L_{md} + L_a & L_{md} & L_{md} \\ L_{md} & L_{md} + L_{kf} + L_f & L_{md} + L_{kf} \\ L_{md} & L_{md} + L_{kf} & L_{md} + L_{kf} + L_{kd} \end{bmatrix} \frac{d}{dt} \begin{bmatrix} i_d \\ i_f \\ i_{kd} \end{bmatrix}$$

where $\nu\Psi_Q$ the *speed voltage term* is given by

$$\Psi_Q = L_a i_q + L_{mq}(i_q + i_{kq}) \tag{8}$$

$\nu$ is the rotational speed, and the subscript $q$ denotes quadrature axis quantities. Inversion of equation(7) gives the standard state variable form,

$$\dot{\underline{X}} = A\underline{X} + B\underline{U} \tag{9}$$

where the state vector $\underline{X}$ contains the currents and the input vector $\underline{U}$ the applied voltages.

The dc line current specifies the field current of the series excited machine. Thus $i_f$ and $\frac{d}{dt} i_f$ are known and equation(7) can be rewritten in the form.

$$\begin{bmatrix} V_d - \nu\Psi_Q - r_a i_d \\ -r_{kd} i_{kd} \end{bmatrix} =$$

$$\begin{bmatrix} L_{md} + L_a & L_{md} \\ L_{md} & L_{md} + L_{kf} + L_{kd} \end{bmatrix} \frac{d}{dt} \begin{bmatrix} i_d \\ i_{kd} \end{bmatrix} + \begin{bmatrix} L_{md} \\ L_{md} + L_{kf} \end{bmatrix} \frac{d}{d}$$

The field voltage ($V_f$), no longer an input parameter, is given by

$$V_f = r_f i_f + \begin{bmatrix} L_{md} & L_{md} + L_{kf} + L_f & L_{md} + L_{kf} \end{bmatrix} \frac{d}{dt} \begin{bmatrix} i_d \\ i_f \\ i_{kd} \end{bmatrix} (1$$

The quadrature axis matrix equation, which is of the same form as (7), need not be modified.

## APPENDIX C: Test System Data

| | |
|---|---|
| Generator: Rating | 90MVA |
| Terminal Voltage | 13.8kV |

| | |
|---|---|
| Direct-axis reactance | $x_d = 1.18$ |
| Direct-axis damper reactance | $x_{kd} = 1.24$ |
| Quadrature-axis reactance | $x_q = 1.05$ |
| Quadrature-axis damper reactance | $x_{kq} = 1.05$ |
| Field Reactance | $x_f = 1.27$ |
| Direct-axis damper resistance | $r_{kd} = 0.021$ |
| Direct-axis sub-transient reactance | $x_d'' = 0.145$ |
| Quadrature axis damper resistance | $r_{kq} = 0.036$ |
| Quadrature axis sub-transient reactance | $x_q'' = 0.145$ |
| Field resistance | $r_f = 0.00068$ |
| Leakage reactance | $x_l = 0.075$ |
| Armature resistance | $r_a = 0.0035$ |
| Direct-axis open circuit time constant | $T_{do} = 0.042s$ |

| | |
|---|---|
| Converter: | |
| Type | 12 pulse |
| Nominal Current | $I_d = 1kA$ |
| Nominal Voltage | $V_d = 40kV$ |

| | |
|---|---|
| Converter Transformers: | |
| Rating | 50 MVA |
| Reactance | $x_t = 5percent$ |
| Voltage | $13.8/30.36kV$ |

## AUTHORS

**Jos Arrillaga** received his BE degree of Spain and his MSc, PhD and DSc of Manchester, where he led the power systems group of UMIST between 1970-74. He has been a Professor at the University of Canterbury since 1975. He is a Fellow of IEE, IEEE, the New Zealand Institution of Engineers and the Royal Society of New Zealand.

**Stuart J. Macdonald** received his BE degree in electrical and electronic engineering from the University of Canterbury (New Zealand) in 1991. He is currently working towards a PhD with an emphasis on unit connected HVdc generation.

**Neville R. Watson** received BE (Hons) and PhD degrees in electrical and electronic engineering from the University of Canterbury (New Zealand) in 1984 and 1987, respectively. He has worked as a lecturer at the University of Canterbury since 1988. His interests include steady state and dynamic analysis of ac/dc power systems and computer graphics.

**Soesi Watson** received ME and PhD degrees in civil engineering from the University of Canterbury (New Zealand) in 1986 and 1989, respectively.

# Test Results From Benmore HVdc station with the Generators operating in Group Connected Mode

S.J. Macdonald W. Enright J. Arrillaga M.T. O'Brien

University of Canterbury
Christchurch, New Zealand

Trans Power NZ Ltd

## Introduction

A recent CIGRE document published in ELECTRA [1] has described the potential benefits of a direct connection of generators to HVdc converters. The steady state capability, operational aspects and transient behaviour of unit connected schemes are well documented from a theoretical point of view [2],[3],[4]. So far, however, there is no practical information on the operation of such schemes and particularly the harmonic content and ratings of the generator units involved.

This paper reports on recent harmonic tests carried out at the Benmore end of the New Zealand HVdc link operating as a group connected scheme, i.e. disconnected from the rest of the South Island system and without filters. While the focus of the paper is on the harmonic current loading issues, it is recognised that other issues, such as governing problems may also need detailed consideration.

There are important differences in the operation of unit and group connected schemes. In the unit connection each machine is directly connected to a 12–pulse converter and the dc line voltage is formed by adding a number of these units in series. Reduced dc power levels may dictate the removal of generating units and this will reduce the dc line voltage and therefore the transmission efficiency. Moreover the inverter end will then operate with larger value of $\gamma$, increasing the reactive power requirements.

In the group connection the generators are connected to a common bus and therefore the removal of generator units does not affect the dc line voltage. However, electrically there is no difference between unit and group connections as the generators, for a given load and firing angle condition should see the same harmonic voltages and currents. Therefore the group connected harmonic test results should be of general applicability to both types of direct connection schemes. Moreover, the results were used to try and verify different simulation techniques presently available.

## The Benmore HVdc Terminal

The recently upgraded New Zealand link consists of a parallel arrangement of two 12–pulse mercury–arc valve converters in pole 1 and a new thyristor valve 12–pulse converter in pole 2. The circuit and components involved in pole 1 are shown in Figure(1). When either of the interconnecting transformers (T2 or T5) are removed from service, poles 1A or 1B can operate in group connection.

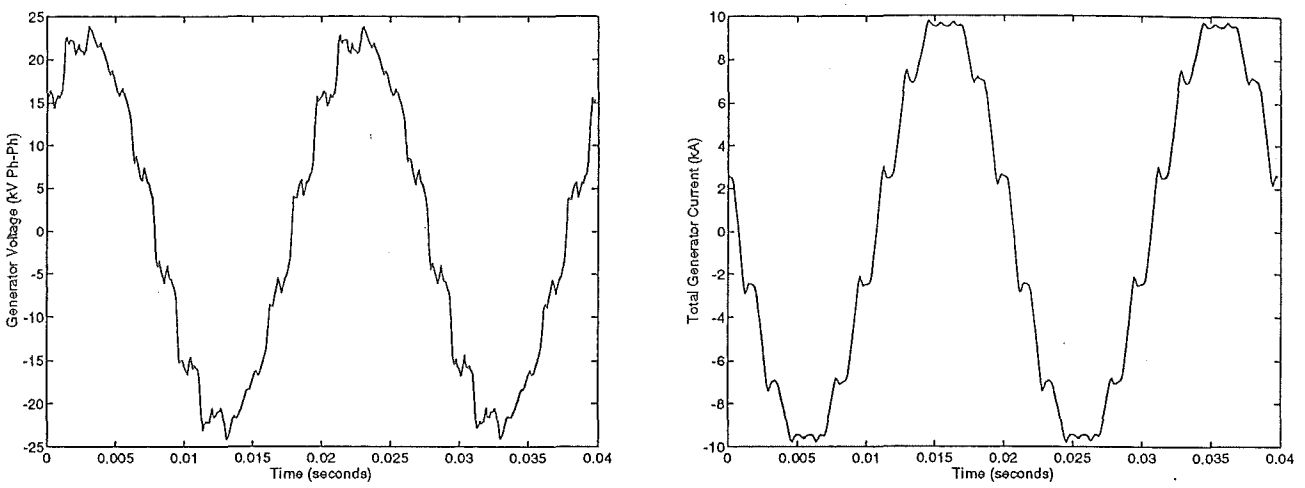


Figure 1: Typical Generator Voltage and Current Waveforms

By arrangement with TRANS POWER, the National Grid Company, the system was available for harmonic tests in the group connected mode (i.e. with no filters and the ac system disconnected) during a recent period of maintenance for transformer T2. The maximum power transmitted under this condition was 212 MW (80 % of full power) with three generator units connected.

# Experimental Procedure

The harmonic measurements were made with a Hewlet Packard Data Aquisition Unit (DAQ) which forms part of the Benmore instrumentation to capture system transients. Three extra channels were installed to record the generators' terminal voltage in one phase and the corresponding currents in each of the two transformers of the 12–pulse converter; these two currents were subsequently added to derive the total generator stator current. Other existing channels of interest were the dc voltage and pole current as well as the firing angle.

The pole 1A mercury–arc valve converter was deblocked and a steady operating point of 350 Amps, 260kV at 15 degrees firing angle was achieved. Throughout the tests the firing angle was maintained at 15 degrees. The waveforms were sampled at 8192 bits per second for a 5 second interval. Further half–pole dc current increments were performed, and after allowing sometime for the system to stabilize, the waveforms were again sampled. The dc current range varied from 350 to 785 amps; a typical set of time data recorded is shown in Figure(1) for the case of a dc current of 650 Amps. From the sampled waveforms the harmonic spectra were calculated.

In all cases the uncharacteristic harmonic levels were insignificant. Moreover the presence of dc side filters also made the dc voltage and current harmonics negligible. The report, therefore, discusses only the generator characteristic harmonic content.

# Comparison between Test and Simulation Results

Figures(2) and (3) compare the recorded machine voltage and current harmonic levels with those predicted by steady state and dynamic simulations. Owing to the difficulty in maintaining a constant generating frequency it is recommended that future tests should use more accurate FFT processing synchronised with the actual fundamental frequency, such as provided by the CHART instrumentation [5].

The steady state formulation, based upon the commutating voltage behind the subtransient reactance [4] in general predicts lower levels of harmonic current content. The agreement for the harmonic voltages is considered fortuitous for this particular system.

The PSCAD [6] dynamic simulation package has been used in the harmonic prediction. The harmonic current levels are quite close to the test results as they are less influenced by the generating operating conditions and more by the dc link firing and current control (which were fixed during the tests). The harmonic voltage trends are consistent, and the discrepancies are seen as a limitation of the generator model.

# Generator Rating

The possibility of a direct connection was envisaged in the design of the Benmore generators and restrictions imposed on the nominal power rating (lowered to 102.3 MVA) and the current harmonic content under such operating conditions. The ratings are listed in table(1) together with the maximum current harmonics monitored during the tests recently carried out. Clearly none of the specified maximum limits were exceeded at the power levels involved.

| Harmonic | rating (pu) | recorded (@212 MW) |
|---|---|---|
| 11th | 0.0744 | 0.0422 |
| 13th | 0.0595 | 0.0267 |
| 23rd | 0.0193 | 0.0067 |
| 25th | 0.0154 | 0.0037 |

Table 1: Machine Stator Current Harmonics

If the dynamic simulation results are extrapolated in the high current region to the maximum dc half–pole current of 1000 amps, the maximum harmonic current levels are still not exceeded. Moreover the total current harmonics are less than 10% of the fully rated positive sequence current.

# Generator Governing

Although this paper does not explore the issue of generator governing, it is known from previous operation of the Benmore generators in both 6 and 12–pulse converter modes, that governor responses differ from those when the generators are interconnected to the South Island system. The governor responses cause operational difficulties which render this aspect worthy of a separate study.

# Conclusions

This paper has presented the first Unit Connection harmonic measurements. Experience gained will be used for future measurement opportunities as they arise. The generator harmonic current levels were well below specified maximum ratings. Present dynamic simulation studies provide slightly conservative estimates of the voltage and current harmonics. Although on the safe side, in a competitive environment the overdesign concept is not necessarily acceptable.

# Acknowledgements

The authors wish to acknowledge the financial and technical support of Trans Power New Zealand for this investigation, the help of P. Thompson and K. Dean during the tests and of Dr's N.R Watson and J. Zavahir with the processing of results.

# References

[1] CIGRE Joint Working Group 11/14-09. Hvdc unit connected generators. *ELECTRA*, 149, August 1993.

[2] J Arrillaga, H J Al-Khashali, and J G Campos-Barros. Dynamic modelling of single generators connected to hvdc convertors. *IEEE Transactions on Power Apparatus and Systems*, 97(4):1018–1029, July 1978.

[3] J Arrillaga, S Sankar, C P Arnold, and N R Watson. Characteristics of unit-connected hvdc generator convertors operating at variable speeds. *Proceedings of the IEE, Part C*, 139(3):295–299, May 1992.

[4] J Arrillaga, S Sankar, N R Watson, and C P Arnold. Operational capability of generator hvdc convertor units. *IEEE Transactions on Power Delivery*, 6(3):1171–1176, July 1991.

[5] A J V Miller. Multichannel continuous harmonic analysis in real time. *IEEE Transactions on Power Delivery*, 7(4):1813–1819, October 1992.

[6] Manitoba Hydro. *The EMTDC Users Manual.* Canada, 1988.

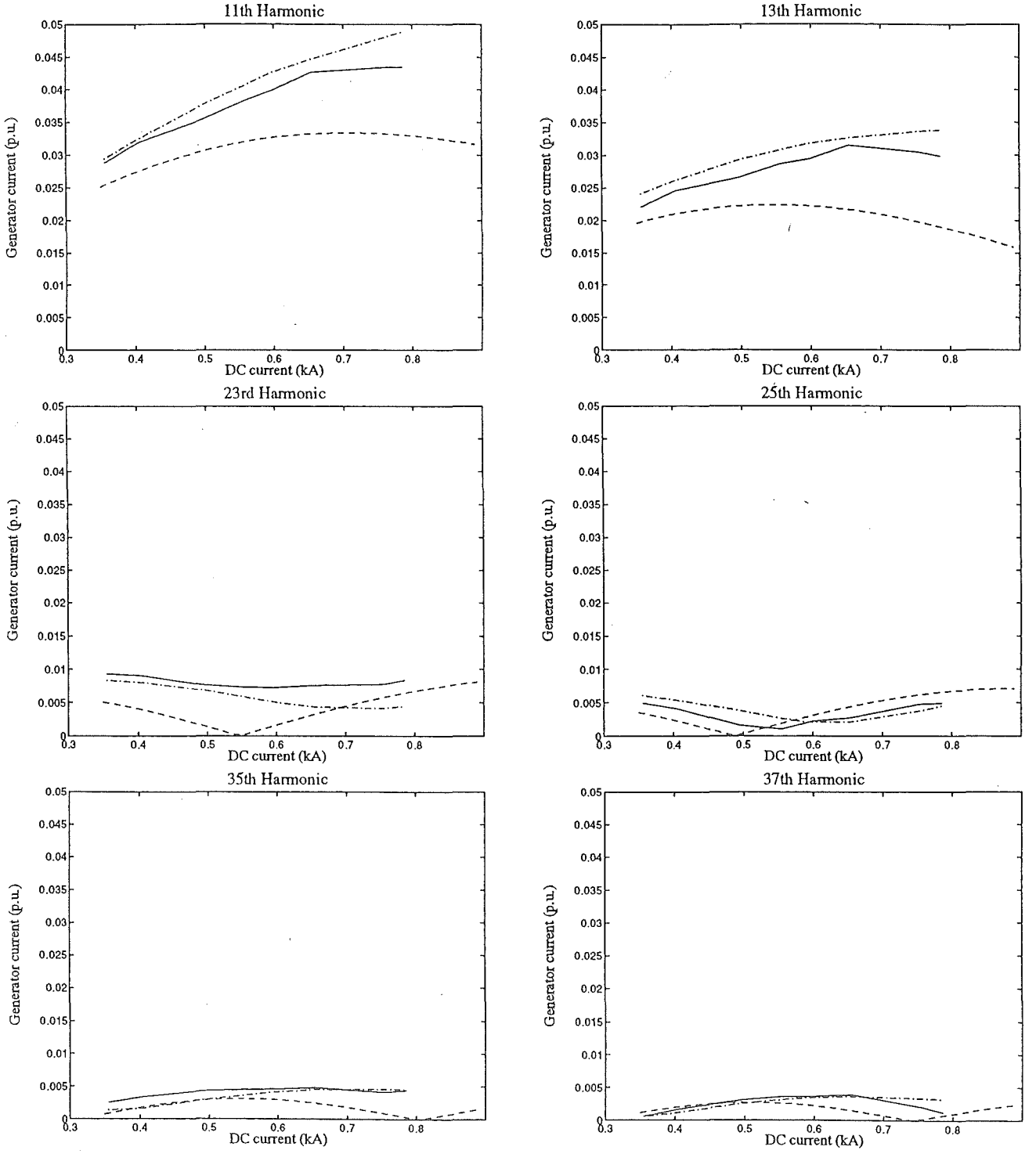


Figure 2: Harmonic comparison of recorded generator current with steady state and dynamic simulation; *Recorded data=Solid, Dynamic simulation=Dash-Dot, Steady state equations=Dash-Dash.*

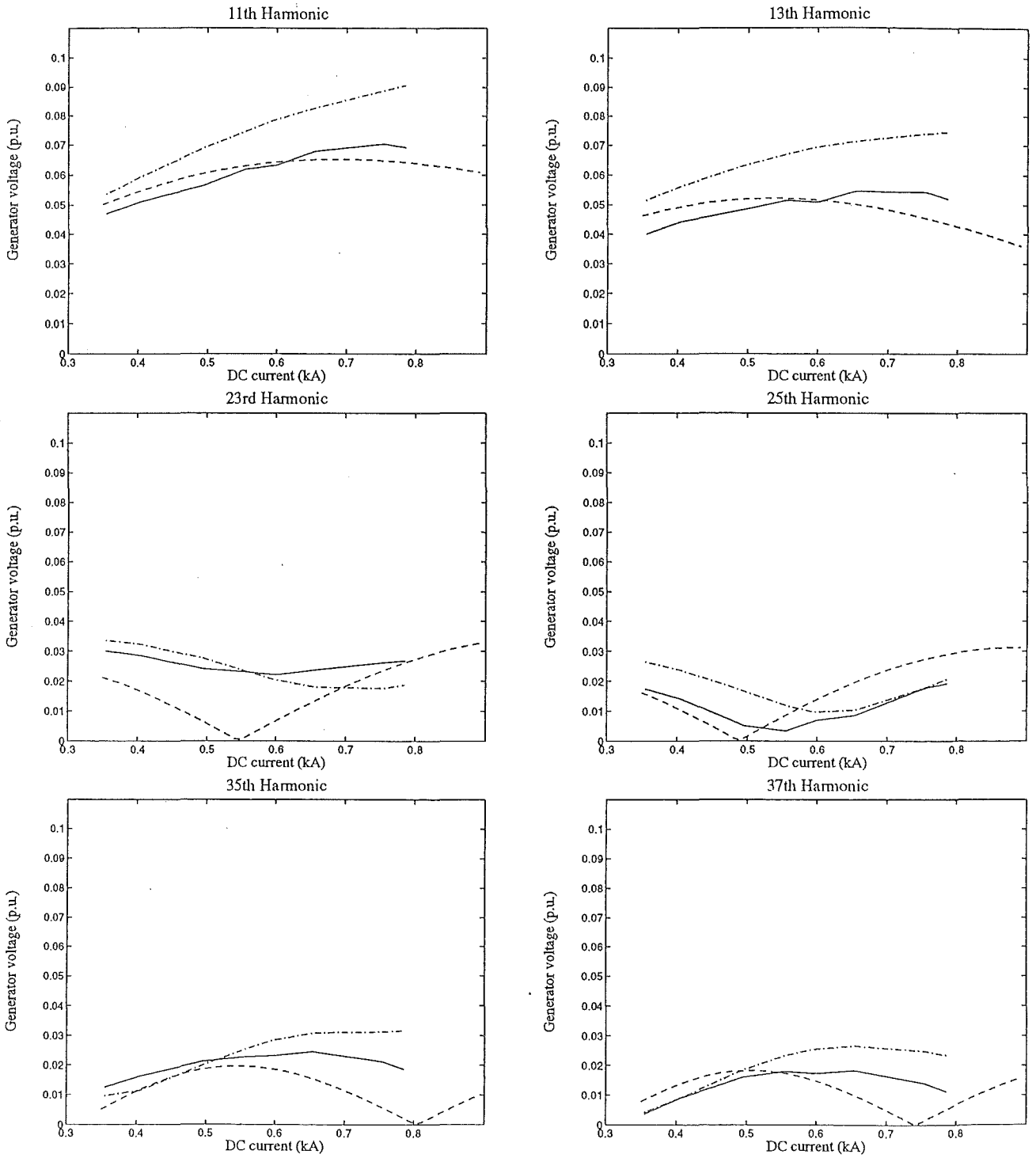


Figure 3: Harmonic comparison of recorded generator voltage with dynamic simulation; *Recorded data=Solid, Dynamic simulation=Dash-Dot, Steady state equations=Dash-Dash.*

# Operating characteristics of unit and group connected generator-HVDC converter schemes

J. Arrillaga, DSc, FIEE
J.R. Camacho, MSc
S.J. MacDonald, BEng
C.P. Arnold, PhD, MIEE

*Indexing terms: Group connection, HVDC converters, Load flow, Unit connection*

**Abstract:** The two alternatives for the direct connection of generators to HVDC converters, i.e. the unit and group connections, are compared under varying steady-state operating conditions at nominal operating frequency. Direct connection is defined as the connection of synchronous generators and converters without AC filters and with the transformer having simultaneously the function of converter and step-up transformer. With all the units in service both schemes display the same characteristics. By reducing the number of generators in service the group connection becomes more efficient at lower power levels. The opposite effect occurs with the unit connection where the efficiency reduces with the power levels, particularly with fewer generators in service. Moreover, in the last-mentioned case the inverter end of the link requires extra reactive power compensation. Therefore for schemes operating at varying power levels and fixed frequency the group connection should be the preferred alternative.

## List of symbols

$E$ = rectifier AC system EMF
$E''$ = rectifier AC system commutating voltage
$x_c$ = Unit-connection commutating reactance
$x'_c$ = Group-connection commutating reactance
$x$ = generator synchronous reactance
$x''$ = generator sub-transient reactance
$x_t$ = converter transformer reactance
$x_B$ = reactance base in ohms
$n$ = total number of generators
$n_s$ = number of generators in service
$V_n$ = direct voltage for one unit-connected generator
$V_d$ = direct voltage for $n_s$ generators
$V_i$ = inverter end voltage per pole of link
$V_r$ = rectifier end voltage per pole of link
$V_B$ = base voltage in kV
$MVA_B$ = MVA base
$I_d$ = direct current of link
$I_p$ = phase current for unit-connected scheme
$R$ = resistance per pole of link
$R(n)$ = residuals in AC–DC load flow
$r$ = voltage ratio of converter transformer
$a$ = tap of converter transformer
$\alpha$ = converter firing angle
$\beta$ = phase angle of commutating voltage
$\phi$ = power factor angle in primary of converter transformer
$\gamma$ = converter extinction angle
$\eta_t$ = turbine efficiency
$\eta_l$ = transmission efficiency
$\eta_l^U$ = transmission efficiency, unit connection
$\eta_l^G$ = transmission efficiency, group connection
$\eta_t^U$ = overall efficiency, unit connection
$\eta_t^G$ = overall efficiency, group connection



Paper 9602C (P9, P10), first received 27th November 1992 and in revised form 30th March 1993

The authors are with the Department of Electrical and Electronic Engineering, University of Canterbury, Christchurch, New Zealand.

## 1 Introduction

Several contributions have discussed the direct connection of generators to HVDC converters. Some have tried to justify the adoption of the unit-connection concept on the basis of substantial cost reductions in power generation and rectification plant [1–3]. Others have described the development of computer models for the incorporation of the unit connection in power system studies [4, 5].

An important disadvantage of the unit-connected scheme is a considerable increase in the number of converter transformers, i.e. two per generator for 12-pulse operation. Consequently a 600 MW (6 × 100 MW units) power station requires 12 converter transformers as compared with only two for the conventional rectifier station.The general cases of $n$ generators connected either as units or as a group are shown in Fig. 1. The possibility of six-pulse operation, which only requires one transformer and bridge per generator, is not considered because of the extra characteristic harmonic problem in the generator and in the DC line.

Operation of the unit-connection configuration with diode rectifier bridges was considered in previous published articles [3, 4], which show the operational limitations and possibilities of operation of a converter

Financial assistance has been provided by the New Zealand Ministry of External Relations and Trade, New Zealand Vice-Chancellors' Committee, by Universidade Federal de Uberlândia — Departamento de Engenharia Elétrica and by CAPES/Ministry of Education of Brazil.

under minimum firing angle equal 0°. The power transmission setting may be determined by the receiving system requirements and generating efficiency. Therefore,

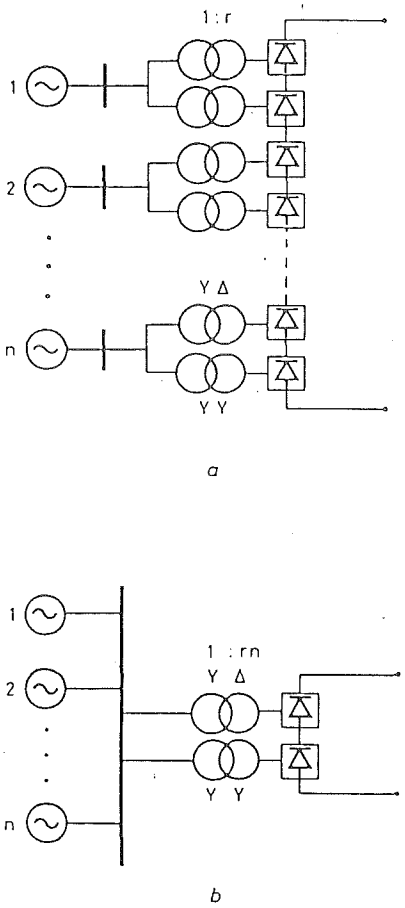


**Fig. 1** *Generator–converter plant*
*a* Unit-connected generation
*b* Group-connected generation

the number of generators in service will vary if the generating plant has been designed for constant (nominal) speed operation. This could be avoided with the use of variable-speed turbines which will permit optimal efficiencies at varying water heads.

The question of direct voltage control at low speeds (and frequencies) has been considered in a recent publication [6] which shows that constant-voltage transmission can be achieved even without the need for on-load tap changers at the rectifier end.

The disconnection of generating units, while ensuring efficient generation, may result in poor transmission efficiency when applied to unit-connected schemes because the voltage is proportional to the number of units connected in series. Moreover, transmission voltage reductions caused by the disconnection of units at the rectifier end will immediately be followed by corresponding firing angle advances at the inverter end, which may require extra VAr compensation.

These problems should not affect the direct group connection of generators to HVDC converters because the generators are paralleled at a common converter busbar and all the converter units in series remain in service following generator removals.

At a time when direct connection is being seriously considered, it is important to compare the operating characteristics of the two alternatives, i.e. unit and group configurations, and assess their effect on the overall system efficiency and receiving end reactive power requirements. The results of such investigation are described here.

## 2 Steady-state analysis

An accurate power flow solution of the unit-connection scheme with representation of saliency effects requires the use of time domain calculated rectifier characteristics [6]. However for a preliminary comparison of the characteristics of unit- and group-connected schemes the conventional AC/DC steady-state power flow [8] provides sufficient information.

By assuming that all the generators in service have identical characteristics and are equally loaded, they can be represented as a single equivalent machine as in Fig. 2.

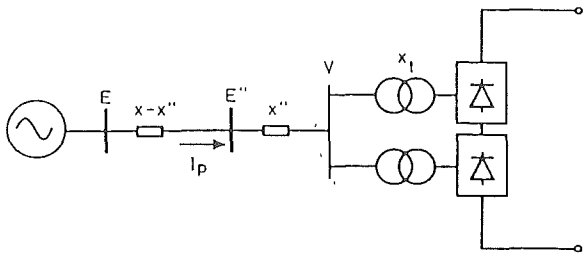


**Fig. 2** *Test system at rectifier end of link*

The internal EMF behind subtransient reactance is not directly controllable. Instead, the generator excitation will be controlled to provide the specified DC link power at the specified firing angle ($\alpha_{min}$).

With reference to Fig. 2, the fictitious bus behind the machine's subtransient reactance is used as the slack busbar on the rectifier side of the load flow solution and the subtransient voltage is used as the commutating voltage for the converter. However the commutating voltage ($E''$) is not known in advance and its magnitude and phase ($\beta$) are obtained as part of the load flow solution.

The vector of independent variables of the converter model is [4]

$$\bar{x} = [V_d, I_d, \cos\alpha, \phi, E, E'', \beta]^T \quad (1)$$

where $T$ is its transpose. Seven residual equations were needed to formulate the load flow problem at the rectifier end. The first two equations are common to the conventional model [8] (with tap variable removed). Therefore,

$$R(1) = V_d - k_1 E'' \cos\phi \quad (2)$$

$$R(2) = V_d - k_1 E'' \cos\alpha - \frac{3}{\pi} I_d x_c \quad (3)$$

where $k_1 = 3\sqrt{(2)}/\pi$. The next two are derived from the generator subtransient phasor diagram of Fig. 3. That is,

$$R(3) = E - E'' \cos\beta - (x - x'')|I_p| \sin(\beta + \phi) \quad (4)$$

$$R(4) = E'' \sin\beta - (x - x'')|I_p| \cos(\beta + \phi) \quad (5)$$

Valid converter control specifications are: direct voltage, direct current, minimum firing angle and DC power at the receiving end. To solve for the seven variables of eqn. 1 three of them must be specified. The second and third specifications will normally be the direct voltage and current fixing the DC power at the rectifier end. However, once the control angle $\alpha$ reaches the minimum level $\alpha_{min}$, this value becomes the second specification instead of the direct voltage. The incorporation of converter equations into the AC/DC power flow solution is

well documented and the results obtained in this paper are based in the algorithms described in References 4 and 8.

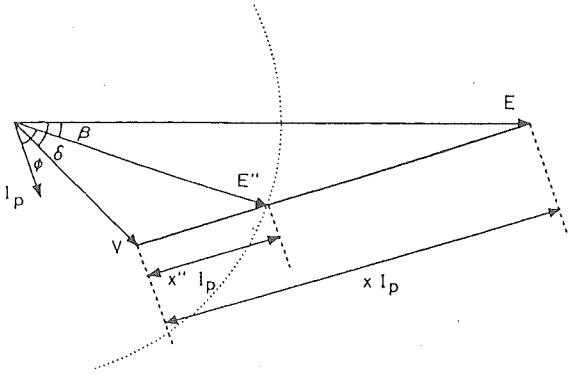


**Fig. 3** *Simplified phasor diagram of unit and group-connected generator*

Figs. 1*a* and *b* display the main components of the two basic unit and group-connection configurations. It is assumed that all the generators are the same and equally excited. If $r$ is the converter transformer voltage ratio of the unit connection, then to derive the same nominal direct voltage and current, the corresponding ratio for the group-connection transformers needs to be $rn$, where $n$ is the total number of generators. Using as a power base the nominal rating of one generator, the commutation reactance of the unit-connection bridges is

$$x_{c(pu)} = x'' + 2x_t \tag{6}$$

or

$$x_c = (x'' + 2x_t)x_B r^2 \tag{7}$$

in ohms, where $x_B = V_B^2/MVA_B$, with $V_B$ being the base voltage at the primary side of the transformer. The direct voltage of a twelve-pulse bridge unit is

$$V_n = 2\left[\frac{3\sqrt{(2)}}{\pi} E''r\cos\alpha - \frac{3}{\pi}(x'' + 2x_t)x_B r^2 I_d\right] \tag{8}$$

and the total direct voltage output with $n_s$ generators in service is

$$V_d = n_s V_n \tag{9}$$

i.e. the output is always proportional to the number of generators in service. Using the same power base, the commutation reactance of the group-connection bridges with $n_s$ generators in service is

$$x'_{c(pu)} = \frac{x''}{n_s} + \frac{2x_t}{n} \tag{10}$$

or

$$x'_c = \left(\frac{x''}{n_s} + \frac{2x_t}{n}\right)x_B(rn)^2 \tag{11}$$

in ohms, and the maximum direct voltage of the group connection is

$$V_n = 2\left[\frac{3\sqrt{(2)}}{\pi} E''rn\cos\alpha - \frac{3}{\pi}\left(\frac{x''}{n_s} + \frac{2x_t}{n}\right)x_B(rn)^2 I_d\right] \tag{12}$$

Eqn. 12 shows that for a given excitation the no-load voltage output remains invariant regardless of the number of generators in service. However, the second term of the equation depends on $n_s$ and therefore the slope of the voltage regulation increases with fewer generators in service. The reverse happens in the case of the unit connection (eqn. 8), where the commutation reactance and hence the slope of the voltage regulator remains invariant while the open-circuit voltage reduces with the number of generators in service.

## 3 Rectifier characteristics

The generator excitation will be designed to keep the converter voltage constant under different specified powers. For the unit-connection configuration however, with a reduced number of units in operation, the exciters of these machines will not be able to maintain the nominal transmission voltage level. Once the maximum excitation is reached the commutating voltage (i.e. $E''$) will reduce with increasing current and therefore the output $V_d/I_d$ characteristic of the rectifier will be non-linear.

The AC/DC load flow, described in Section 2, is used to derive the rectifier characteristics of the unit and group connections. The results for the test system specified in the Appendix are shown in Fig. 4 and 5. Points *a* to *f* and

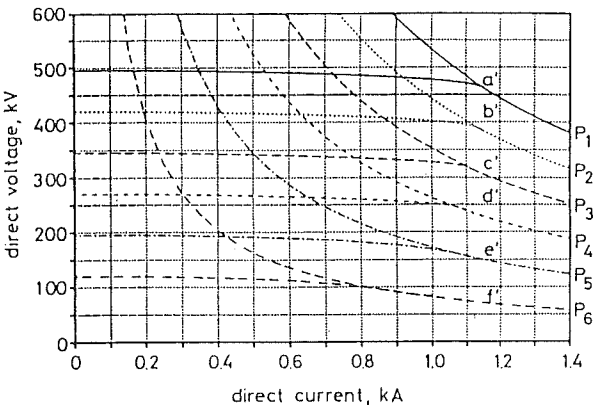


**Fig. 4** *Characteristics for Unit-connected generation at rectifier end*

——— 6 machines
····· 5
– – – – 4
------- 3
—·—· 2
— — 1

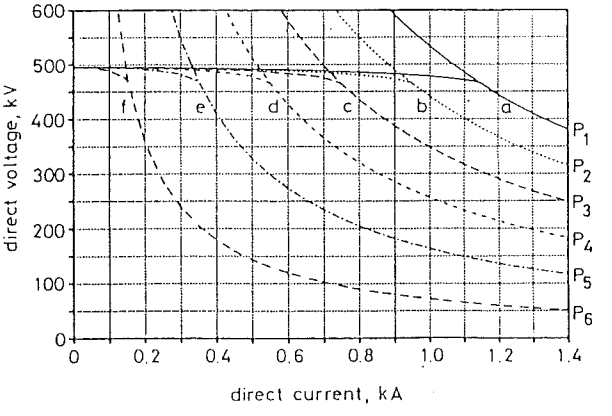


**Fig. 5** *Characteristics for group-connected generation at rectifier end*

——— 6 machines
····· 5
– – – – 4
------- 3
—·—· 2
— — 1

*a'* to *f'* in those Figures indicate the nominal operation of the test system when changing the number of machines in service from 6 to 1, respectively.

With all the generators in service the unit and group configurations follow the same characteristic. In both cases the intersection of this curve and the maximum specified power level ($P_1$ = 520 MW) (i.e. point *a*) determines the operating current required (i.e. 1.16 kA in the test system). At a reduced power setting ($P_2$ = 430 MW) and with one generator removed, the unit and group characteristics are different, giving rise to the operating points *b* in Fig. 4 (1.15 kA) and 5 (0.955 kA), the last requiring less current and thus resulting in better transmission efficiency. Although the commutation voltage loss is larger in the case of the group connection, the reduced open-circuit voltage of the unit connection demands more current for a given power setting.

Further generator removals result in operating points *c*, *d*, *e* and *f* in Figs. 4 and 5, which show a practically constant voltage for the case of the group connection. For these points the currents in Fig. 4 are, respectively, 1.125, 1.1, 1.09 and 1.01 kA. In Fig. 5 the currents for the same points are 0.75, 0.55, 0.35 and 0.153 kA. The curved lines are the $V_d/I_d$ characteristics for the rectifier in Figs. 4 (unit connection) and 5 (group connection) and for the inverter in Fig. 6 (unit and group connection). Table 1

**Table 1: Maximum power received at inverter end**

| Number of machines | Power received | Power designation |
|---|---|---|
| | MW | |
| 6 | 520 | $P_1$ |
| 5 | 430 | $P_2$ |
| 4 | 340 | $P_3$ |
| 3 | 250 | $P_4$ |
| 2 | 160 | $P_5$ |
| 1 | 70 | $P_6$ |

shows the maximum power at the receiving end for each number of machines in operation.

## 4 Inverter characteristics

In Fig. 6 the constant-power characteristics are combined with the inverter constant extinction angle characteristics

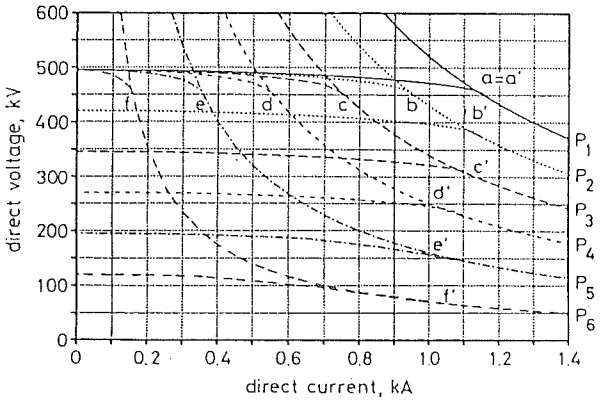


Fig. 6 *Characteristics for unit- and group-connected generation at inverter end*

——— 6 machines
····· 5
– – – – 4
------- 3
—·—· 2
— — 1

to give the same operating points described in the previous section, after taking into account the effect of DC line resistance. Clearly, in the unit-connection case a gradual reduction in the number of generating units reduces the transmission voltage and transfers the constant-current control from the rectifier to the inverter end which then operates with increasing firing angle advances and reduced power factors. This is illustrated in Fig. 7 which shows reactive versus active power levels at

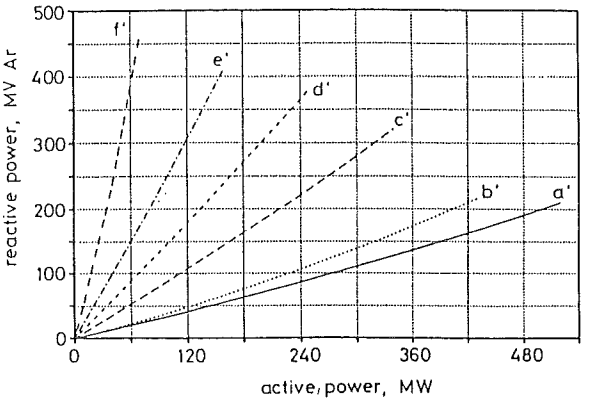


Fig. 7 *Power characteristics for unit-connected generation at inverter end*

——— 6 machines
····· 5
– – – – 4
------- 3
—·—· 2
— — 1

the inverter end for different numbers of unit-connected machines at the rectifier. The difference between the reactive demands with 6 and 5 machines is small (points *a'* and *b'*, respectively) because the complete range of tap variation is first used to delay the extra reactive demand with one machine disconnected. Once the tap change range is exhausted such demand increases fast. For instance when changing from six to four machines (points *a'* and *c'*, respectively) the inverter reactive power increases from about 210 to 320 MVAr.

On the other hand, the group connection permits operation with fewer generating units in service while reducing the inverter reactive power demand. This is illustrated in Fig. 8 where the reactive versus active

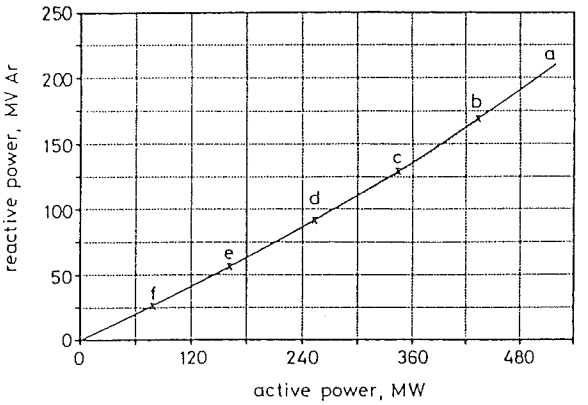


Fig. 8 *Power characteristics for group-connected generation at inverter end*

——— 6 machines
····· 5
– – – – 4
------- 3
—·—· 2
— — 1

power characteristics with different number of machines are practically coincident. In this case a 3.2% tap variation of the inverter end transformers can accommodate

the small extra voltage regulation caused by the increased commutation reactance at the rectifier end.

## 5 Efficiency considerations

### 5.1 Turbine efficiency

If the station is designed for a fixed-speed turbine operation to generate power at the nominal frequency (i.e. 50 or 60 Hz), the optimum turbine torque varies with the water head level. Therefore, in the absence of other possible considerations justifying less efficient power transmission, minimum water utilisation will be achieved by varying such power with the water head level. This implies the disconnection of turbine–generator groups at reducing power levels.

The performance characteristics of the 90 MW hydroturbines of the Pan Jia Kou scheme [7] are used to illustrate this effect. For a water head level of 86 metres, the turbine efficiency ($\eta_t$) against power ($P$) curve for a power range between 45 and 90 MW can be approximated by the following 3rd-order polynomial

$$\eta_t = -0.6735P^3 + 1.1620P^2 - 0.4151P + 0.9220 \quad (13)$$

with $\eta_t$ being the turbine efficiency in pu and $P$ the power of one unit in pu at 90 MW power base.

### 5.2 Transmission efficiency

The line voltage is the critical factor affecting transmission efficiency. By comparison the generator, transformer and converter plant efficiencies are high and practically constant. Thus for the purpose of our comparison the efficiency of an HVDC transmission line can be expressed as

$$\eta_l = \frac{V_i}{V_r} = 1 - \frac{RI_d}{V_r} \quad (14)$$

As shown in eqns. 8 and 9 the voltage of a unit-connected scheme is proportional to the number of units in service, and the direct voltage in each pole of the transmission line at the rectifier end is

$$V_r = \left(\frac{n_s}{2}\right)V_n \quad (15)$$

The transmission line efficiency of a unit-connected scheme is then

$$\eta_l^U = 1 - \frac{RI_d}{(n_s/2)V_n} \quad (16)$$

Similarly, Fig. 4 shows that the rectifier voltage output of a group-connected scheme remains practically constant regardless of the number of generators in service, and the transmission line efficiency in this case becomes

$$\eta_l^G = 1 - R\left(\frac{P}{V_r^2}\right) \quad (17)$$

### 5.3 Test system efficiencies

The test system, described in the Appendix, consists of six generators connected to an HVDC link. The nominal voltage and current rating of the 500 km line are 270 kV and 1.2 kA, respectively, and the line resistance 11.86 ohms. The overall operating efficiency results from the combined effect of turbine and transmission efficiency components, i.e.

$$\eta_t^U = \eta_t \eta_l^U \quad (18)$$

for the unit connection, and

$$\eta_t^G = \eta_t \eta_l^G \quad (19)$$

for the group connection.

For the turbine characteristic represented by eqn. 13 the overall efficiencies against power with one to six machines in service are shown in Fig. 9. With fewer units

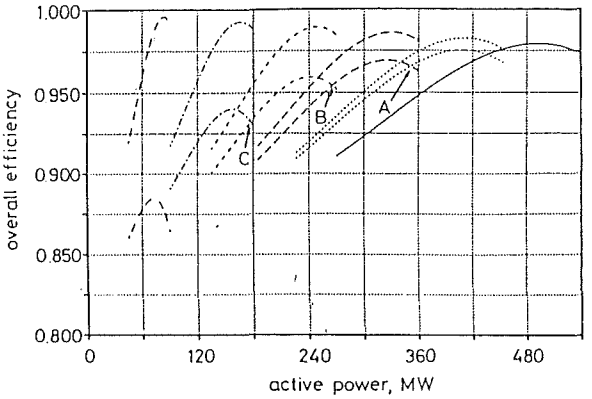


**Fig. 9** *Comparison of overall efficiency of unit and group-connected generation*

——— 6 machines
····· 5
– – – – 4
------- 3
—·—·— 2
— — 1

in service, the transmission efficiency reduction in the case of the unit connection predominates. The opposite effect occurs with the group connection, where the nominal voltage can be maintained with lower powers and machine numbers. Hence the group connection provides higher overall operating efficiencies with reducing powers.

Regarding unit-connection performance, the crossings between the efficiency curves in Fig. 9 (i.e. points A, B and C) indicate the power boundaries for the number of units to be used for highest efficiency (even though the efficiencies are considerably lower than for the group connection). However, these points may occur at power levels beyond the capability of the machines. Moreover, Fig. 7 has shown that for reducing active power levels, operation with fewer machines demands increasing reactive power provision at the inverter end, a condition unlikely to be acceptable.

## 6 Conclusions

The characteristics of unit and group HVDC-connected generation have been derived for a wide range of operating powers. Although there is no difference between the alternative configurations when all the generators are in service, the transmission voltages of the unit connection deteriorate fast with fewer generators in service resulting in low transmission efficiencies. Moreover, operation with reduced generators in service requires a transfer of power control to the inverter end, which increases substantially the reactive power demand at that end. Group connection presents no problems in this respect, being capable of maintaining the required transmission voltage with fewer generators in service and thus providing efficient transmission at different power levels. The group

connection also permits efficient inversion without the need for unrealistic on load tap change ranges.

The effect of turbine efficiencies taking into account the hydrowater levels has been incorporated in the overall comparison to define the optimal operating strategies in each case.

It is recognised that factors other than optimum efficiency may dictate the power transmission levels via the HVDC link but if water conservation becomes a critical factor (such as the likelihood of frequent dry years) the foregoing considerations may influence the decision on the type of direct connection to be selected.

## 7 References


1 CALVERLEY, T.E., OTTAWAY, C.H., and TUFNELL, D.H.A.: 'Concept of a unit generator convertor transmission system'. IEE conference on *High voltage DC and AC transmission*, London, 1973, pp. 53–59

2 KRISHNAYYA, P.C.S.: 'Review of unit generator–convertor connections for HVDC transmission'. IEEE/CSEE joint conference on *High voltage transmission systems*, Beijing, China, 1987

3 BOWLES, J.P.: 'Multiterminal HVDC transmission systems incorporating diode rectifier stations', *Trans. IEEE*, 1981, **PAS-100**, (4), pp. 1674–1678

4 ARRILLAGA, J., ARNOLD, C.P., CAMACHO, J.R., and SANKAR, S.: 'AC–DC load flow with unit-connected generator–converter infeeds'. Presented at IEEE summer power meeting, 1992, paper 92 SM 593–4 PWRS

5 GALVÃO, L.C.R., DOS REIS, L.B., PENTEADO, A.A., CRISTINE, S.V., MITTIO, H., DONHA, D.C., and ELLERY Fo., E.H.: 'HVDC unit connection schemes & dimensioning turbines and generators and characteristics and advantages of the operation with variable speed'. III SEPOPE — symposium of specialists in electric operation and expansion planning, Belo Horizonte, Brazil, May 1992

6 ARRILLAGA, J., SANKAR, S., ARNOLD, C.P., and WATSON, N.R.: 'Characteristics of unit connected HVDC generator convertors operating at variable speeds', *Proc. IEE C*, 1992, **139**, (3), pp. 295–299

7 JAQUET, M.: 'The Pan Jia Kou pumped storage station, part I: hydraulic equipment'. 4th ASME International Symposium *Hydropower Fluid Machinery*, December 1986

8 ARRILLAGA, J., ARNOLD, C.P., and HARKER, B.J.: 'Computer modelling of electrical power systems' (Wiley, London, 1983)


## 8 Appendix

### 8.1 Test system

The New Zealand North Island primary transmission system is used at the inverter end of the link and the Benmore power station, without filters and disconnected from the New Zealand South Island AC system, is used as the unit and/or the group connected scheme. The rectifier end of the DC link for the unit connection is shown in Fig. 2. The circuit configuration pertinent to the group connection is as shown in Fig. 1*b*. The relevant parameters for each of the six generators at the Benmore power station are

rating = 112.5 (MVA)
voltage = 16.0 (kV)
$x$ = 1.140 (pu)
$x'_d$ = 0.264 (pu)
$x''_d$ = 0.174 (pu)
$x''_q$ = 0.190 (pu)
$R_a$ = 0.003 (pu)

Convertor transformers reactance: 11.5%